Supplementary Information

TEMPO-Promoted Thioacid–Amine Coupling for Peptide Synthesis

Surya Pratap Singh[†a], Upasana Chatterjee[†a], Daniel T. Glatzhofer[a] and Indrajeet Sharma*[a]

[a]Department of Chemistry and Biochemistry, University of Oklahoma, 101 Stephenson Parkway, Norman, Oklahoma 73019- 5251, United States

Correspondence to: isharma@ou.edu

Content

Materials and methods

Reagents:

Reagents and solvents were obtained from Sigma-Aldrich (www.sigma-aldrich.com), Chem-Impex (www.chemimpex.com) or Acros Organics (www.fishersci.com) and used without further purification unless otherwise indicated. Dry solvents (acetonitrile) were obtained from Acros Organics (www.fishersci.com), and dichloromethane was distilled over CaH_2 under N_2 unless otherwise indicated. THF purchased from Sigma-Aldrich was distilled over Na metal with benzophenone indicator. Toluene was obtained from Sigma-Aldrich.

Reactions:

All reactions were performed in flame-dried glassware under positive N_2 pressure with magnetic stirring unless otherwise noted. Liquid reagents and solutions were transferred through rubber septa via syringes flushed with N_2 before use. Cold baths were generated as follows: 0 °C with wet ice/water and −78 °C with dry ice/acetone.

Chromatography:

TLC was performed on 0.25 mm E. Merck silica gel 60 F254 plates and visualized under UV light (254 nm) or by staining with potassium permanganate ($KMnO_4$), cerium ammonium molybdate (CAM), phosphomolybdic acid (PMA), and ninhydrin. Silica flash chromatography was performed on Sorbtech 230–400 mesh silica gel 60.

Analytical Instrumentation:

NMR spectra were recorded on a Varian VNMRS 400 and 500 MHz NMR spectrometer in $CDCl_3$ unless otherwise indicated. Chemical shifts are expressed in ppm relative to solvent signals: $CDCl_3$ (^1H, 7.26 ppm, ^{13}C, 77.0 ppm); coupling constants are expressed in Hz. NMR spectra were processed using Mnova (www.mestrelab.com/software/mnova-nmr). Mass spectra were obtained at the OU Analytical Core Facility on an Agilent 6538 High-Mass-Resolution QTOF Mass Spectrometer and an Agilent 1290 UPLC.

Nomenclature:

N.B.: Atom numbers shown in chemical structures herein correspond to IUPAC nomenclature, which was used to name each compound.

List of thioacids used in TEMPO-promoted peptide bond formation:

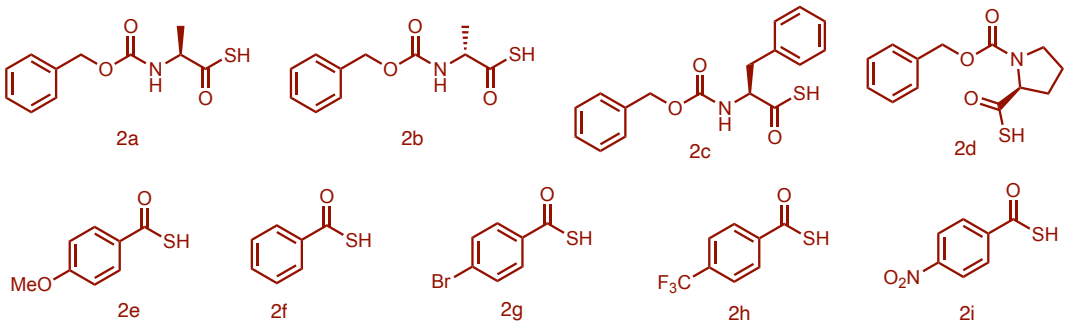

Figure S1: List of thioacids screened in this study.

All the above-stated thioacids (**2a**[1,2], **2b**[2], **2c**[3], **2d**[4], **2e**[5, 6], **2f**[6], **2g**[7], **2h**[8], **and 2i**[9]) were synthesized using the known synthetic procedures in the literature, as stated below.

General Procedure for the synthesis of peptides using thioacid and amines:

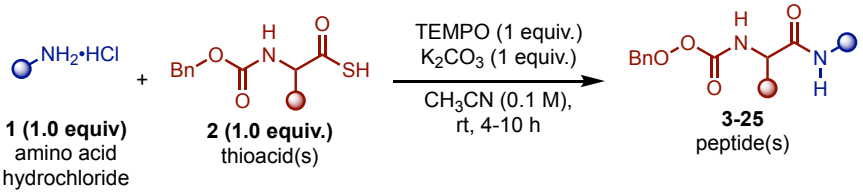

Figure S2: General scheme for the synthesis of peptides

In an oven-dried vial equipped with a stir bar, amino acid methyl ester hydrochloride salt (0.1 mmol) was combined with thioacid (0.1 mmol, 1.0 equiv.), TEMPO (1.0 equiv.), K_2CO_3 (1.0 equiv.) was dissolved in CH_3CN (0.1M). The mixture was stirred at room temperature for 6h - 8h. The reaction was monitored with thin-layer chromatography. The reaction mixture was diluted with ethyl acetate and washed with brine. The organic layer was combined, dried over Na_2SO_4, and evaporated to dryness. The crude was purified with column chromatography (EtOAc: Hexane) to afford the dipeptides and tripeptides.

Optimization of the reaction conditions:

We initiated our studies using L-alanine methyl ester hydrochloride (**1a**) as a model amine and *Z*-L-Ala-SH (**2a**) as a model thioacid. To neutralize the amine hydrochloride salt, we employed K_2CO_3 as a base and screened TEMPO as an oxidant in acetonitrile. The reaction proceeded efficiently, delivering the desired peptide (**3**) in good yield within 6 hours (entry 1). Next, we evaluated DDQ as an alternative oxidant, which did lead to product formation, albeit in significantly lower yield (entry 2). Following this, we screened molecular oxygen (20 psi) as an oxidant, leading to peptide formation with poor yields (entry 3), confirming TEMPO as the best oxidant. We also tested diisopropylethylamine (DIPEA) as an organic base (entry 4), which yielded a good result, although K_2CO_3 remained superior in terms of efficiency and reproducibility. Having optimized the oxidant and base, we turned our attention to solvents. In pursuit of greener and industrially viable conditions, we screened methanol (entry 5) and ethanol (entry 6), both of which afforded the product in good yields. However, when we tested tetrahydrofuran (THF), a coordinating and basic solvent (entry 7), and toluene, an aromatic solvent (entry 8), we observed only trace amounts of product, indicating incompatibility. Since biological peptide construction typically occurs in aqueous media, we also explored aqueous solvent systems (entries 9-13). Acetonitrile containing up to 30% water supported product formation in reasonable yields but increasing the water content to 40% and 50% drastically reduced the yield to trace levels. To further improve productivity, we increased the loading of thioacid to 1.5 equivalents (entry 14), and significant yield improvement was observed. We also performed reactions in the dark (entry 15) and in the presence of 440 nm blue light (entry 16). However, the outcome was unaffected and produced identical results. In summary, the optimized conditions involve using TEMPO as the oxidant, K_2CO_3 as the base, CH_3CN as the solvent, and 1.0–1.5 equivalents of the thioacid; equimolar amounts were preferred for scope exploration.

Table S1: Optimization of the reaction conditions for TEMPO-mediated peptide bond formation.[a]

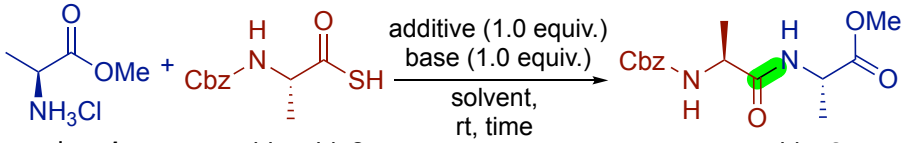

amine, **1a** (1.0 equiv.) thioacid, **2a** (1.0 equiv.)

entry	additive	base	solvent	time	**3**, yield%[b]
1.	TEMPO	K_2CO_3	CH_3CN	6 h	65(60)[c]
2.	DDQ	K_2CO_3	CH_3CN	6 h	50
3.	O_2 (15 psi)	K_2CO_3	CH_3CN	24 h	19
4.	TEMPO	DIPEA	CH_3CN	6 h	58
5.	TEMPO	K_2CO_3	MeOH	24 h	55
6.	TEMPO	K_2CO_3	EtOH	24 h	50
7.	TEMPO	K_2CO_3	THF	24 h	<10
8.	TEMPO	K_2CO_3	toluene	24 h	<10
9.	TEMPO	K_2CO_3	CH_3CN:H_2O (9:1)	8 h	50
10.	TEMPO	K_2CO_3	CH_3CN:H_2O (8:2)	9 h	43
11.	TEMPO	K_2CO_3	CH_3CN:H_2O (7:3)	9 h	46
12.	TEMPO	K_2CO_3	CH_3CN:H_2O (6:4)	12 h	33
13.	TEMPO	K_2CO_3	CH_3CN:H_2O (1:1)	15 h	<10
14.[d]	TEMPO	K_2CO_3	CH_3CN	6 h	80
15.[e]	TEMPO	K_2CO_3	CH_3CN	6 h	65
16.[f]	TEMPO	K_2CO_3	CH_3CN	6 h	63

[a]All reactions were conducted with amine 1 (0.1 mmol, 1.0 equiv.), thioacid 2 (1.0 equiv.), additive (1.0 equiv.), and solvent (1.0 mL, 0.1 M). [b]Yields were calculated by analyzing 1H-NMR of crude sample with 1,3,5-trimethoxybenzene as an internal standard. [c]Isolated yield. [d]1.5 equiv. thioacid was added. [e]Reaction was performed in the dark. [f]Reaction was irradiated with 440 nm blue light.

Substrate scope of this methodology

Synthesis of Z-D-Ala-SH (2b)

Following the literature-known procedure[2], thioacid (**2b**) was synthesized as a viscous liquid.

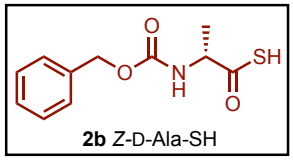

2b Z-D-Ala-SH

^{1}H NMR (500 MHz, $CDCl_3$) δ 7.36 (s, 5H), 5.36 (d, *J* = 8.1 Hz, 1H), 5.14 (s, 2H), 4.49 – 4.34 (m, 1H), 1.41 (d, *J* = 7.3 Hz, 3H).

^{13}C NMR (500 MHz, $CDCl_3$) δ 200.4, 155.7, 136.0, 128.7, 128.5, 128.3, 67.4, 57.7, 18.2.

LRMS: calc. for $C_{11}H_{14}NO_3S$ (M+H): 240.1; found: 240.2.

Scope of amino acid methyl esters

Synthesis of *Z*-L-Ala-L-Ala-OMe (3)

With 1.0 equivalent of thioacid: following the general procedure, L-alanine methyl ester hydrochloride salt (14.0 mg, 100.0 µmol) was coupled with thioacid **2a** (24.0 mg, 100.0 µmol) to afford **3** (20.0 mg, 64.9 µmol, 65% yield) as a white solid.
With 1.5 equivalents of thioacid: following the general procedure, L-alanine methyl ester hydrochloride salt (14.0 mg, 100.0 µmol) was coupled with thioacid **2a** (36.0 mg, 150.0 µmol) to afford **4** (23.6 mg, 80.2 µmol, 80% yield) as a white solid.
R_f = 0.4 (EtOAc: Hexane = 1:1).

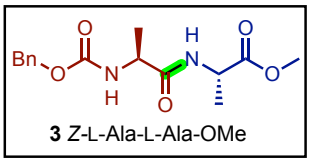

3 *Z*-L-Ala-L-Ala-OMe

Gram Scale synthesis: Following the general procedure, L-alanine methyl ester hydrochloride salt (850 mg, 6.09 mmol) was coupled with thioacid **2a** (1.46 g, 6.09 mmol) to afford **3** (1.31 g, 4.25 mmol, 70% yield) as a white solid.
R_f = 0.4 (EtOAc: Hexane = 1:1).

^{1}H NMR (500 MHz, $CDCl_3$) δ 7.38 – 7.30 (m, 5H), 6.50 (s, 1H), 5.36 – 5.28 (m, 1H), 5.11 (s, 2H), 4.56 (t, *J* = 7.3 Hz, 1H), 4.26 (t, *J* = 7.5 Hz, 1H), 3.75 (s, 3H), 1.39 (d, *J* = 7.1 Hz, 6H).

^{13}C NMR (500 MHz, $CDCl_3$) δ 172.7, 170.3, 156.2, 136.2, 128.7, 128.4, 128.2, 67.2, 52.5, 50.5, 41.3, 18.6. The data are identical to the literature report.[10]

Synthesis of *Z*-L-Ala-Gly-OMe (4)

With 1.0 equivalent of thioacid: following the general procedure, L-glycine methyl ester hydrochloride salt (12.5 mg, 100.0 µmol) was coupled with thioacid **2a** (24.0 mg, 100.0 µmol) to afford **4** (18.5 mg, 62.9 µmol, 63% yield) as a white solid.
With 1.5 equivalents of thioacid: following the general procedure, L-glycine methyl ester hydrochloride salt (12.5 mg, 100.0 µmol) was coupled with thioacid **2a** (35.74 mg, 150.0 µmol) to afford **4** (25 mg, 84.9 µmol, 85% yield) as a white solid.
R_f = 0.4 (EtOAc: Hexane = 1:1).

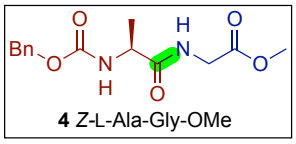

4 *Z*-L-Ala-Gly-OMe

^{1}H NMR (500 MHz, $CDCl_3$) δ 7.38 – 7.28 (m, 5H), 6.70 (s, 1H), 5.42 (d, *J* = 7.7 Hz, 1H), 5.11 (q, *J* = 12.2 Hz, 2H), 4.34 – 4.27 (m, 1H), 4.02 (dd, *J* = 5.6, 2.8 Hz, 2H), 3.74 (s, 3H), 1.40 (d, *J* = 7.1 Hz, 3H).

^{13}C NMR (500 MHz, $CDCl_3$) δ 172.7, 170.3, 156.2, 136.2, 128.7, 128.4, 128.2, 67.2, 52.54, 50.5, 41.3, 18.6. The data are identical to the literature report.[11]

Synthesis of *Z*-L-Ala-D-Ala-OMe (5)

With 1.0 equivalent of thioacid: following the general procedure, D-alanine methyl ester hydrochloride salt (14.0 mg, 100.0 µmol) was coupled with thioacid **2a** (24.0 mg, 100.0 µmol) to afford **5** (18.5 mg, 62.9 µmol, 63% yield) as a white solid.
With 1.5 equivalents of thioacid: following the general procedure, D-alanine methyl ester hydrochloride salt (14.0 mg, 100.0 µmol) was coupled with thioacid **2a** (36.0 mg, 150.0 µmol) to afford **5** (25.4 mg, 82.4 µmol, 82% yield) as a white solid.
R_f = 0.4 (EtOAc: Hexane = 1:1).

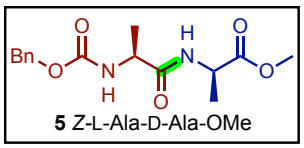

5 *Z*-L-Ala-D-Ala-OMe

^{1}H NMR (500 MHz, $CDCl_3$) δ 7.39 – 7.30 (m, 5H), 6.57 (s, 1H), 5.26 (s, 1H), 5.13 (d, *J* = 3.2 Hz, 2H), 4.56 (p, *J* = 7.3 Hz, 1H), 4.27 (d, *J* = 9.8 Hz, 1H), 3.74 (s, 3H), 1.40 (t, *J* = 6.1 Hz, 6H).

^{13}C NMR (500 MHz, $CDCl_3$) δ 173.3, 171.8, 156.1, 136.2, 128.7, 128.4, 128.3, 67.3, 52.7, 50.6, 48.2, 18.6, 18.4. The data are identical to the literature report.[12]

Synthesis of *Z*-L-Ala-L-Pro-OMe (6)

With 1.0 equivalent of thioacid: following the general procedure, L-proline methyl ester hydrochloride salt (16.6 mg, 100.0 µmol) was coupled with thioacid **2a** (24.0 mg, 100.0 µmol) to afford **6** (22.1 mg, 66.0 µmol, 66% yield) as a yellow oil.

With 1.5 equivalents of thioacid: following the general procedure, L-proline methyl ester hydrochloride salt (16.6 mg, 100.0 µmol) was coupled with thioacid **2a** (38.4 mg, 150.0 µmol) to afford **6** (28.8 mg, 86.2 µmol, 86% yield) as a white solid.

R_f = 0.4 (EtOAc: Hexane = 1:1)

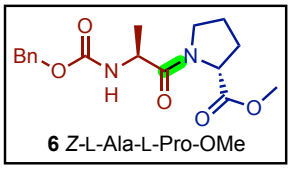

6 *Z*-L-Ala-L-Pro-OMe

^{1}H NMR (500 MHz, $CDCl_3$) δ 7.36 – 7.28 (m, 5H), 5.68 (d, *J* = 8.0 Hz, 1H), 5.12 – 5.04 (m, 2H), 4.52 (dd, *J* = 8.7, 5.0 Hz, 2H), 3.71 (d, *J* = 2.0 Hz, 3H), 3.69 – 3.66 (m, 1H), 3.63 – 3.56 (m, 1H), 2.25 – 2.15 (m, 1H), 2.09 – 1.94 (m, 3H), 1.41 – 1.35 (m, 3H).

^{13}C NMR (500 MHz, $CDCl_3$) δ 172.5, 171.4, 155.8, 136.5, 128.6, 128.2, 128.1, 66.9, 58.8, 52.4, 48.4, 46.9, 29.1, 25.0, 18.5. The data are identical to the literature report.[13]

Synthesis of *Z*-L-Ala-L-Met-OMe (7)

With 1.0 equivalent of thioacid: following the general procedure, L-methionine methyl ester hydrochloride salt (20.0 mg, 100.0 µmol) was coupled with thioacid **2a** (24.0 mg, 100.0 µmol) to afford **7** (21.7 mg, 59.0 µmol, 59% yield) as a white solid.

With 1.5 equivalents of thioacid: following the general procedure, L-methionine methyl ester hydrochloride salt (20.0 mg, 100.0 µmol) was coupled with thioacid **2a** (36.0 mg, 150.0 µmol) to afford **7** (29.2 mg, 79.2 µmol, 79% yield) as a white solid.

R_f = 0.4 (EtOAc: Hexane = 1:1)

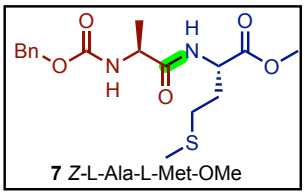

7 *Z*-L-Ala-L-Met-OMe

^{1}H NMR (500 MHz, $CDCl_3$) δ 7.38 – 7.30 (m, 5H), 6.74 – 6.68 (m, 1H), 5.33 (d, *J* = 7.6 Hz, 1H), 5.11 (s, 2H), 4.69 (td, *J* = 7.6, 5.0 Hz, 1H), 4.27 (s, 1H), 3.75 (s, 3H), 2.49 (t, *J* = 7.4 Hz, 2H), 2.17 (dt, *J* = 14.1, 6.8 Hz, 1H), 2.07 (s, 3H), 1.99 (dt, *J* = 14.2, 7.1 Hz, 1H), 1.40 (d, *J* = 7.0 Hz, 3H).

^{13}C NMR (500 MHz, $CDCl_3$) δ 172.3, 172.2, 156.1, 136.2, 128.7, 128.4, 128.2, 52.7, 51.7, 31.5, 30.0, 15.6. The data are identical to the literature report.[14]

Synthesis of *Z*-L-Pro-L-Phe-OMe (8)

With 1.0 equivalent of thioacid: following the general procedure, L-phenylalanine methyl ester hydrochloride salt (21.6 mg, 100.0 µmol) was coupled with thioacid **2d** (26.5 mg, 100.0 µmol) to afford **8** (25.4 mg, 62.0 µmol, 62% yield) as a white
solid.

With 1.5 equivalents of thioacid: following the general procedure, L-phenylalanine methyl ester hydrochloride salt (21.6 mg, 100.0 µmol) was coupled with thioacid **2d** (39.9 mg, 150.0 µmol) to afford **8** (33.3 mg, 81.1 µmol, 81% yield) as a white solid.

R_f = 0.4 (EtOAc: Hexane = 1:1).

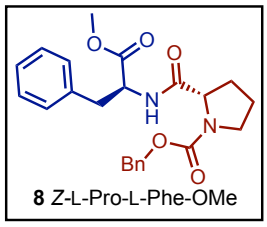

8 *Z*-L-Pro-L-Phe-OMe

^{1}H NMR (500 MHz, $CDCl_3$) δ 7.40 – 7.29 (m, 6H), 7.23 (d, *J* = 7.2 Hz, 3H), 7.09 – 7.01 (m, 2H), 5.20 – 5.05 (m, 2H), 4.84 (d, *J* = 7.1 Hz, 1H), 4.34 (d, *J* = 7.2 Hz, 1H), 3.69 (d, *J* = 36.5 Hz, 3H), 3.49 – 3.30 (m, 2H), 3.22 – 3.08 (m, 1H), 2.99 (dd, *J* = 13.6, 7.2 Hz, 1H), 2.04 (s, 1H), 1.82 (s, 2H), 1.63 (s, 1H).

^{13}C NMR (500 MHz, $CDCl_3$) δ 172.0, 171.7, 171.3, 156.2, 155.1, 136.5, 136.2, 129.4, 129.2, 128.7, 128.5, 128.2, 128.1, 127.3, 127.0, 77.4, 77.2, 76.9, 67.5, 60.9, 60.3, 53.3, 52.8, 52.5, 47.5, 47.0, 38.0, 30.9, 28.0, 24.6, 23.5. The data are identical to the literature report.[15]

Synthesis of *Z*-L-Ala-L-Phe-OMe (9)

Following the general procedure, L-phenylalanine methyl ester hydrochloride salt (21.6 mg, 100.0 µmol) was coupled with thioacid **2a** (24.0 mg, 100.0 µmol) to afford **9** (25.9 mg, 67.3 µmol, 67% yield) as a white solid. R_f = 0.4 (EtOAc: Hexane = 1:1).

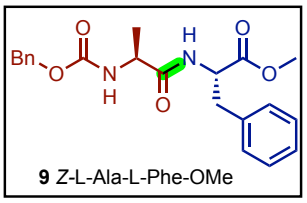

9 *Z*-L-Ala-L-Phe-OMe

^{1}H NMR (500 MHz, $CDCl_3$) δ 7.39 – 7.30 (m, 5H), 7.27 (d, *J* = 6.9 Hz, 1H), 7.26 – 7.21 (m, 2H), 7.08 (d, *J* = 7.1 Hz, 2H), 6.41 (d, *J* = 7.8 Hz, 1H), 5.21 (d, *J* = 7.4 Hz, 1H), 5.11 (t, *J* = 10.8 Hz, 2H), 4.85 (q, *J* = 6.2 Hz, 1H), 4.21 (t, *J* = 7.3 Hz, 1H), 3.73 (s, 3H), 3.19 – 3.04 (m, 2H), 1.34 (d, *J* = 7.0 Hz, 3H)

^{13}C NMR (500 MHz, $CDCl_3$) δ 171.8, 171.8, 136.3, 135.7, 129.4, 128.7, 128.7, 128.4, 128.2, 127.3, 67.2, 53.3, 52.6, 50.5, 37.9. The data are identical to the literature report.[16]

Synthesis of *Z*-L-Ala-L-Trp-OMe (10)

Following the general procedure, L-tryptophan methyl ester hydrochloride salt (25.5 mg, 100.0 µmol) was coupled with thioacid **2** (24.0 mg, 100.0 µmol) to afford **10** (22.8 mg, 53.8 µmol, 54% yield) as a yellowish white solid. R_f = 0.4 (EtOAc: Hexane = 1:1).

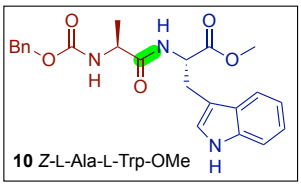

10 *Z*-L-Ala-L-Trp-OMe

^{1}H NMR (500 MHz, $CDCl_3$) δ 8.17 (s, 1H), 7.50 (d, *J* = 7.9 Hz, 1H), 7.33 (dd, *J* = 13.1, 6.8 Hz, 5H), 7.15 (d, *J* = 7.7 Hz, 1H), 7.08 (t, *J* = 7.5 Hz, 1H), 6.93 (s, 1H), 6.63 (d, *J* = 7.9 Hz, 1H), 5.35 (d, *J* = 7.9 Hz, 1H), 5.04 (t, *J* = 14.3 Hz, 2H), 4.93 – 4.85 (m, 1H), 4.25 (t, *J* = 7.4 Hz, 1H), 3.66 (s, 3H), 3.29 (d, *J* = 5.4 Hz, 2H), 1.29 (dd, *J* = 18.6, 7.1 Hz, 4H).

^{13}C NMR (500 MHz, $CDCl_3$) δ 172.2, 172.1, 156, 136.4, 136.2, 128.7, 128.3, 128.2, 127.6, 123.2, 122.3, 119.7, 118.5, 111.5, 109.6, 67.0, 53.0, 52.6, 50.5, 27.6, 18.7. The data are identical to the literature report.[17]

Synthesis of *Z*-L-Ala-L-Leu-OMe (11)

Following the general procedure, L-leucine methyl ester hydrochloride salt (18.2 mg, 100.0 µmol) was coupled with thioacid **2a** (24.0 mg, 100.0 µmol) to afford **11** (18.7 mg, 55.5 µmol, 55% yield) as a yellowish white solid. R_f = 0.4 (EtOAc: Hexane = 1:1).

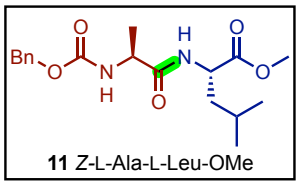

11 *Z*-L-Ala-L-Leu-OMe

^{1}H NMR (500 MHz, $CDCl_3$) δ 7.38 – 7.28 (m, 5H), 6.57 (d, *J* = 8.2 Hz, 1H), 5.47 (d, *J* = 7.8 Hz, 1H), 5.10 (s, 2H), 4.59 (td, *J* = 8.7, 4.6 Hz, 1H), 4.30 (p, *J* = 7.2 Hz, 1H), 3.72 (s, 3H), 1.62 (t, *J* = 4.1 Hz, 2H), 1.53 (t, *J* = 8.5 Hz, 1H), 1.38 (d, *J* = 7.0 Hz, 3H), 0.90 (d, *J* = 6.0 Hz, 6H).

^{13}C NMR (500 MHz, $CDCl_3$) δ 173.3, 172.2, 156.0, 136.3, 128.7, 128.3, 128.1, 67.1, 52.4, 50.8, 50.4, 41.5, 24.9, 22.9, 21.9, 18.7. The data are identical to the literature report.[18]

Synthesis of *Z*-L-Ala-D-Leu-OMe (12)

Following the general procedure, D-leucine methyl ester hydrochloride salt (18.2 mg, 100.0 µmol) was coupled with thioacid **2a** (24.0 mg, 100.0 µmol) to afford **12** (19.3 mg, 57.3 µmol, 57% yield) as a yellowish white solid. R_f = 0.4 (EtOAc: Hexane = 1:1).

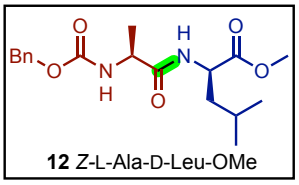

12 *Z*-L-Ala-D-Leu-OMe

^{1}H NMR (400 MHz, $CDCl_3$) δ 7.34 (d, *J* = 4.0 Hz, 5H), 6.72 (d, *J* = 8.3 Hz, 1H), 5.51 (d, *J* = 7.7 Hz, 1H), 5.10 (s, 2H), 4.59 (td, *J* = 8.7, 4.2 Hz, 1H), 4.32 (q, *J* = 7.5 Hz, 1H), 3.69 (s, 3H), 1.58 (dq, *J* = 33.7, 8.6 Hz, 3H), 1.38 (d, *J* = 7.0 Hz, 3H), 0.91 (d, *J* = 5.6 Hz, 6H).

^{13}C NMR (400 MHz, $CDCl_3$) δ 173.4, 172.3, 156.1, 136.3, 128.7, 128.3, 128.1, 77.5, 77.2, 76.8, 67.1, 52.4, 50.8, 50.5, 41.4, 24.9, 22.9, 21.9, 18.8. The data are identical to the literature report.[19]

Synthesis of *Z*-L-Ala-L-Asp-OMe (13)

Following the general procedure, L-Aspartic acid, 1,4-dimethyl ester, hydrochloride salt (20.0 mg, 100.0 µmol) was coupled with thioacid **2a** (24.0 mg, 100.0 µmol) to afford **13** (19.4 mg, 52.9 µmol, 53% yield) as a white solid. R_f = 0.4 (EtOAc: Hexane = 1:1)

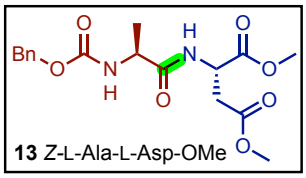

13 *Z*-L-Ala-L-Asp-OMe

^{1}H NMR (500 MHz, $CDCl_3$) δ 7.39 – 7.29 (m, 5H), 6.90 (d, *J* = 8.3 Hz, 1H), 5.43 – 5.35 (m, 1H), 5.11 (s, 2H), 4.84 (dt, *J* = 8.9, 4.4 Hz, 1H), 4.32 – 4.18 (m, 1H), 3.75 (s, 3H), 3.68 (s, 3H), 2.94 (ddd, *J* = 103.3, 17.3, 4.5 Hz, 2H), 1.41 (d, *J* = 7.0 Hz, 3H).

^{13}C NMR (500 MHz, $CDCl_3$) δ 172.2, 171.6, 171.0, 128.7, 128.3, 128.2, 67.1, 53.0, 52.2, 50.6, 48.6, 36.0, 18.9. The data are identical to the literature report. [17]

Synthesis of *Z*-D-Ala-L-Ala-OMe (14)

Following the general procedure, L-alanine methyl ester hydrochloride salt (14.0 mg, 100.0 µmol) was coupled with thioacid **2b** (24.0 mg, 100.0 µmol) to afford **14** (20.7 mg, 67.0 µmol, 67% yield) as a white solid. R_f = 0.4 (EtOAc: Hexane = 1:1)

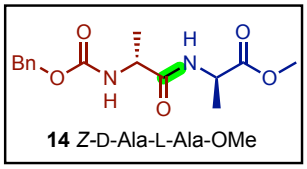

14 Z-D-Ala-L-Ala-OMe

^{1}H NMR (500 MHz, $CDCl_3$) δ 7.37 – 7.29 (m, 5H), 6.76 (s, 1H), 5.46 (t, *J* = 7.7 Hz, 1H), 5.10 (q, *J* = 6.2 Hz, 2H), 4.55 (q, *J* = 6.6 Hz, 1H), 4.29 (q, *J* = 6.8 Hz, 1H), 3.71 (d, *J* = 4.5 Hz, 3H), 1.37 (t, *J* = 6.0 Hz, 6H).

^{13}C NMR (500 MHz, $CDCl_3$) δ 173.4, 172.0, 156.1, 136.3, 128.7, 128.3, 128.2, 67.2, 52.6, 50.5, 48.1, 18.7, 18.3. The data are identical to the literature report.[12]

Synthesis of *Z*-L-Phe-L-Ala-OMe (15)

Following the general procedure, L-alanine methyl ester hydrochloride salt (14.0 mg, 100.0 µmol) was coupled with thioacid **2c** (31.5 mg, 100.0 µmol) to afford **15** (21.9 mg, 57.3 µmol, 57% yield) as a white solid. R_f = 0.4 (EtOAc: Hexane = 1:1).

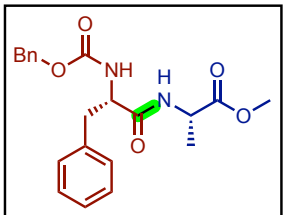

15 *Z*-L-Phe-L-Ala-OMe

^{1}H NMR (500 MHz, $CDCl_3$) δ 7.38 – 7.27 (m, 7H), 7.25 – 7.16 (m, 3H), 6.35 (d, *J* = 7.0 Hz, 1H), 5.42 – 5.24 (m, 1H), 5.08 (s, 2H), 4.47 (dt, *J* = 20.2, 7.3 Hz, 2H), 3.71 (s, 3H), 3.08 (qd, *J* = 13.8, 6.6 Hz, 2H), 1.33 (d, *J* = 7.1 Hz, 3H).

^{13}C NMR (500 MHz, $CDCl_3$) δ 171.8, 171.8, 156.0, 136.3, 135.7, 129.4, 128.7, 128.7, 128.4, 128.2, 127.3, 77.4, 77.2, 76.9, 67.2, 53.3, 52.6, 50.5, 37.9, 18.5. The data are identical to the literature report.[20]

Synthesis of Tripeptides:

Synthesis of *Z*-L-Ala-L-Ala-L-Ala-OMe (16)

Following the general procedure, L-alanine-L-alanine methyl ester (17.2 mg, 100.0 µmol) was coupled with thioacid **2a** (23.9 mg, 100.0 µmol) to afford **16** (23.5 mg, 61.9 µmol, 62% yield) as a white solid. R_f = 0.2 (EtOAc: Hexane = 7:3)

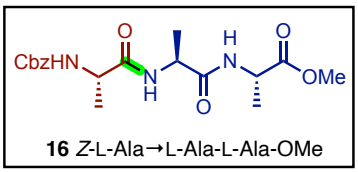

16 *Z*-L-Ala→L-Ala-L-Ala-OMe

^{1}H NMR (500 MHz, $CDCl_3$) δ 7.41 – 7.29 (m, 5H), 6.62 (d, *J* = 7.8 Hz, 2H), 5.31 (d, *J* = 6.8 Hz, 1H), 5.11 (d, *J* = 2.4 Hz, 2H), 4.52 (dq, *J* = 31.6, 7.2 Hz, 2H), 4.29 – 4.16 (m, 1H), 3.75 (s, 3H), 1.39 (q, *J* = 6.4 Hz, 9H)

^{13}C NMR (500 MHz, $CDCl_3$) δ 173.2, 172.2, 171.5, 156.1, 136.2, 128.7, 128.4, 128.3, 77.41, 77.16, 67.3, 52.7, 50.8, 49.0, 48.3, 29.8, 27.7, 18.7, 18.3. The data are identical to the literature report.[21]

Synthesis of *Z*-D-Ala-L-Ala-L-Ala-OMe (17)

Following the general procedure, L-alanine-L-alanine methyl ester (17.2 mg, 100.0 µmol) was coupled with thioacid **2b** (23.9 mg, 100.0 µmol) to afford **17** (17.1 mg, 45.1 µmol, 45% yield) as a white solid. R_f = 0.2 (EtOAc: Hexane = 7:3)

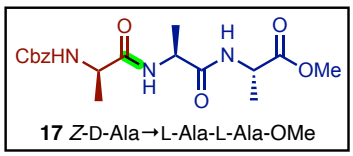

17 *Z*-D-Ala→L-Ala-L-Ala-OMe

^{1}H NMR (500 MHz, $CDCl_3$) δ 7.37 – 7.30 (m, 5H), 6.83 (d, *J* = 7.3 Hz, 1H), 6.71 (d, *J* = 7.7 Hz, 1H), 5.43 (d, *J* = 7.3 Hz, 1H), 5.10 (q, *J* = 12.2 Hz, 2H), 4.57 – 4.48 (m, 2H), 4.27 – 4.19 (m, 1H), 3.72 (s, 3H), 1.38 (d, *J* = 7.0 Hz, 9H).

^{13}C NMR (500 MHz, $CDCl_3$) δ 173.2, 172.3, 171.6, 156.2, 136.2, 128.7, 128.4, 128.3, 67.3, 52.6, 50.8, 48.9, 48.2, 18.6, 18.3, 18.2. The data are identical to the literature report.[22]

Synthesis of *Z*-L-Phe-L-Ala-L-Ala-OMe (18)

Following the general procedure, L-alanine-L-alanine methyl ester (17.4 mg, 100.0 µmol) was coupled with thioacid **2c** (31.3 mg, 100.0 µmol) to afford **18** (26.4 mg, 57.9 µmol, 58% yield) as a white solid. R_f = 0.2 (EtOAc: Hexane = 7:3)

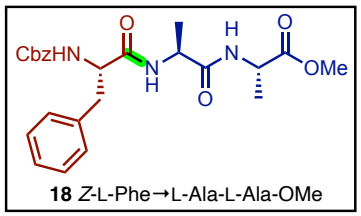

18 *Z*-L-Phe→L-Ala-L-Ala-OMe

^{1}H NMR (500 MHz, $CDCl_3$) δ 7.37 – 7.26 (m, 6H), 7.26 – 7.19 (m, 2H), 7.17 – 7.14 (m, 2H), 6.87 (d, *J* = 7.4 Hz, 1H), 6.68 (d, *J* = 7.5 Hz, 1H), 5.50 (d, *J* = 7.7 Hz, 1H), 5.10 – 5.02 (m, 2H), 4.50 (p, *J* = 7.1 Hz, 3H), 3.72 (s, 3H), 3.07 (d, *J* = 6.7 Hz, 2H), 1.34 (dd, *J* = 24.2, 7.1 Hz, 6H).

^{13}C NMR (500 MHz, $CDCl_3$) δ 173.2, 171.4, 170.9, 129.4, 128.8, 128.7, 128.4, 128.2, 67.2, 52.6, 48.9, 48.2, 18.5, 18.3. The data are identical to the literature report.[15]

Scope of aryl thiocarboxylic acids:

Synthesis of Methyl(4-methoxybenzoyl)-L-alaninate (19)

Following the general procedure, L-alanine methyl ester hydrochloride salt (14.0 mg, 100.0 µmol) was coupled with thioacid **2e** (16.8 mg, 100.0 µmol) to afford **19** (19.0 mg, 80.0 µmol, 80% yield) as a white solid. R_f = 0.2 (EtOAc: Hexane = 3:7)

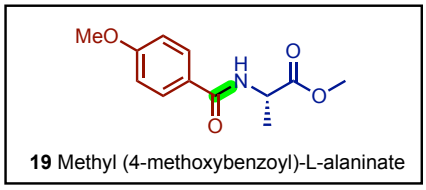

19 Methyl (4-methoxybenzoyl)-L-alaninate

^{1}H NMR (500 MHz, $CDCl_3$) δ 7.81 – 7.73 (m, 2H), 6.96 – 6.89 (m, 2H), 6.65 (d, *J* = 7.3 Hz, 1H), 4.79 (p, *J* = 7.2 Hz, 1H), 3.85 (s, 3H), 3.79 (s, 3H), 1.51 (d, *J* = 7.1 Hz, 3H).

^{13}C NMR (500 MHz, $CDCl_3$) δ 174.0, 166.4, 162.5, 129.0, 126.3, 113.9, 55.5, 52.7, 48.5, 18.9. The data are identical to the literature report.[23]

Synthesis of Methyl benzoyl-L-alaninate (20)

Following the general procedure, L-alanine methyl ester hydrochloride salt (14.0 mg, 100.0 µmol) was coupled with thioacid **2f** (13.8 mg, 100.0 µmol) to afford **20** (15.1 mg, 73.0 µmol, 73% yield) as a white solid. R_f = 0.2 (EtOAc: Hexane = 3:7)

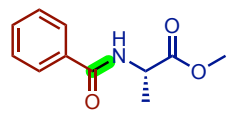

20 Methyl benzoyl-L-alaninate

^{1}H NMR (500 MHz, $CDCl_3$) δ 7.81 (dq, *J* = 7.1, 1.4 Hz, 2H), 7.55 – 7.41 (m, 3H), 6.81 – 6.72 (m, 1H), 4.81 (pd, *J* = 7.2, 1.4 Hz, 1H), 3.79 (d, *J* = 1.4 Hz, 3H), 1.53 (dd, *J* = 7.1, 1.4 Hz, 3H).

^{13}C NMR (500 MHz, $CDCl_3$) δ 173.9, 166.9, 134.0, 131.9, 128.7, 127.2, 52.7, 48.6, 18.8. The data are identical to the literature report.[24]

Synthesis of Methyl(4-bromobenzoyl)-L-alaninate (21)

Following the general procedure, L-alanine methyl ester hydrochloride salt (14.0 mg, 100 µmol) was coupled with thioacid **2g** (21.7 mg, 100 µmol) to afford **21** (20.3 mg, 71.0 µmol, 71% yield) as a white solid. R_f = 0.2 (EtOAc: Hexane = 3:7)

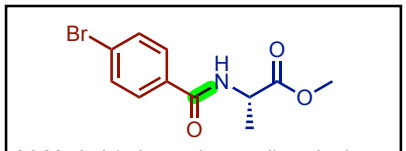

21 Methyl (4-bromobenzoyl)-L-alaninate

^{1}H NMR (500 MHz, $CDCl_3$) δ 7.67 (d, *J* = 8.4 Hz, 2H), 7.60 – 7.55 (m, 2H), 6.74 (d, *J* = 7.3 Hz, 1H), 4.78 (t, *J* = 7.2 Hz, 1H), 3.79 (s, 3H), 1.52 (d, *J* = 7.1 Hz, 3H)

^{13}C NMR (500 MHz, $CDCl_3$) δ 173.7, 165.9, 132.8, 131.9, 128.8, 126.6, 52.8, 48.6, 18.7. The data are identical to the literature report.[25]

Synthesis of Methyl(4-trifluoromethyl)-L-alaninate (22)

Following the general procedure, L-alanine methyl ester hydrochloride salt (14.0 mg, 100.0 µmol) was coupled with thioacid **2h** (20.6 mg, 100.0 µmol) to afford **22** (13.0 mg, 47.2 µmol, 47% yield) as a white solid. R_f = 0.2 (EtOAc: Hexane = 3:7)

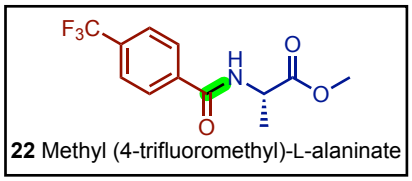

22 Methyl (4-trifluoromethyl)-L-alaninate

^{1}H NMR (500 MHz, $CDCl_3$) δ 7.92 (d, *J* = 7.9 Hz, 2H), 7.71 (d, *J* = 7.9 Hz, 2H), 6.80 (d, *J* = 7.3 Hz, 1H), 4.81 (td, *J* = 7.2, 1.8 Hz, 1H), 3.81 (d, *J* = 1.9 Hz, 3H), 1.54 (dd, *J* = 7.2, 1.9 Hz, 3H).

^{13}C NMR (500 MHz, $CDCl_3$) δ 173.7, 165.6, 127.7, 125.8, 125.8, 125.8, 125.7, 52.9, 48.8, 18.7. The data are identical to the literature report.[26]

Synthesis of Methyl(4-nitrobenzoyl)-L-alaninate (23)

Following the general procedure, L-alanine methyl ester hydrochloride salt (14.0 mg, 100.0 µmol) was coupled with thioacid **2i** (18.3 mg, 100.0 µmol) to afford **23** (9.83 mg, 39.0 µmol, 39% yield) as a yellow solid. R_f = 0.2 (EtOAc: Hexane = 3:7)

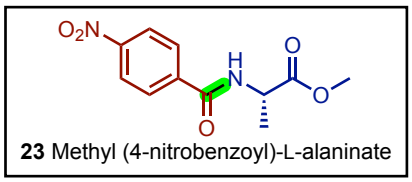

23 Methyl (4-nitrobenzoyl)-L-alaninate

^{1}H NMR (500 MHz, $CDCl_3$) δ 8.30 (dq, *J* = 9.2, 2.6 Hz, 2H), 8.02 – 7.93 (m, 2H), 6.85 (s, 1H), 4.80 (qd, *J* = 7.2, 2.4 Hz, 1H), 3.82 (d, *J* = 2.5 Hz, 3H), 1.56 (dd, *J* = 7.2, 2.3 Hz, 3H).

^{13}C NMR (500 MHz, $CDCl_3$) δ 173.5, 164.9, 139.6, 128.4, 124.0, 53.0, 48.9, 18.7. The data are identical to the literature report.[27]

Mechanistic Studies:

Synthesis of *Z*-L-Ala-NH-Bn (24)

Following the general procedure, benzyl amine (10.7 mg, 100.0 µmol) was coupled with thioacid **2a** (24.0 mg, 100.0 µmol) to afford **24** (26.2 mg, 84.0 µmol, 84% yield) as a white solid. R_f = 0.2 (EtOAc: Hexane = 3:7)

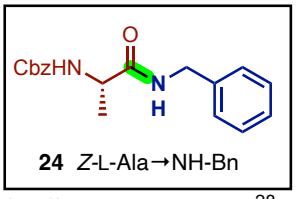

24 *Z*-L-Ala→NH-Bn

^{1}H NMR (500 MHz, $CDCl_3$) δ 7.38 – 7.26 (m, 8H), 7.25 (d, *J* = 9.3 Hz, 2H), 6.37 (s, 1H), 5.31 (s, 1H), 5.08 (d, *J* = 1.9 Hz, 2H), 4.44 (t, *J* = 5.5 Hz, 2H), 4.28 – 4.23 (m, 1H), 1.41 (d, *J* = 7.1 Hz, 3H).

^{13}C NMR (500 MHz, $CDCl_3$) δ 172.2, 156.1, 138.0, 136.2, 128.9, 128.73, 128.4, 128.2, 127.8, 127.7, 67.2, 50.8, 46.0, 43.7, 18.7, 8.7. The data are identical to the literature report.[28]

Synthesis of *Z*-L-Ala-TEMPO (25)

Following the general procedure, TEMPO was coupled with thioacid **2a** (24.0 mg, 100.0 µmol) to afford **25** (29.0 mg, 80.0 µmol, 80% yield) as a white solid. R_f = 0.2 (EtOAc: Hexane = 3:7)

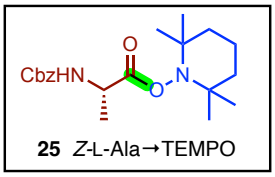

25 *Z*-L-Ala→TEMPO

^{1}H NMR (500 MHz, $CDCl_3$) δ 7.37 – 7.29 (m, 5H), 5.42 (d, *J* = 7.8 Hz, 1H), 5.11 (s, 2H), 4.45 (p, *J* = 7.3 Hz, 1H), 1.66 (p, *J* = 13.2 Hz, 3H), 1.57 – 1.36 (m, 6H), 1.10 (d, *J* = 50.2 Hz, 12H).

^{13}C NMR (500 MHz, $CDCl_3$) δ 172.8, 155.6, 136.4, 128.6, 128.3, 128.2, 67.0, 60.4, 49.0, 39.2, 39.1, 32.0, 31.8, 20.6, 20.5, 19.3, 17.0.

LRMS[16]: calc. for $C_{20}H_{31}N_2O_4$ (M+H): 363.23; found: 363.33

Procedure for the experiments to understand the reactivity of the TEMPO-adduct and diacyl disulfide

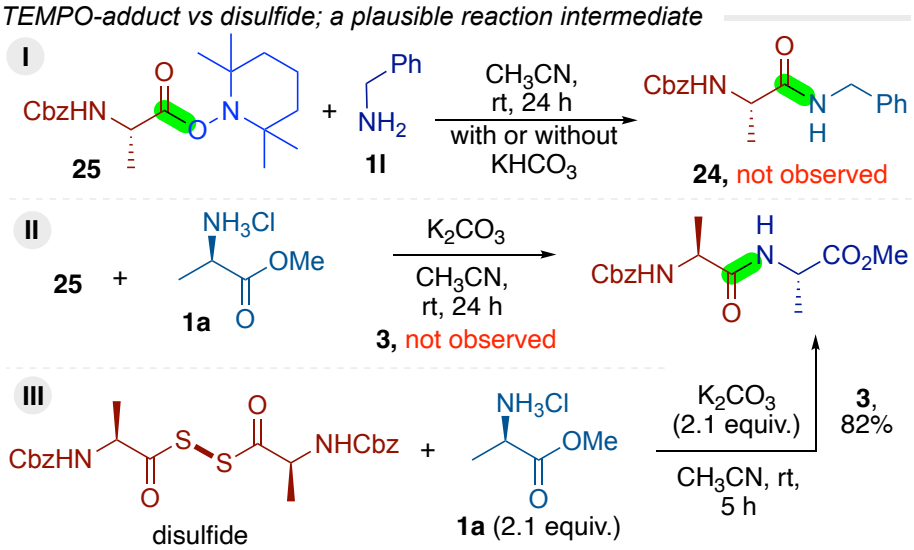

I. In an oven-dried vial charged with a magnetic stir bar, TEMPO-adduct 20 (1.0 equiv.) and benzylamine (1.0 equiv.) were dissolved in CH_3CN. Then, to this solution, $KHCO_3$ (1.0 equiv.) was added, and the reaction was stirred at room temperature for the next 24 hours. After stirring for 24 hours starting material remained unreactive. The ^{1}H-NMR analysis of the crude reaction mixture further confirmed the presence of starting materials.

Note: Reaction was also performed without $KHCO_3$, and the starting materials remained unreactive.

II. In an oven-dried vial charged with a magnetic stir bar, TEMPO-adduct 20 (1.0 equiv.) and L-alanine methyl ester hydrochloride (1.0 equiv.) were dissolved in CH_3CN. Then, to this solution, K_2CO_3 (1.0 equiv.) was added, and the reaction was stirred at room temperature for the next 24 hours. After stirring for 24 hours starting material remained unreactive. The ^{1}H-NMR analysis of the crude reaction mixture further confirmed the presence of starting materials.

III. In an oven-dried vial charged with a magnetic stir bar, L-Alanine diacyl disulfide (1.0 equiv.) and L-alanine methyl ester hydrochloride (2.1 equiv.) were dissolved in CH_3CN. Then, to this solution, K_2CO_3 (2.1 equiv.) was added, and the reaction was stirred at room temperature. The reaction progress was monitored by TLC, after stirring for 5 hours at room temperature, complete consumption of diacyl disulfide was observed. Reaction was diluted by adding ethyl acetate, and the organic layer was washed with brine. The combined organic layers were dried over anhydrous Na_2SO_4, filtered, and evaporated under reduced pressure to afford viscous crude material. The crude material was purified by column chromatography to produce **3** (82%) as a white solid.

Reactivity of nucleophilicity of aliphatic and aromatic amines

Nucleophilicity of TEMPOH, aliphatic, and aromatic amines

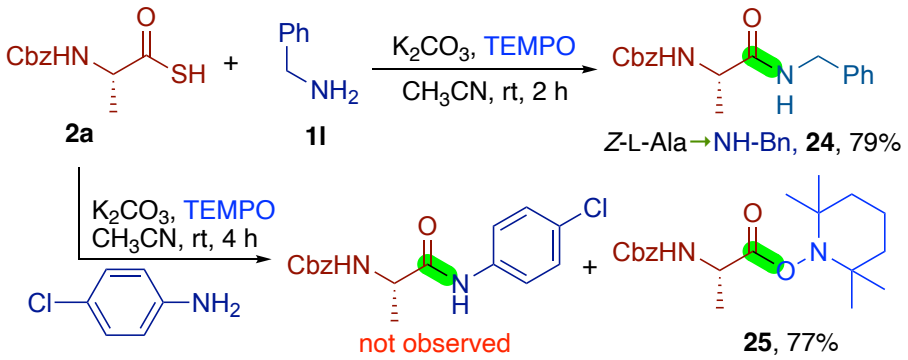

With Aliphatic amine: In an oven-dried vial charged with a magnetic stir bar, L-ala-SH **2a** (1.5 equiv.), benzyl amine (1.0 equiv.), and TEMPO (1.0 equiv.) were dissolved in CH_3CN. Then, to this solution, K_2CO_3 (1.0 equiv.) was added, and the reaction was stirred at room temperature for 2 hours. The reaction progress was monitored by TLC upon complete consumption of both starting materials. Reaction was diluted by adding ethyl acetate, and the organic layer was washed with brine. The combined organic layers were dried over anhydrous Na_2SO_4, filtered, and evaporated under reduced pressure to afford viscous crude material. The crude material was purified by column chromatography to produce **19** (79%) as a white solid.

With Aromatic amine: In an oven-dried vial charged with a magnetic stir bar, L-ala-SH **2a** (1.5 equiv.), 4-chloro aniline (1.0 equiv.), and TEMPO (1.0 equiv.) were dissolved in CH_3CN. Then, to this solution, K_2CO_3 (1.0 equiv.) was added, and the reaction was stirred at room temperature for 4 hours. The reaction progress was monitored by TLC upon complete consumption of both starting materials. Reaction was diluted by adding ethyl acetate, and the organic layer was washed with brine. The combined organic layers were dried over anhydrous Na_2SO_4, filtered, and evaporated under reduced pressure to afford viscous crude material. The crude material was purified by column chromatography to produce exclusively byproduct TEMPO adduct **20** (79%) as a white solid.

Note: This outcome indicates that the in situ formed TEMPOH is more nucleophilic than 4-chloroaniline and shows excellent competitive reactivity with diacyl disulfide. Whereas despite in access 4-chloroanilne did not engage with diacyl disulfide.

Physical Observations of the Reaction Mixtures:

Physical appearance of the reaction mixture was observed to change from bright orange to colorless (Figure S3-A and B). Separately, Thioacid + TEMPO, TEMPO + K_2CO_3, and thioacid + K_2CO_3 combinations were observed. More specifically, in the case of thioacid + TEMPO, a significant color change was observed. While the initial color was bright yellow/orange (Figure S3-C, left vial), after 2 hours bright color faded (Figure S3-D, left vial), and eventually the color disappeared (Figure S3-E, left vial). These color changes strongly suggested the disproportionation of TEMPO under thioacid conditions. More specifically, the oxoammonium ion ($TEMPO^+$) and TEMPOH are formed; this oxoammonium ion further oxidizes thioacid to diacyl disulfide. In the case of the other two combinations, no color change was observed; instead, some turbidity formation was seen.

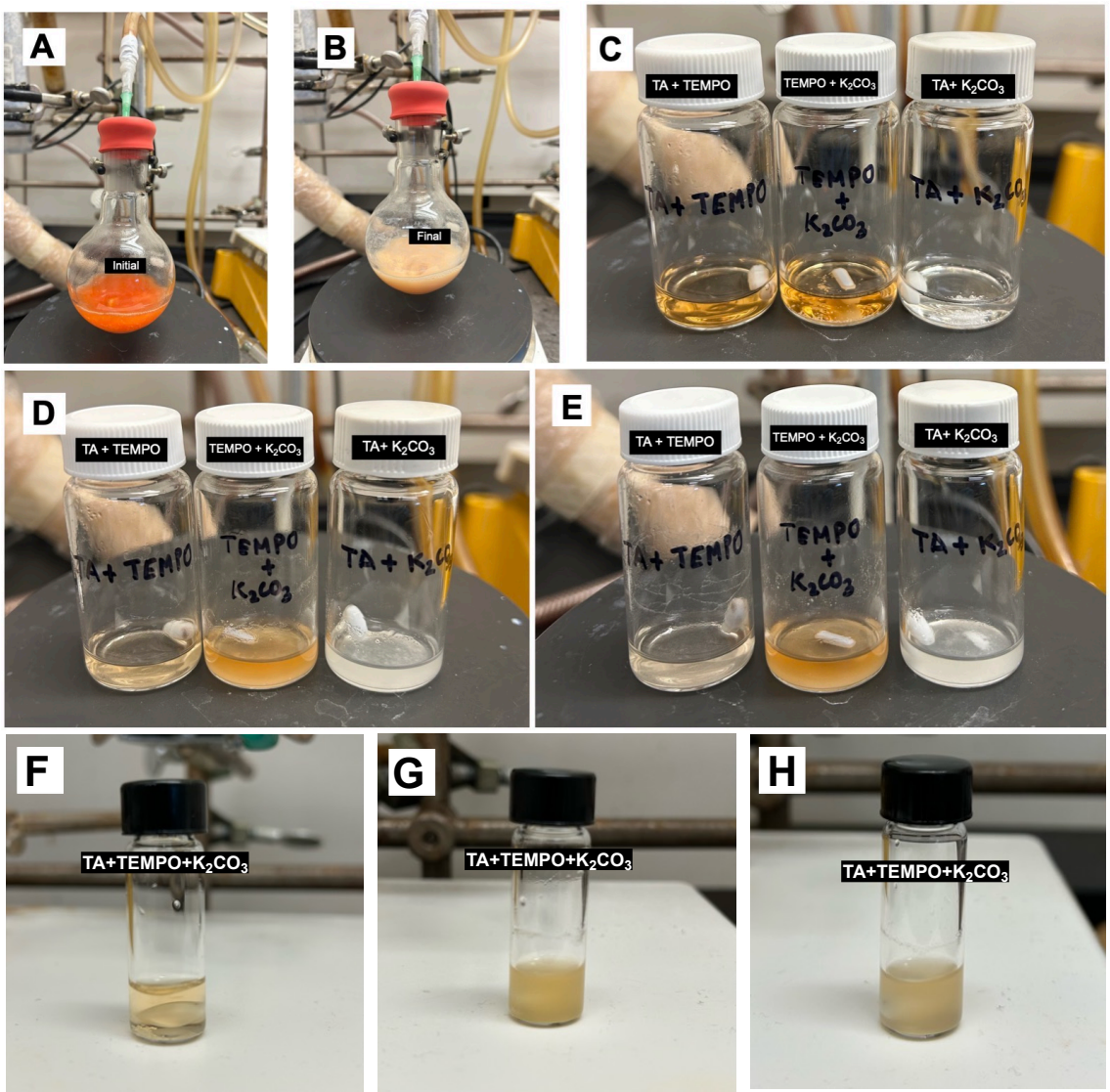

Figure S3: A: Initial color of the reaction mixture (for gram-scale) having thioacid (TA), amino acid hydrochloride, TEMPO, and K_2CO_3 **B:** Final color of the reaction mixture (for gram-scale) having thioacid (TA), amino acid hydrochloride, TEMPO, and K_2CO_3 **C:** Color of the reaction mixtures at t = 0 having TA + TEMPO, TEMPO + K_2CO_3 and TA + K_2CO_3 **D:** Color of the reaction mixtures at t = 120 minutes having TA + TEMPO, TEMPO + K_2CO_3 and TA + K_2CO_3 **E:** Color of the reaction mixtures at t = 240 mins having TA + TEMPO, TEMPO + K_2CO_3 and TA + K_2CO_3 **F:** Color of the reaction mixture at t=0 mins having TA + TEMPO + K_2CO_3 **G:** Color of the reaction mixture at t=180 mins having TA + TEMPO + K_2CO_3 **H:** Color of the reaction mixture at t=360 mins having TA + TEMPO + K_2CO_3.

UV-Visible Studies of the Starting Materials and Reaction Mixtures

Spectra a: Stock solutions (0.1 M) were prepared in acetonitrile for all the starting materials, such as thioacid, thioacid+K_2CO_3, and TEMPO. These solutions were further diluted to 0.01 M before performing UV analysis.

Spectra b: The molarity of reaction mixtures was 0.1M in acetonitrile, and it was diluted to 0.01M before performing UV analysis. In the reaction mixture after 2.5 hours the TEMPO absorbance peak was observed to reduced, confirming the consumption of TEMPO.[29]

Spectra c: A subtracted spectrum for the reaction mixture, final and initial, clearly indicated the appearance of a new absorbance peak at around 420-430 nm which is distinct than the original peak of TEMPO.

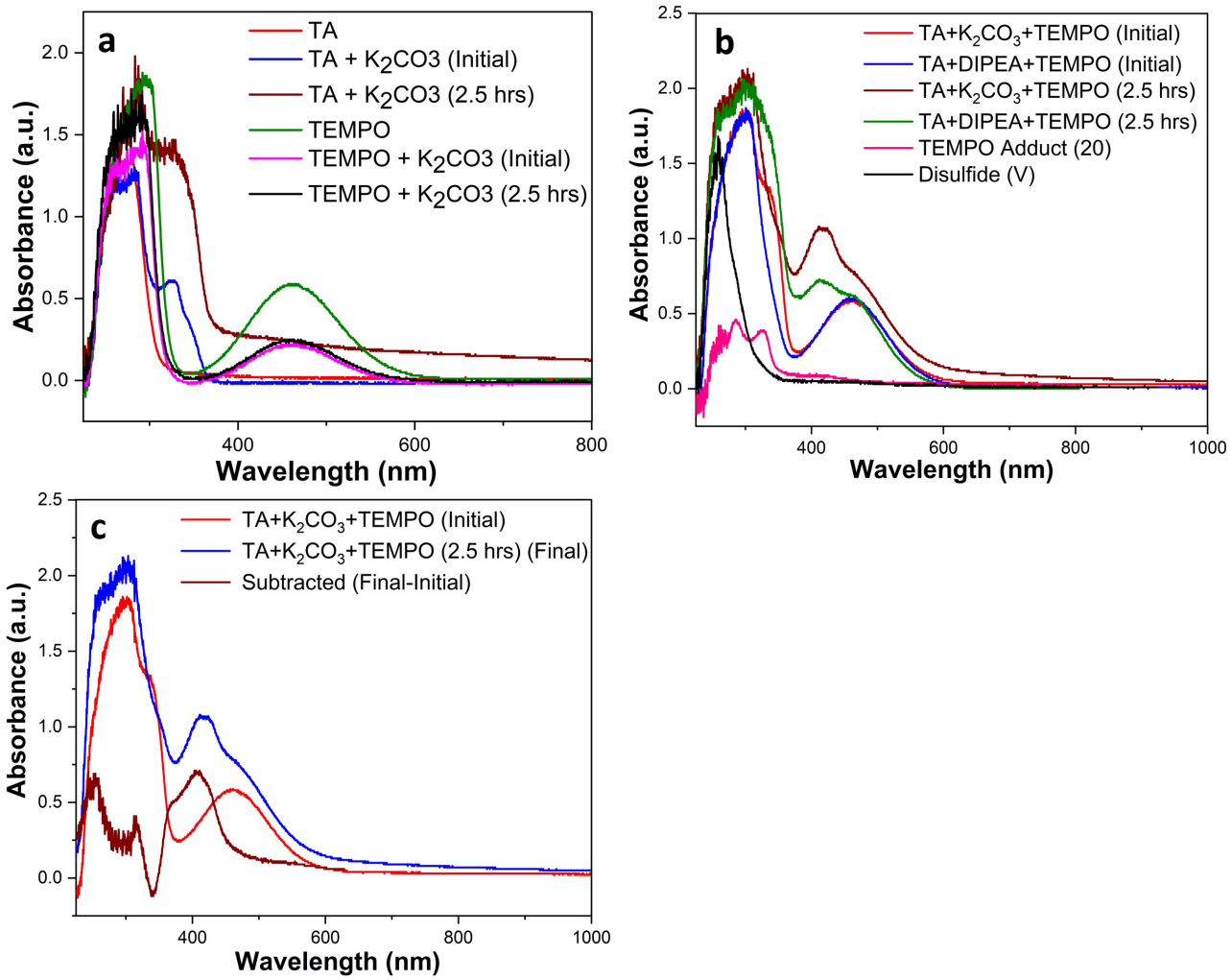

Figure S4: UV-Visible studies. **a)** UV-Visible studies of the starting materials, **b)** UV-Visible studies of the reaction mixture (initial and final), TEMPO-adduct, and diacyl disulfide, **c**) Subtracted spectra of the reaction mixture (final and initial).

Cyclic Voltammetry study for thioacetate and TEMPO

We performed the cyclic voltammetry studies for both thioacetate and the oxidant. The oxidation potential of thioacetate was observed to be 0.246V (vs Ferrocene), and the reduction potential of TEMPO was observed to be -1.37V (vs Ferrocene). Experimentally, the free energy for an outer-sphere electron transfer was found to be +37.4 kcal/mol. These values suggest that this process is non-spontaneous and requires external energy to occur. Hence, the single electron transfer (SET) between thioacetate and TEMPO is highly unlikely and eliminates any possibility of a direct SET process between them. More specifically, it also indicates a reaction pathway highly likely to occur via the formation of a reactive activator, possibly the oxoammonium ion.

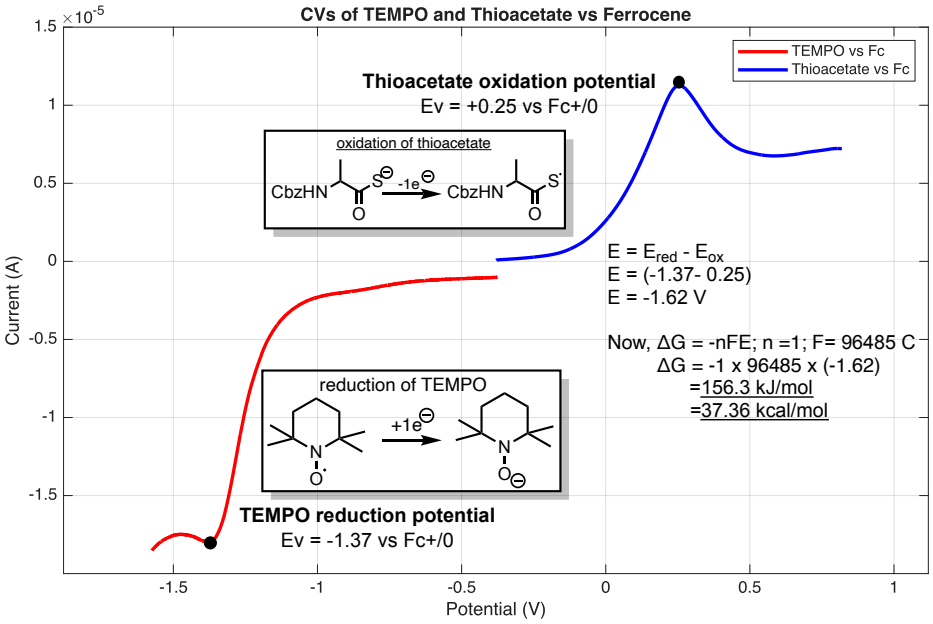

Figure S5. Cyclic voltammetry of thioacetate (oxidation) and TEMPO (reduction).

Plausible, detailed mechanistic pathway(s)

Possibility 1

Based on our mechanistic findings and literature precedents[30-32], we propose the pathway depicted in **Figure S6**. First, under standard reaction conditions, TEMPO disproportionates to $TEMPO^+$ and TEMPOH (Figure S7, SI).[30-32] Then, the sequence begins with base-assisted deprotonation of thioacid **2** to generate thioacetate intermediate **I**. This nucleophile can engage the oxoammonium species ($TEMPO^+$, **II**) through two plausible routes to form the intermediate diacyl disulfide **IV**. In path **I**, thioacetate **I** attacks the nitrogen center of **II**, producing the transient quaternary ammonium intermediate **int-I**. A second thioacetate then attacks at sulfur, releasing $TEMPO^-$ [20] and furnishing diacyl disulfide **IV**. In path **II**, thioacetate **I** attacks the oxygen atom of **II**, generating the oxygen-bound intermediate **int-II**. Subsequent nucleophilic attack by another thioacetate at the sulfur center again affords $TEMPO^-$ [20] and diacyl disulfide **IV**, which then undergoes aminolysis with the amine to yield the peptide product. Notably, $TEMPO^-$ [20] is rapidly protonated to TEMPOH, and TEMPO itself can undergo disproportionation under the reaction conditions.

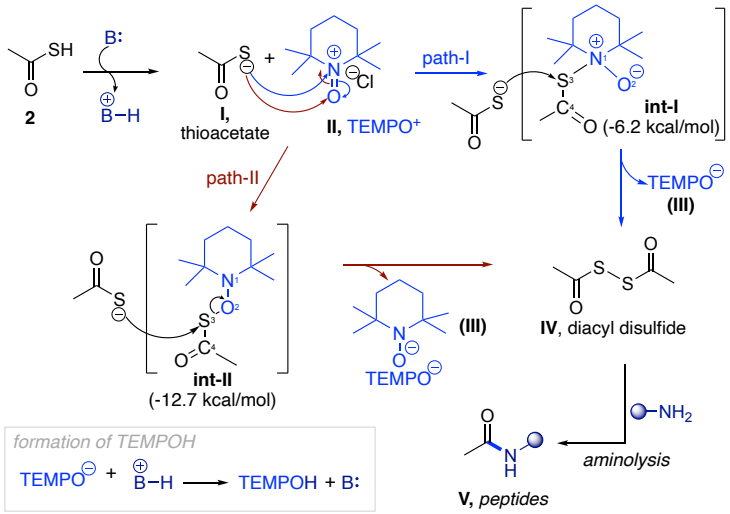

Figure S6. Detailed, Plausible Mechanistic pathway (s) for this transformation via oxoammonium ion.

To further elucidate the mechanistic landscape, we conducted density functional theory (DFT) calculations. The results show that **int-II** is 6.5 kcal/mol more stable than **int-I,** indicating a thermodynamic preference for **path-II**. Next, to understand the site of nucleophilic attack by thioacetate **I**, we evaluated the electrophilicity of all four reactive centers using Fukui functions (**Figure S8**, SI). In both intermediates, the sulfur atom (S^3) was calculated as the most electrophilic site, making it the preferred position for nucleophilic attack. This analysis strongly supports our proposed formation of the diacyl disulfide **IV** as a key mechanistic intermediate.

Possibility 2

After an important suggestion by Reviewer 2 and performing experiments, we proposed another pathway (**Figure S7**). The reaction initiated by the interaction of thioacid **2** and TEMPO leads to the formation of thioketyl radical **II** and TEMPOH **I.** The thioketyl radical **I** further interact with another molecule of TEMPO and forms a transient intermediate **III,** which further fragments into intermediate **IV** and tetramethyl piperidine **V**. Then, the intermediate **IV** reacts with another molecule of thioacid and produces diacyl disulfide **VI**, which, upon aminolysis, forms a peptide and species **VIII,** which can protonate tetramethyl piperidinium salt **IX.**

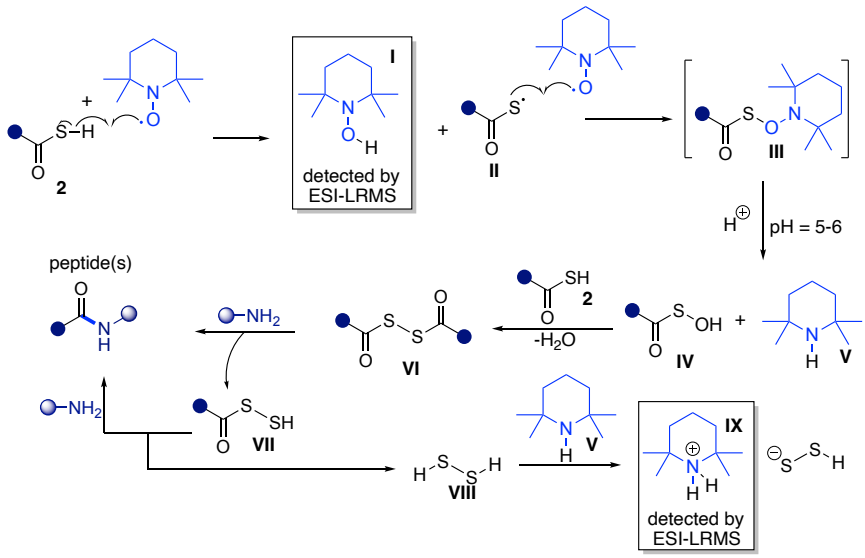

Figure S7. Mechanistic pathway initiated by the formation of thioketyl radical via TEMPO.

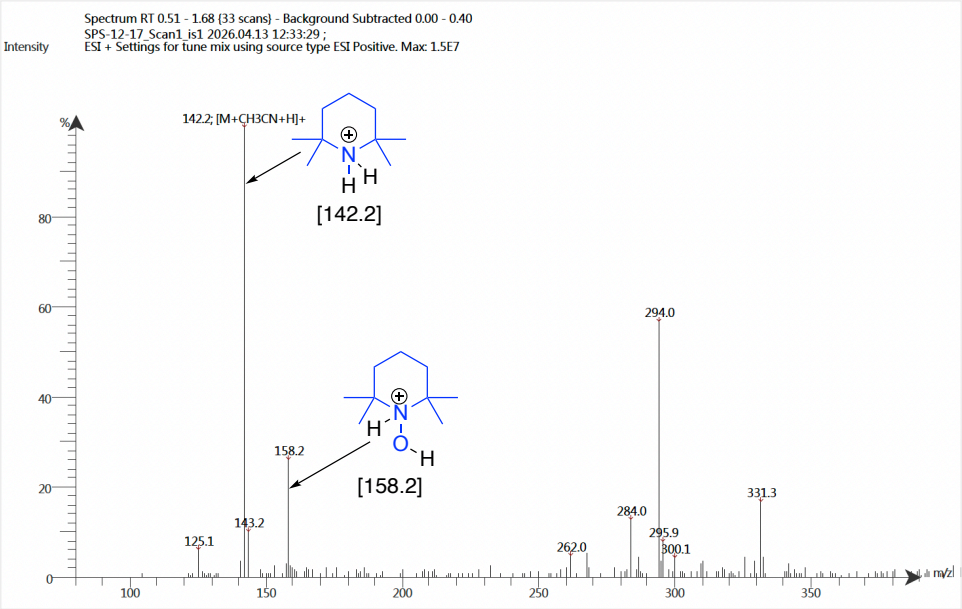

Figure S8. ESI-LRMS analysis of the reaction mixture for the synthesis of **3**.

Thiocarboxylic acid and amine coupling using Bobbitt's salt as a coupling agent.

In an oven-dried vial charged with a magnetic stir bar, L-ala-SH **2a** (1.5 equiv.), L-alanine methyl ester hydrochloride (1.0 equiv.), and Bobbitt's salt (1.0 equiv.) were dissolved in CH_3CN. Then, to this solution, K_2CO_3 (1.0 equiv.) was added, and the reaction was stirred at room temperature for 6 hours. The reaction progress was monitored by TLC upon complete consumption of both starting materials. Reaction was diluted by adding ethyl acetate, and the organic layer was washed with brine. The combined organic layers were dried over anhydrous Na_2SO_4, filtered, and evaporated under reduced pressure to afford viscous crude material. The crude material was purified by column chromatography to produce **3** (54%) as a white solid.

Computational Studies:

All computations were performed using density functional theory (DFT) as implemented in the *Gaussian 16*[33] software package at the 6-31G(d) level of theory with the B3LYP hybrid exchange-correlation functional[34]. This level of theory was chosen due to its relatively high accuracy and low computational cost. Solvent effects were treated implicitly using the PCM solvent model[35] for MeCN. Dispersion was treated using Grimme's D3-BJ[36] dispersion correction. All stationary points were analyzed using Hessian vibrational analysis and confirmed as either intermediates (zero imaginary vibrational frequencies and a zero gradient) or transition states (exactly one physically relevant, imaginary vibrational frequency). See attached txt file for XYZ coordinates, electronic energies, and relevant frequencies of all optimized geometries. All transition states were discovered using relaxed potential energy surface scans. Molecular structures were visualized in the *GaussView* molecular viewer. Thermodynamic parameters were calculated using the FREQ keyword.

Calculation of K_{eq} for TEMPO disproportionation reaction:

It is well known that TEMPO can readily disproportionate under acidic or oxidizing conditions, generating **TEMPO$^+$** and **TEMPO$^-$**. Since our reaction condition is slightly acidic due to the presence of the thioacid, we propose that an equilibrium like that shown in **Figure S6** exists. To probe the equilibrium constant ($\mathbf{K_{eq}}$) for the disproportionation reaction of TEMPO to **TEMPO$^+$** and **TEMPO$^-$**, the Gibbs Free Energy of the respective species **TEMPO**, **TEMPO$^+$,** and **TEMPO$^-$** is calculated by DFT calculations using the above level of theory. Then those values are used in the formula mentioned below:

$\mathbf{K_{eq} = e^{-\Delta G/RT}}$, where **R = 1.9 x 10^{-3} kcal/mol** and **T = 298K**

$\mathbf{\Delta G = \sum G_{Products} - \sum G_{Reactants} = (G_{TEMPO\_Cation} + G_{TEMPO\_Anion}) - 2*G_{TEMPO}}$

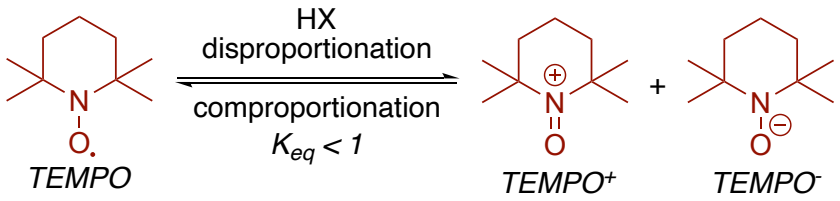

Figure S9: Disproportionation reaction of TEMPO.

Calculation of Fukui Function:

To find out the most electrophilic site on the intermediates (i.e., **int-I** and **int-II**), the electrophilic Fukui function was calculated by the formula:

$f_+ (r) = \rho_{N+1} (r) - \rho_N (r)$

For the above calculations, we considered the ESP charges of the anionic and neutral centers and then subtracted the charge of the neutral center from that of the anionic one. For the next step to occur, the thioacetate anion (i.e., the nucleophile) should attack the most electropositive site of the molecule. The calculation showed that for both intermediates (i.e., **int-I** and **int-II**), the *S*-atom was the most electropositive center, indicating that the second nucleophilic attack occurs at the sulfur center, which in turn produces the disulfide as the product.

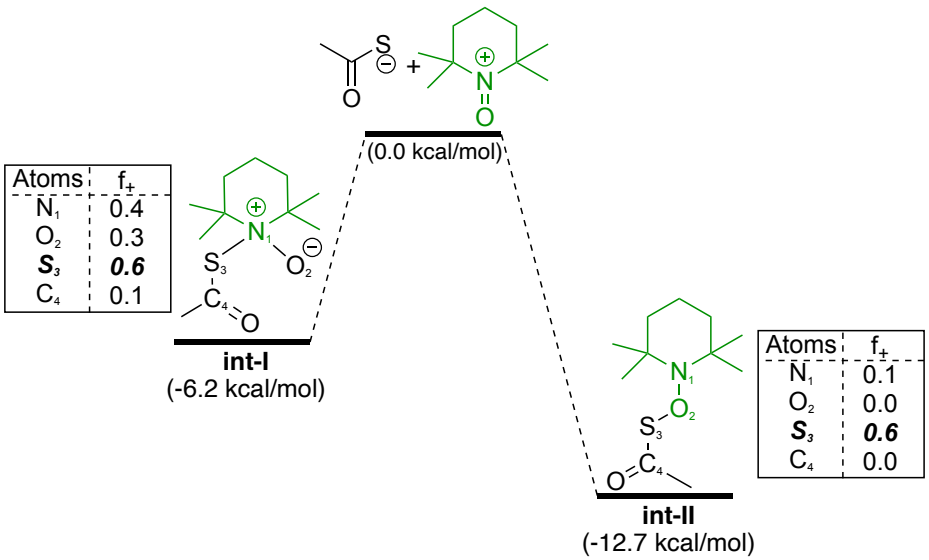

Figure S10: Energy Diagram showing the electrophilic Fukui functions and intermediates.

Transition State Modeling

Relaxed potential energy surface scans were employed to identify the transition state connecting the starting materials (**SM**) and the major intermediate (**int-I**). We were able to identify a transition state (**TS-II**), which was confirmed by the presence of a single imaginary vibrational frequency. Due to the strong electrostatic attraction between the $TEMPO^+$ cation and the thioacetate anion, the exact quantification of this barrier is difficult; however, it is likely to be very small. We have presented the geometry, vibrational frequencies, and electronic energy of this intermediate in a separate text document for completeness. The existence of this intermediate further supports our mechanistic hypothesis.

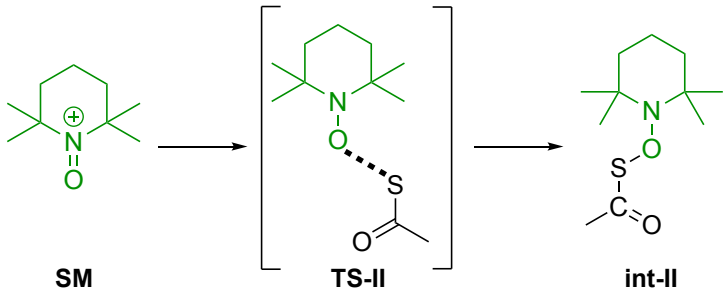

Figure S11: Prediction of the transition state by PES scans.

XYZ coordinates and frequencies of the optimized structures:

All final geometries optimized and frequencies
computed at *DFT B3LYP-B3(BJ) 6-31G(d) PCM(MeCN)* level of theory

****
* Stationary points along the minimum energy pathway *
****

Thioacetate_Anion:
electronic energy: -551.585534 Eh
geometry:

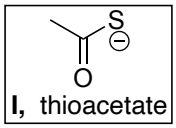

I, thioacetate

-1 1

C	0.37374100	0.21891300	-0.00060000
C	1.32231100	-0.98241200	-0.00019000
H	1.15658200	-1.60012800	0.88909400
H	1.13731700	-1.61894600	-0.87197300
H	2.36152700	-0.63769900	-0.01431100
O	0.85320700	1.35505200	0.00015100
S	-1.35358700	-0.15016500	0.00004500

Frequencies:

Frequencies --	16.2318	360.4980	488.3338
Frequencies --	536.6452	660.4087	954.1980
Frequencies --	1024.1888	1125.9728	1389.3908
Frequencies --	1482.4673	1493.0631	1663.4491
Frequencies --	3049.3834	3122.3614	3130.1108

****

TEMPO^{+}:
electronic energy: -483.591143 Eh
geometry:

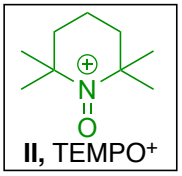

II, TEMPO^{+}

1 1

C	0.00114500	2.15377800	-0.00342300
H	0.41483900	2.80515200	-0.77722400
H	-0.41068000	2.81071500	0.76664300
C	-1.12365800	1.30996500	-0.63581600
H	-0.95510100	1.17664800	-1.70800600
H	-2.08228200	1.82776500	-0.54446100
C	1.12373200	1.31060300	0.63366900
H	0.95279700	1.18024500	1.70582400
H	2.08285100	1.82769300	0.54328000
C	1.33037100	-0.07639800	0.01304100
C	-1.33030300	-0.07589000	-0.01166500
C	-2.32829300	-0.92225600	-0.80439300
H	-2.51154600	-1.88654700	-0.32860100
H	-3.26974200	-0.36946800	-0.84331200
H	-1.97839200	-1.08388200	-1.82772700
C	-1.74585700	-0.00146600	1.48086500
H	-2.72837200	0.47787900	1.50161800
H	-1.82883900	-1.00466300	1.90475300
H	-1.06083100	0.59184400	2.08623700

C	1.75028700	-0.00544000	-1.47816800
H	2.73297000	0.47361900	-1.49760200
H	1.83399400	-1.00954600	-1.89976300
H	1.06683100	0.58677400	-2.08654900
C	2.32399400	-0.92292200	0.81119900
H	2.50618800	-1.88905200	0.33878200
H	3.26669600	-0.37233000	0.85123700
H	1.97068600	-1.08044100	1.83404100
O	-0.00071600	-2.00357900	-0.00531400
N	-0.00069100	-0.80765900	-0.00121700

Frequencies:

Frequencies --	21.1355	130.5190	156.4647
Frequencies --	189.0318	201.1801	232.7792
Frequencies --	258.7081	259.4839	275.2751
Frequencies --	284.8314	340.8604	359.1866
Frequencies --	368.9835	373.5139	397.9614
Frequencies --	451.1833	465.6090	536.8676
Frequencies --	575.6657	701.6855	733.0432
Frequencies --	749.2985	793.6109	843.2744
Frequencies --	887.6549	912.0112	938.1191
Frequencies --	968.9575	973.3766	975.5547
Frequencies --	998.9628	1025.2235	1039.0298
Frequencies --	1087.9851	1113.5215	1128.8674
Frequencies --	1138.7991	1178.9741	1218.5280
Frequencies --	1258.4806	1274.1231	1280.4576
Frequencies --	1282.0119	1314.9280	1393.0014
Frequencies --	1396.3094	1417.3784	1421.2923
Frequencies --	1423.3801	1449.0015	1450.2193
Frequencies --	1489.5591	1494.6415	1504.2202
Frequencies --	1504.4976	1512.0441	1516.2955
Frequencies --	1523.1728	1531.7148	1532.3709
Frequencies --	1536.7597	1542.6370	1717.6302
Frequencies --	3081.4240	3081.7411	3085.7279
Frequencies --	3086.7442	3088.7722	3089.8464
Frequencies --	3096.7129	3119.1555	3128.6101
Frequencies --	3140.6579	3158.7026	3158.9874
Frequencies --	3164.3175	3164.4004	3176.6981
Frequencies --	3176.8596	3189.3168	3190.1525

****

TEMPO$^-$:
electronic energy: -483.836736 Eh
geometry:

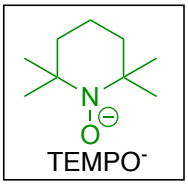

-1 1

C	0.06335000	2.13028300	0.31428200
H	0.05832900	3.20513000	0.08707400
H	0.25404000	2.02928400	1.38859800
C	-1.29105700	1.51111300	-0.04644100
H	-1.57878800	1.86293600	-1.04676800
H	-2.06238400	1.88479500	0.63959100
C	1.15155200	1.41067800	-0.47712500

H	2.12510300	1.90700200	-0.36170900
H	0.89803100	1.47630300	-1.54471400
C	-1.27285200	-0.05135800	-0.03776600
C	1.26659000	-0.07126500	-0.05115000
C	1.71282300	-0.95410800	-1.23260000
H	2.79272400	-0.87971900	-1.41409400
H	1.43998600	-1.97713600	-0.95526800
H	1.19782400	-0.68934300	-2.16177600
C	-1.51017900	-0.63002600	-1.44942300
H	-1.22813300	-1.68674800	-1.40852000
H	-2.56069100	-0.54358200	-1.75906700
H	-0.90004200	-0.12507100	-2.20569000
C	-2.41019600	-0.54649500	0.87198200
H	-3.38359900	-0.19114600	0.50938300
H	-2.40011600	-1.63662400	0.90870500
H	-2.26229000	-0.16766100	1.89112900
C	2.31310800	-0.19939600	1.07319900
H	2.26551800	-1.21710000	1.46998900
H	3.32945200	0.00825300	0.71313900
H	2.08436500	0.49611800	1.89001300
O	-0.01684900	-1.94873600	0.68246600
N	-0.01048000	-0.53748000	0.58721500

Frequencies:

Frequencies --	32.3258	103.8545	201.5889
Frequencies --	217.0742	236.8423	258.4500
Frequencies --	262.5288	301.8318	312.2891
Frequencies --	322.9180	349.5965	372.6824
Frequencies --	380.9591	402.3653	415.6425
Frequencies --	464.8328	480.6812	503.6952
Frequencies --	578.8801	594.9263	663.8719
Frequencies --	775.1677	779.4724	852.9710
Frequencies --	892.0269	917.9234	930.4969
Frequencies --	938.1147	954.5404	982.5179
Frequencies --	987.8088	1001.0104	1036.4275
Frequencies --	1047.2040	1062.7521	1077.0499
Frequencies --	1109.1491	1148.7241	1196.6045
Frequencies --	1229.2368	1239.3609	1255.7274
Frequencies --	1265.5057	1278.3518	1326.6679
Frequencies --	1358.4392	1366.4403	1377.2123
Frequencies --	1382.3371	1390.0697	1395.2298
Frequencies --	1400.0655	1490.8167	1494.8814
Frequencies --	1503.6981	1508.7792	1515.9343
Frequencies --	1520.7734	1521.3867	1524.1748
Frequencies --	1532.2397	1535.0328	1541.5392
Frequencies --	3012.8380	3016.8686	3021.6264
Frequencies --	3023.2569	3029.7830	3031.5949
Frequencies --	3036.3992	3045.9129	3051.2181
Frequencies --	3083.4439	3084.1353	3087.1480
Frequencies --	3088.7689	3100.0281	3121.9426
Frequencies --	3126.0764	3128.8659	3156.9850

****

TEMPO:
electronic energy: -483.773065 Eh
geometry:

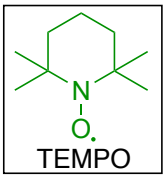

0 2

C	0.00024500	2.15331300	0.00016500
H	0.41875700	2.81098700	-0.76882400
H	-0.41779600	2.81153800	0.76893700
C	-1.11638800	1.30399600	-0.63757100
H	-0.90539100	1.15235900	-1.70182600
H	-2.07241900	1.83666000	-0.58959900
C	1.11638100	1.30352000	0.63805800
H	0.90501500	1.15151800	1.70218100
H	2.07252800	1.83603000	0.59062200
C	1.31242900	-0.08276600	0.00215300
C	-1.31243400	-0.08252200	-0.00221300
C	-2.29997500	-0.89357400	-0.85039100
H	-2.47676800	-1.87811100	-0.41436800
H	-3.25191000	-0.35594700	-0.90666400
H	-1.91659600	-1.02869700	-1.86684500
C	1.83234000	0.01008000	-1.44479300
H	2.84230900	0.43413800	-1.45317500
H	1.87169300	-0.99043800	-1.88665200
H	1.19442600	0.63842400	-2.07176300
C	2.29935700	-0.89441400	0.85044000
H	2.47637500	-1.87869900	0.41394600
H	3.25128600	-0.35687100	0.90762700
H	1.91534300	-1.03012900	1.86657400
C	-1.83163300	0.00954800	1.44503900
H	-2.84166800	0.43343600	1.45404800
H	-1.87065400	-0.99120700	1.88639100
H	-1.19360200	0.63768300	2.07207700
O	-0.00027200	-2.07955700	-0.00035100
N	-0.00009800	-0.79418500	-0.00074400

Frequencies:

Frequencies --	48.9918	121.3039	147.9379
Frequencies --	158.9631	214.0586	219.9413
Frequencies --	255.8550	256.7512	280.3235
Frequencies --	301.1738	325.9700	357.1640
Frequencies --	360.1006	383.3120	385.8251
Frequencies --	462.4682	467.4279	506.5534
Frequencies --	540.0610	596.4674	704.9504
Frequencies --	746.0731	821.0058	837.2822
Frequencies --	886.3122	927.7868	950.9811
Frequencies --	955.3224	986.5244	1002.8158
Frequencies --	1002.8184	1028.9421	1045.1155
Frequencies --	1093.1182	1110.3552	1144.2834
Frequencies --	1168.9825	1216.1850	1217.6062
Frequencies --	1260.0740	1276.7612	1284.6445
Frequencies --	1309.2181	1327.8950	1384.7172
Frequencies --	1393.0639	1408.4481	1417.2947
Frequencies --	1418.7277	1427.5293	1437.5845

Frequencies --	1455.7018	1498.5343	1502.7440
Frequencies --	1508.1957	1509.7343	1513.3605
Frequencies --	1514.2198	1520.7287	1528.5240
Frequencies --	1532.1426	1533.0222	1536.6941
Frequencies --	3055.1273	3057.2144	3058.9643
Frequencies --	3059.1277	3064.3327	3066.0165
Frequencies --	3071.0430	3084.4737	3096.5415
Frequencies --	3108.9335	3127.3269	3127.6055
Frequencies --	3131.3941	3131.8816	3144.1180
Frequencies --	3144.2253	3160.3973	3160.6308

****

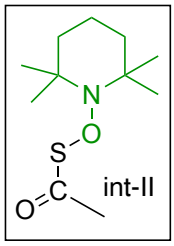

Int-II:
electronic energy: -1035.209098 Eh
geometry:
0 1

C	2.96731700	0.45515800	-1.22327000
H	3.97587200	0.78221800	-1.49970000
H	2.55730200	-0.07203300	-2.09223600
C	3.01942700	-0.49145900	-0.02878800
H	3.39198000	0.05287200	0.84739800
H	3.71953600	-1.31585100	-0.20263200
C	2.09829300	1.67571400	-0.89052000
H	1.77322400	2.15241100	-1.82103700
H	2.69771200	2.41832900	-0.35148900
C	0.84706300	1.35021000	-0.01194000
C	1.62825400	-1.09593900	0.27825300
C	1.54425200	-1.48478500	1.76517200
H	0.60886300	-2.00283800	1.98821000
H	2.37384900	-2.16161600	1.99855200
H	1.62401900	-0.61746500	2.42345700
C	1.05404700	1.80313000	1.44682100
H	1.07448900	2.89775300	1.49033600
H	0.23328400	1.45462900	2.08136300
H	1.99618300	1.44143000	1.86511400
C	1.41327400	-2.35769700	-0.57481100
H	2.13976100	-3.12971400	-0.29889400
H	0.41194900	-2.77116900	-0.41745500
H	1.52867300	-2.13373900	-1.63975400
C	-0.35243000	2.11456100	-0.59170200
H	-1.23283100	2.04594400	0.04926700
H	-0.08932200	3.17376800	-0.68034900
H	-0.60656300	1.73735500	-1.58655500
O	-0.63340200	-0.46191800	0.51903000
N	0.59336000	-0.10783600	-0.17071400
S	-1.81066200	-0.98891100	-0.60144000
C	-3.29289000	-0.09617900	-0.12867100
C	-3.29682200	0.74489700	1.12102100
H	-2.33726400	0.73512300	1.63661000
H	-3.56782800	1.77159000	0.85394500
H	-4.07555700	0.35501300	1.78500300
O	-4.26146900	-0.28086400	-0.84159300

Frequencies:

Frequencies --	45.0992	49.2276	62.9918
Frequencies --	84.9610	93.9487	135.6720
Frequencies --	152.0386	180.2635	209.8163
Frequencies --	231.8973	241.7435	276.1420
Frequencies --	286.0889	292.2970	313.7014
Frequencies --	315.2028	340.6954	355.6437
Frequencies --	360.7550	390.9899	402.4082
Frequencies --	407.4866	425.9713	455.5228
Frequencies --	481.8048	509.9063	520.6729
Frequencies --	561.3986	589.9205	623.7840
Frequencies --	651.6981	760.2875	794.5660
Frequencies --	800.8615	852.0014	893.2059
Frequencies --	920.3141	927.1507	942.5259
Frequencies --	948.0430	987.0976	991.1137
Frequencies --	1001.6612	1013.2354	1028.9482
Frequencies --	1031.3530	1057.2474	1075.5578
Frequencies --	1091.4408	1126.3968	1142.4214
Frequencies --	1170.5941	1220.7496	1229.2906
Frequencies --	1250.0177	1272.1729	1276.7093
Frequencies --	1291.4715	1338.4481	1385.0899
Frequencies --	1390.6151	1402.9254	1406.3996
Frequencies --	1419.1750	1422.5776	1437.3354
Frequencies --	1440.7993	1486.0458	1499.6341
Frequencies --	1502.9603	1508.7933	1511.6296
Frequencies --	1513.0927	1517.8720	1520.5459
Frequencies --	1527.6839	1529.4719	1533.8523
Frequencies --	1537.3165	1539.6397	1754.0591
Frequencies --	3050.5479	3052.5621	3055.4573
Frequencies --	3057.7223	3059.7832	3067.6369
Frequencies --	3069.7439	3071.0644	3087.3588
Frequencies --	3092.6514	3103.1064	3122.3236
Frequencies --	3122.9049	3131.5067	3132.9994
Frequencies --	3135.6389	3135.8963	3146.4018
Frequencies --	3164.3159	3168.3163	3191.1432

****

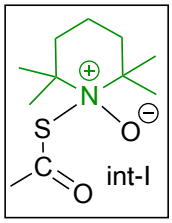

Int-I:
electronic energy: -1035.200876 Eh
geometry:
0 1

C	2.79555500	0.34682500	-1.41948000
H	3.75458800	0.60145700	-1.88362000
H	2.20600600	-0.17642500	-2.18153700
C	3.00472900	-0.56299900	-0.21329900
H	3.50642800	0.00080600	0.58338100
H	3.65548500	-1.40998500	-0.45410800
C	2.07982600	1.62864200	-0.98526500
H	1.70530000	2.15608500	-1.86844000
H	2.80511600	2.29757600	-0.50828400
C	0.90518500	1.39808800	0.01722900
C	1.66333100	-1.12176000	0.30217300
C	1.78260000	-1.54581900	1.77567800
H	0.83327900	-1.94774300	2.13991800

H	2.54913600	-2.32179600	1.87709300
H	2.06745500	-0.69870800	2.40655800
C	1.24583800	1.97160700	1.40785400
H	1.36640500	3.05896300	1.34697300
H	0.44174100	1.75043400	2.11734700
H	2.17840700	1.55212700	1.79648200
C	1.23923600	-2.33489200	-0.54469100
H	1.98783300	-3.12742400	-0.44667800
H	0.28066000	-2.73596100	-0.20515400
H	1.14890500	-2.07172700	-1.60287900
C	-0.34908700	2.09984800	-0.52052600
H	-1.18463700	2.04256300	0.17905900
H	-0.10989800	3.15642600	-0.67597700
H	-0.65879000	1.67237300	-1.47803400
O	-0.54429900	-0.38636800	0.65325800
N	0.63192400	-0.06151500	0.14356800
S	-1.88361100	-0.97889800	-0.66578400
C	-3.34393400	-0.09929300	-0.12922900
C	-3.32683100	0.57979000	1.21911000
H	-2.33220400	0.60714400	1.66383200
H	-3.72288300	1.59412500	1.10860000
H	-4.00160200	0.02686700	1.88278900
O	-4.32334000	-0.12543600	-0.85414300

Frequencies:

Frequencies --	42.1255	53.3794	90.0131
Frequencies --	116.2569	123.5762	131.4734
Frequencies --	163.9442	184.9668	210.8558
Frequencies --	235.9800	274.7024	275.0972
Frequencies --	287.6807	297.5337	304.2990
Frequencies --	330.9609	338.2362	352.2351
Frequencies --	371.4044	381.8101	392.4388
Frequencies --	413.2221	429.5378	457.0995
Frequencies --	466.7216	498.6592	517.4666
Frequencies --	539.6072	553.1947	605.3170
Frequencies --	635.8888	705.5727	771.5087
Frequencies --	810.7292	855.7717	889.6945
Frequencies --	895.3144	949.9921	964.1917
Frequencies --	969.6129	972.9759	990.3445
Frequencies --	997.4695	1026.6075	1040.0886
Frequencies --	1045.5559	1062.6893	1094.1957
Frequencies --	1137.7055	1142.9209	1146.6195
Frequencies --	1188.8972	1235.3013	1244.2704
Frequencies --	1246.8263	1262.5165	1302.1464
Frequencies --	1338.9541	1375.7287	1379.9507
Frequencies --	1383.7695	1408.8293	1412.6933
Frequencies --	1422.4093	1433.5815	1443.5967
Frequencies --	1450.0617	1481.6735	1495.4497
Frequencies --	1503.9325	1506.9840	1509.8815
Frequencies --	1510.9486	1517.3815	1517.9058
Frequencies --	1525.0430	1528.3942	1531.4793
Frequencies --	1540.2169	1546.6507	1728.6702
Frequencies --	3055.0567	3065.5816	3068.9450
Frequencies --	3071.8452	3074.3802	3075.8492
Frequencies --	3078.6022	3083.4390	3102.7237

Frequencies --	3109.9639	3123.2262	3126.9717
Frequencies --	3140.2691	3142.5871	3146.1452
Frequencies --	3152.6494	3157.8563	3168.7006
Frequencies --	3177.6593	3177.9649	3200.6971

****

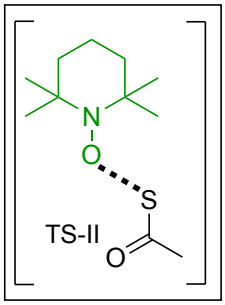

TS-II:
electronic energy: -1035.202110 Eh
geometry:
0 1

C	2.64579400	0.29154800	-1.55504700
H	3.56294400	0.54313900	-2.09808000
H	2.02313300	-0.28722700	-2.24695900
C	2.96438900	-0.55692500	-0.32759900
H	3.52458900	0.04182200	0.40047800
H	3.60281600	-1.40794200	-0.58592600
C	1.91764000	1.57887300	-1.14943100
H	1.38913200	1.98436000	-2.01825700
H	2.65265600	2.33503000	-0.85208500
C	0.91179900	1.40651500	0.03020400
C	1.67656000	-1.10853400	0.31580200
C	1.92489200	-1.52339700	1.77580300
H	1.00235800	-1.89782900	2.22863600
H	2.67785100	-2.31799200	1.81409900
H	2.28663000	-0.67774900	2.36800800
C	1.47841600	2.00915600	1.33421100
H	1.61375400	3.08972400	1.21489800
H	0.78477700	1.83346000	2.16279800
H	2.44805800	1.57689000	1.59510300
C	1.17137000	-2.32598000	-0.47868300
H	1.93892900	-3.10559000	-0.46088900
H	0.26256200	-2.73786300	-0.03394200
H	0.96200200	-2.07190000	-1.52175400
C	-0.39518100	2.12794200	-0.31657100
H	-1.10743100	2.10716100	0.51009000
H	-0.15432900	3.17335400	-0.53269500
H	-0.86576300	1.69505600	-1.20238400
O	-0.53409400	-0.38111500	0.72486000
N	0.64065000	-0.04056200	0.27465200
S	-1.86748200	-0.98455800	-0.65070300
C	-3.33625700	-0.10903500	-0.13787100
C	-3.35434400	0.53149700	1.23103300
H	-2.37844500	0.51920000	1.71586800
H	-3.71607400	1.56018700	1.13475800
H	-4.07186600	-0.01822100	1.85103300
O	-4.30010600	-0.09765600	-0.88551200

Frequencies:

Frequencies --	-220.1416	28.3000	36.7365
Frequencies --	42.5391	58.6421	77.7138

Frequencies --	116.0652	138.7477	147.2148
Frequencies --	224.7202	243.3615	262.5306
Frequencies --	282.6589	291.6156	310.5078
Frequencies --	322.7378	326.1515	331.6611
Frequencies --	356.3506	371.3090	396.7514
Frequencies --	407.5920	417.2528	431.6702
Frequencies --	448.6633	482.1354	525.5701
Frequencies --	532.9155	580.8777	593.0582
Frequencies --	627.4336	663.0854	802.6274
Frequencies --	812.9552	860.4620	899.6197
Frequencies --	929.8393	941.6825	947.0401
Frequencies --	983.6259	991.2543	999.8520
Frequencies --	1012.8442	1031.1761	1035.4317
Frequencies --	1052.6816	1090.8177	1095.2411
Frequencies --	1117.1003	1130.8965	1167.2229
Frequencies --	1172.7200	1214.0132	1228.6615
Frequencies --	1252.8945	1270.0492	1285.7340
Frequencies --	1298.3783	1341.6908	1386.2036
Frequencies --	1394.7023	1403.6871	1408.1641
Frequencies --	1417.8236	1421.1802	1437.2220
Frequencies --	1441.4357	1485.9140	1501.2279
Frequencies --	1502.2367	1508.0138	1510.7615
Frequencies --	1512.9219	1516.7946	1519.3097
Frequencies --	1525.2248	1528.6812	1531.8205
Frequencies --	1535.6643	1536.9684	1736.5308
Frequencies --	3047.7985	3052.5046	3055.3229
Frequencies --	3058.5362	3060.0871	3066.1057
Frequencies --	3066.1212	3072.9480	3090.7326
Frequencies --	3097.2907	3103.4116	3122.6935
Frequencies --	3128.8982	3131.9704	3133.9502
Frequencies --	3135.3277	3139.3403	3142.4384
Frequencies --	3145.4380	3166.7523	3184.2304

****

References:

(1) Elagawany, M.; Hegazy, L.; Elgendy, B. Catalyst- and organic solvent-free synthesis of thioacids in water. *Tetrahedron Letters* **2019**, *60* (30), 2018-2021.

(2) Khaybullin, R.; Panda, S. S.; Al-Youbi, A. O.; Katritzky, A. R. A Facile Synthesis of Thioacids from N-Acylbenzotriazoles. *Synlett* **2014**, *25* (02), 247-250.

(3) Madhu, C.; Vishwanatha, T.; Sureshbabu, V. V. An efficient synthesis of Nα-protected amino and peptide acid aryl amides via iodine-mediated oxidative acylation of Nα-protected amino and peptide thioacids. *Synthesis* **2013**, *45* (19), 2727-2736.

(4) Madhu, C.; Basavaprabhu; Vishwanatha, T. M.; Sureshbabu, V. V. T3P (propylphosphonic anhydride) mediated conversion of Nα-protected amino/peptide acids into thioacids. *Tetrahedron Lett.* **2012**, *53* (11), 1406-1409.

(5) Smedley, C. J.; Li, G.; Barrow, A. S.; Gialelis, T. L.; Giel, M. C.; Ottonello, A.; Cheng, Y.; Kitamura, S.; Wolan, D. W.; Sharpless, K. B. Diversity oriented clicking (DOC): divergent synthesis of SuFExable pharmacophores from 2-substituted-alkynyl-1-sulfonyl fluoride (SASF) hubs. *Angewandte Chemie* **2020**, *132* (30), 12560-12569.

(6) Murai, T.; Asai, F. Three-Component Coupling Reactions of Thioformamides with Organolithium and Grignard Reagents Leading to Formation of Tertiary Amines and a Thiolating Agent. *J. Am. Chem. Soc.* **2007**, *129* (4), 780-781.

(7) Zhao, B.; Liu, Y.-X.; Liang, P.-P.; Hu, G.-Q.; Liu, J.-H. S-Arylation of Thioic S-Acid Using Thianthrenium Salts via Photoactivation of Electron Donor–Acceptor Complex. *J. Org. Chem.* **2024**, *89* (17), 12508-12513.

(8) Elagawany, M.; Hegazy, L.; Elgendy, B. Catalyst- and organic solvent-free synthesis of thioacids in water. *Tet. Lett.* **2019**, *60* (30), 2018-2021.

(9) Fu, Z.; Rong, B.; Huang, L. Pd-Catalyzed Coupling of Aryl Chloride, Isocyanides, and Thiocarboxylate To Synthesize Thioamides. *Org. Lett.* **2025**, *27* (11), 2782-2787.

(10) Chen, H.; Xu, X.; Liu, L. L.; Tang, G.; Zhao, Y. Phosphorus oxychloride as an efficient coupling reagent for the synthesis of esters , amides and peptides under mild conditions. *RSC Adv.* **2013**, *3* (37), 16247-16250.

(11) Kokare, N.; Nagawade, R.; Rane, V.; Shinde, D. B. Design, synthesis and utilization of 1-substituted sulphonyloxy-2-phenyl benzimidazole as a novel peptide coupling reagents. *Protein Pept. Lett.* **2007**, *14* (3), 259-263.

(12) Hill, R. R.; Birch, D.; Jeffs, G. E.; North, M. Enantioselection in peptide bond formation. *Org. Biomol. Chem.* **2003**, *1* (6), 965-972.

(13) Baxendale, I. R.; Ley, S. V.; Smith, C. D.; Tranmer, G. K. A flow reactor process for the synthesis of peptides utilizing immobilized reagents, scavengers and catch and release protocols. *Chem. Comm.* **2006**, (46), 4835-4837, 10.1039/B612197G.

(14) Hoogwater, D. A.; Peereboom, M. Kinetics of the alkaline hydrolysis of several n-benzyloxycarbonyldipeptide methyl and ethyl esters. *Tetrahedron* **1990**, *46* (15), 5325-5332.

(15) Kon, K.; Kohari, Y.; Murata, M. Unnatural tripeptide as highly enantioselective organocatalyst for asymmetric aldol reaction of isatins. *Tet. Lett.* **2019**, *60* (5), 415-418.

(16) Fraczyk, J.; Kaminski, Z. J.; Katarzynska, J.; Kolesinska, B. 4-(4, 6-Dimethoxy-1, 3, 5-triazin-2-yl)-4-methylmorpholinium Toluene-4-sulfonate (DMT/NMM/TsO−) Universal Coupling Reagent for Synthesis in Solution. *Helv. Chim. Acta* **2018**, *101* (1), e1700187.

(17) Chen, H.; He, M.; Wang, Y.; Zhai, L.; Cui, Y.; Li, Y.; Li, Y.; Zhou, H.; Hong, X.; Deng, Z. Metal-free direct amidation of peptidyl thiol esters with α-amino acid esters. *Green Chem.* **2011**, *13* (10), 2723-2726.

(18) Nuijens, T.; Cusan, C.; van Dooren, T. J.; Moody, H. M.; Merkx, R.; Kruijtzer, J. A.; Rijkers, D. T.; Liskamp, R. M.; Quaedflieg, P. J. Fully enzymatic peptide synthesis using C-terminal tert-butyl ester interconversion. *Adv. Synth. Catal.* **2010**, *352* (14-15), 2399-2404.

(19) Vescovi, A.; Knoll, A.; Koert, U. Synthesis and functional studies of THF–gramicidin hybrid ion channels. *Org. Biomol. Chem.* **2003**, *1* (16), 2983-2997.
(20) Camacho, L. A., III; Lampkin, B. J.; VanVeller, B. A Bottom-Up Approach To Preserve Thioamide Residue Stereochemistry during Fmoc Solid-Phase Peptide Synthesis. *Org. Lett.* **2019**, *21* (17), 7015-7018.
(21) Markowicz, M. W.; Dembinski, R. Fluorous coupling reagents: application of 2-chloro-4, 6-bis [(heptadecafluorononyl) oxy]-1, 3, 5-triazine in peptide synthesis. *Synthesis* **2004**, *2004* (01), 80-86.
(22) OKADA, Y.; OKINAKA, M.; YAGYU, M.; WATABE, K.; SANo, K.; KAKIUCHI, Y. Amino acids and peptides. II. Synthesis of stereoisomeric alanine containing peptide derivatives and their effects on germination of Bacillus thiaminolyticus spores. *Chem. Pharm. Bull.* **1976**, *24* (12), 3081-3084.
(23) Xie, M.-S.; Huang, B.; Li, N.; Tian, Y.; Wu, X.-X.; Deng, Y.; Qu, G.-R.; Guo, H.-M. Rational Design of 2-Substituted DMAP-N-oxides as Acyl Transfer Catalysts: Dynamic Kinetic Resolution of Azlactones. *J. Am. Chem. Soc.* **2020**, *142* (45), 19226-19238.
(24) Jaganathan, A.; Staples, R. J.; Borhan, B. Kinetic Resolution of Unsaturated Amides in a Chlorocyclization Reaction: Concomitant Enantiomer Differentiation and Face Selective Alkene Chlorination by a Single Catalyst. *J. Am. Chem. Soc.* **2013**, *135* (39), 14806-14813.
(25) Tian, X.; Kaur, J.; Yakubov, S.; Barham, J. P. α-Amino Radical Halogen Atom Transfer Agents for Metallaphotoredox-Catalyzed Cross-Electrophile Couplings of Distinct Organic Halides. *ChemSusChem* **2022**, *15* (15), e202200906.
(26) Tallon, S.; Manoni, F.; Connon, S. J. A Practical Aryl Unit for Azlactone Dynamic Kinetic Resolution: Orthogonally Protected Products and A Ligation-Inspired Coupling Process. *Angew. Chem.* **2015**, *127* (3), 827-831.
(27) Mahesh, M.; Veladi, P.; Girish, P.; Roopesh, K. L.; Venkata, R. P.; and Sureshbabu, V. V. Oxidative amidation of benzyl alcohols with amino acid esters mediated by N-hydroxysuccinimide/phenyliodine diacetate. *Synth. Commun.* **2017**, *47* (7), 716-721.
(28) Saito, Y.; Ouchi, H.; Takahata, H. Carboxamidation of carboxylic acids with 1-tert-butoxy-2-tert-butoxycarbonyl-1,2-dihydroisoquinoline (BBDI) without bases. *Tetrahedron* **2008**, *64* (49), 11129-11135.
(29) Zhao, X.; Yang, J.-D.; Cheng, J.-P. Revisiting the Electrochemistry of TEMPOH Analogues in Acetonitrile. *J. Org. Chem.* **2023**, *88* (1), 540-547.
(30) Golubev, V.; Rozantsev, E.; Neiman, M. Some reactions of free iminoxyl radicals with the participation of the unpaired electron. *Bull. Acad. Sci. USSR, Div. Chem. Sci.* **1965**, *14* (11), 1898-1904.
(31) Maeda, H.; Wu, H.-Y.; Yamauchi, Y.; Ohmori, H. Important Role of the 3-Mercaptopropionamide Moiety in Glutathione: Promoting Effect on Decomposition of the Adduct of Glutathione with the Oxoammonium Ion of TEMPO. *J. Org. Chem.* **2005**, *70* (21), 8338-8343.
(32) Weierbach, S. M.; Reynolds, R. P.; Stephens, S. M.; Vlasakakis, K. V.; Ritter, R. T.; White, O. M.; Patel, N. H.; Hayes, E. C.; Dunmire, S.; Lambert, K. M. Chemoselective Oxidation of Thiols with Oxoammonium Cations. *J. Org. Chem.* **2023**, *88* (16), 11392-11410.
(33) M. J. Frisch, G. W. T., H. B. Schlegel, G. E. Scuseria, M. A. Robb, J. R. Cheeseman, G. Scalmani, V. Barone, G. A. Petersson, H. Nakatsuji, X. Li, M. Caricato, A. V. Marenich, J. Bloino, B. G. Janesko, R. Gomperts, B. Mennucci, H. P. Hratchian, J. V. Ortiz, A. F. Izmaylov, J. L. Sonnenberg, D. Williams-Young, F. Ding, F. Lipparini, F. Egidi, J. Goings, B. Peng, A. Petrone, T. Henderson, D. Ranasinghe, V. G. Zakrzewski, J. Gao, N. Rega, G. Zheng, W. Liang, M. Hada, M. Ehara, K. Toyota, R. Fukuda, J. Hasegawa, M. Ishida, T. Nakajima, Y. Honda, O. Kitao, H. Nakai, T. Vreven, K. Throssell, J. A. Montgomery, Jr., J. E. Peralta, F. Ogliaro, M. J. Bearpark, J. J. Heyd, E. N. Brothers, K. N. Kudin, V. N. Staroverov, T. A. Keith, R. Kobayashi, J. Normand, K. Raghavachari, A. P. Rendell, J. C. Burant, S. S. Iyengar, J. Tomasi, M. Cossi, J. M. Millam, M. Klene, C. Adamo, R. Cammi, J. W. Ochterski, R. L. Martin, K. Morokuma, O. Farkas, J. B. Foresman, and D. J. Fox. Gaussian 16, Revision C.01, Gaussian, Inc., Wallingford CT. **2016**.
(34) Becke, A. D. Density-functional thermochemistry. III. The role of exact exchange. *J. Chem. Phys.* **1993**, *98* (7), 5648-5652.

(35) Scrocco, S.; Tomasi, J. Electrostatic Interaction of a Solute with a Continuum. A Direct Utilization of Ab Initio Molecular Potentials for the Prevision of Solvent Effects. *Chem. Phys.* **1981**, *55*.
(36) Grimme, S.; Antony, J.; Ehrlich, S.; Krieg, H. A consistent and accurate ab initio parametrization of density functional dispersion correction (DFT-D) for the 94 elements H-Pu. *J. Chem. Phys.* **2010**, *132* (15).

Copies of NMR spectra

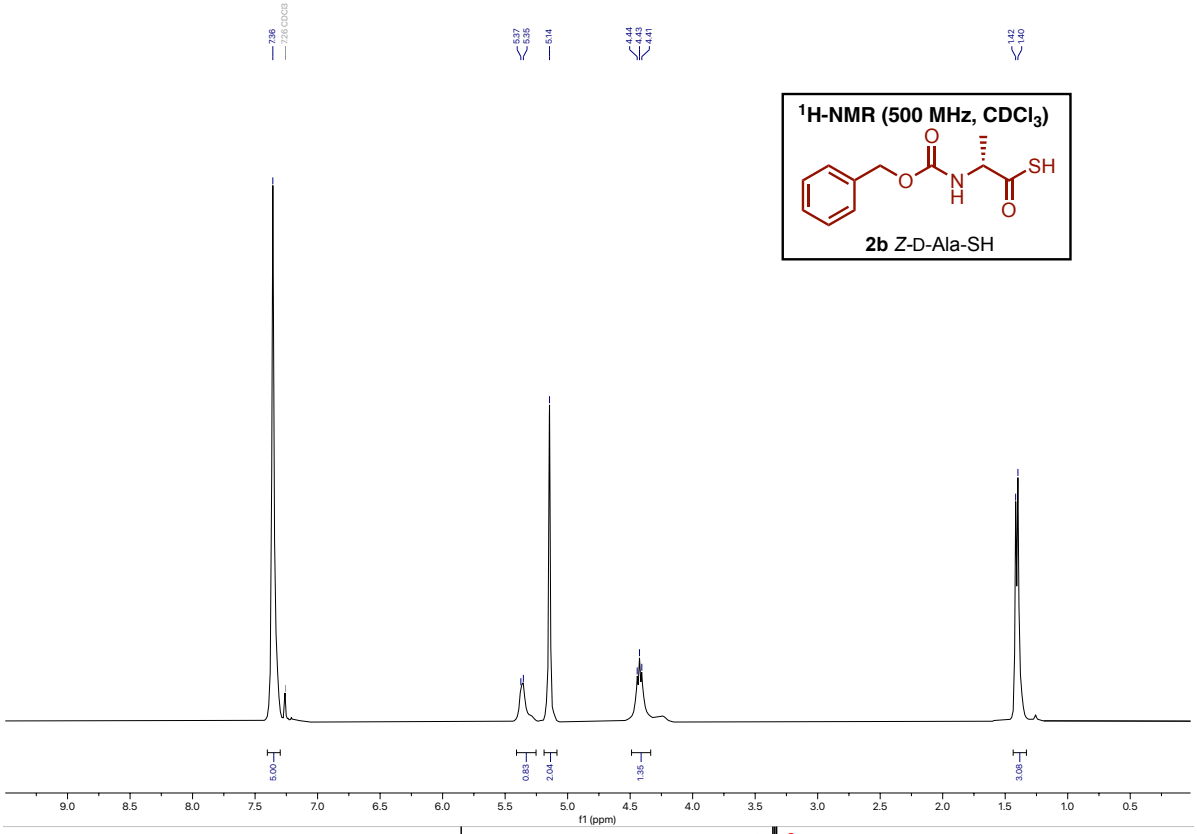

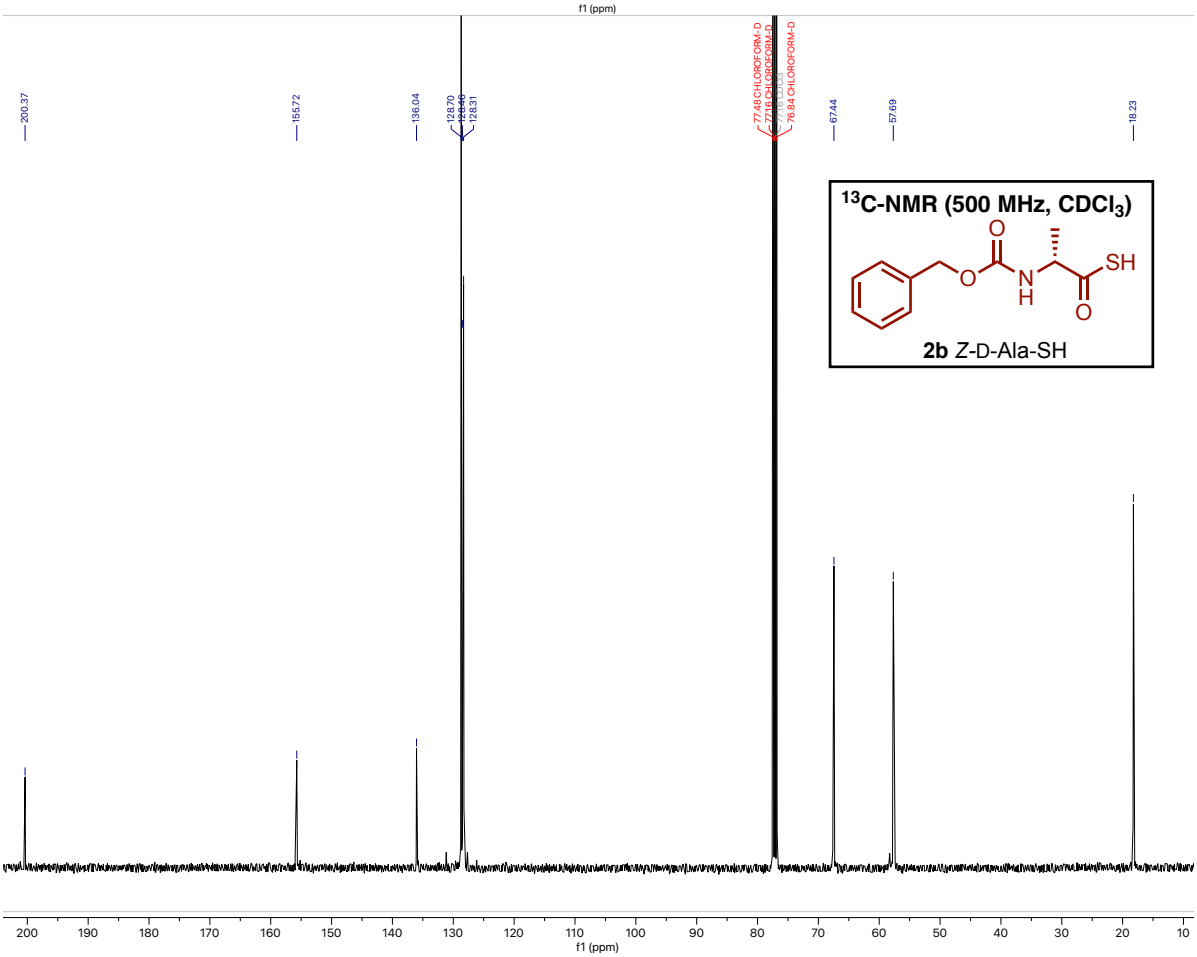

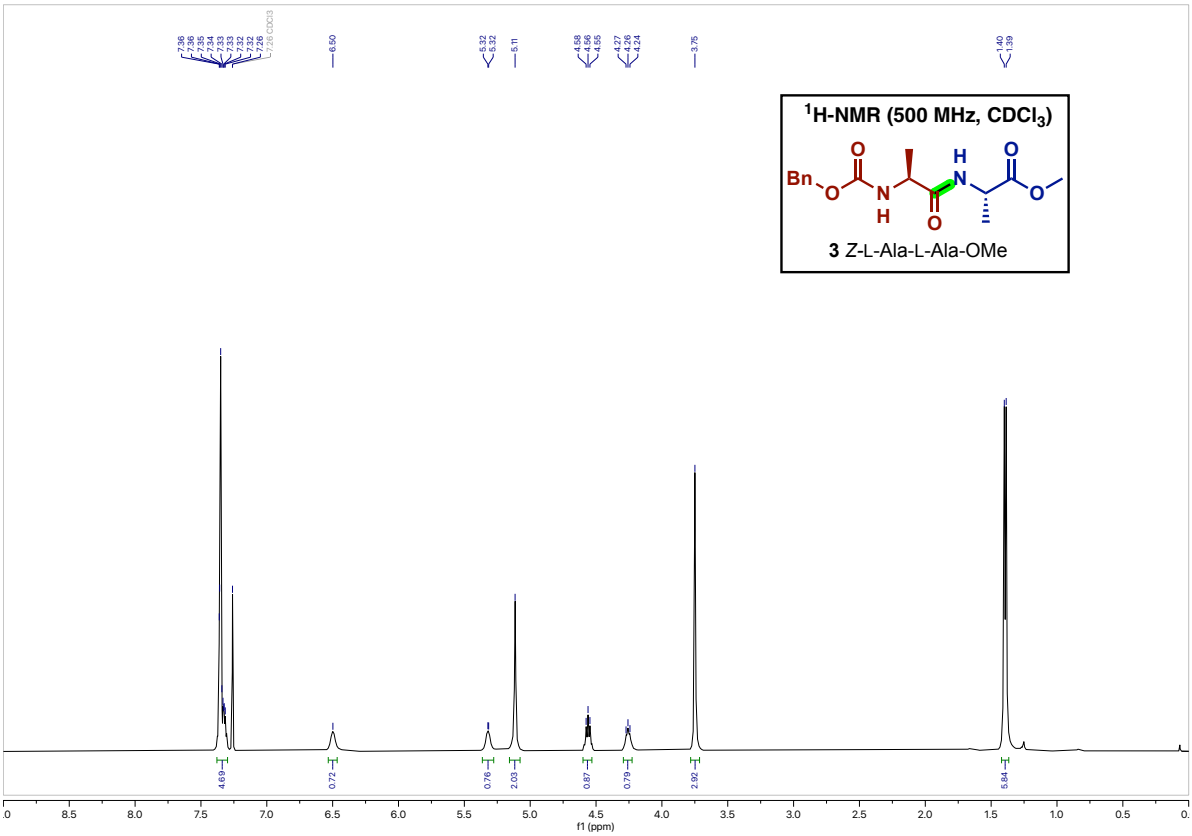
^{1}H-NMR (500 MHz, $CDCl_3$)
3 Z-L-Ala-L-Ala-OMe
f1 (ppm)

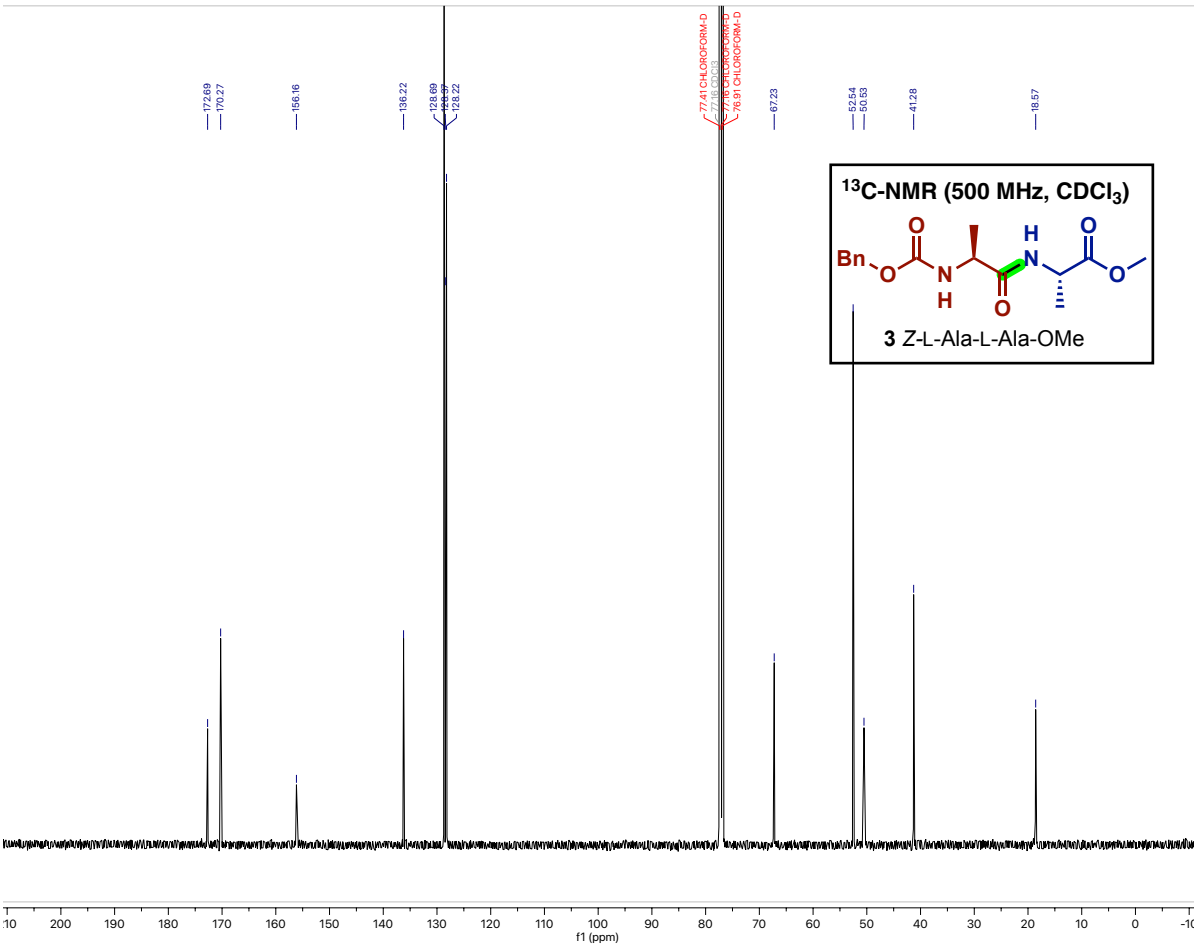
^{13}C-NMR (500 MHz, $CDCl_3$)
3 Z-L-Ala-L-Ala-OMe
f1 (ppm)

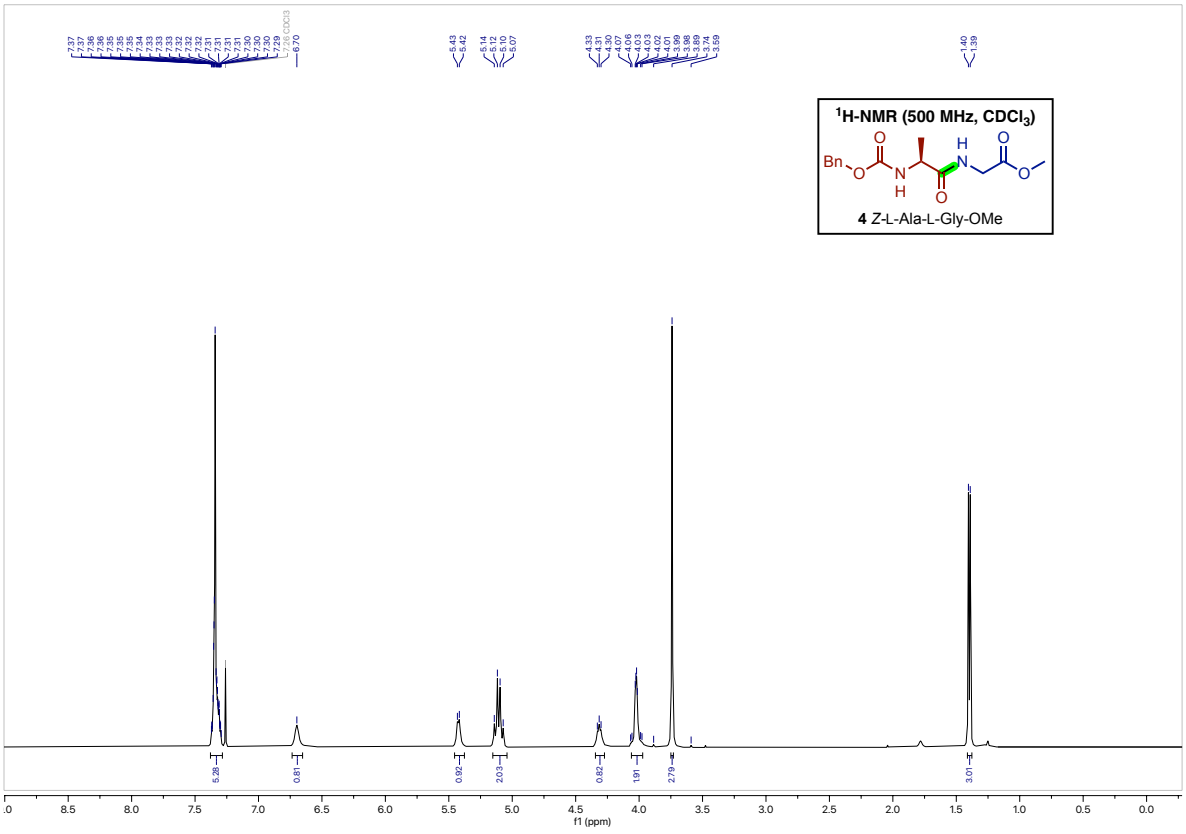
^{1}H-NMR (500 MHz, $CDCl_3$)
4 Z-L-Ala-L-Gly-OMe
f1 (ppm)

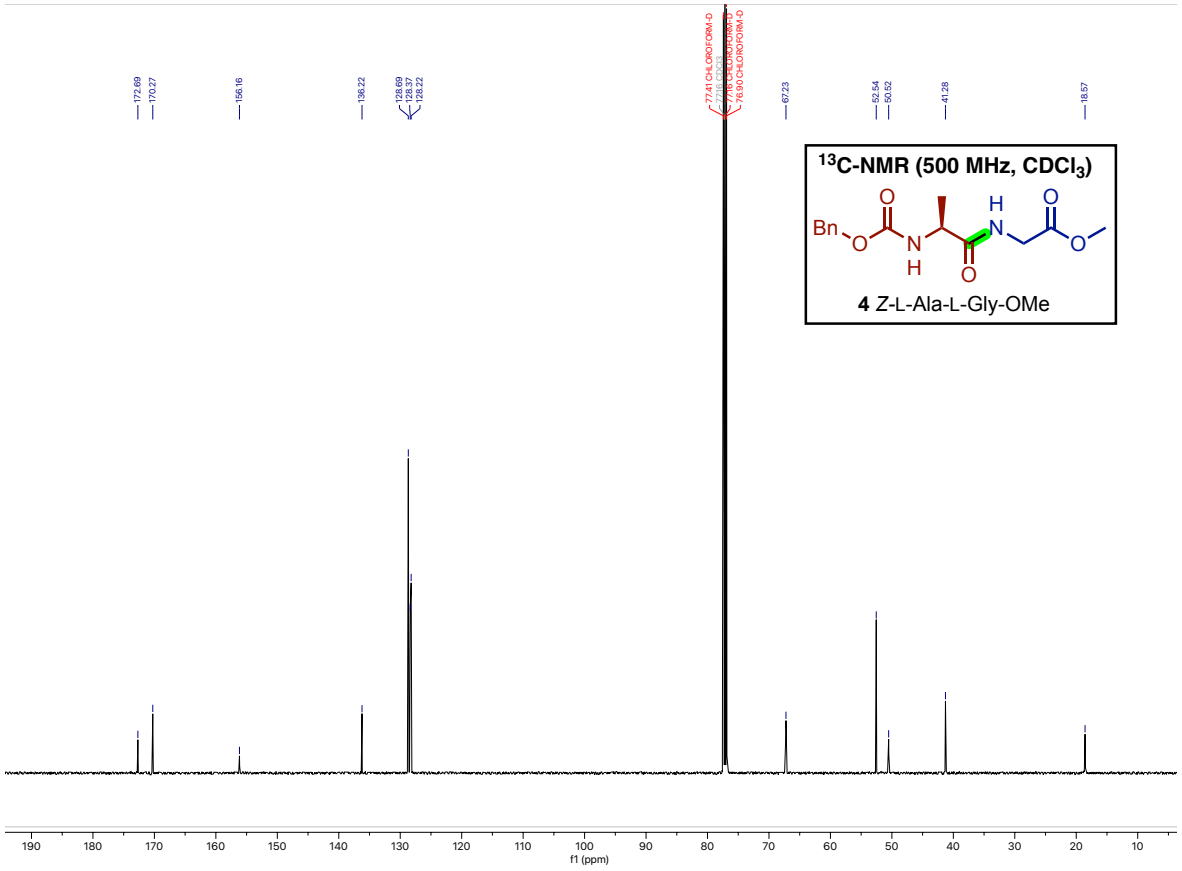
^{13}C-NMR (500 MHz, $CDCl_3$)
4 Z-L-Ala-L-Gly-OMe
f1 (ppm)

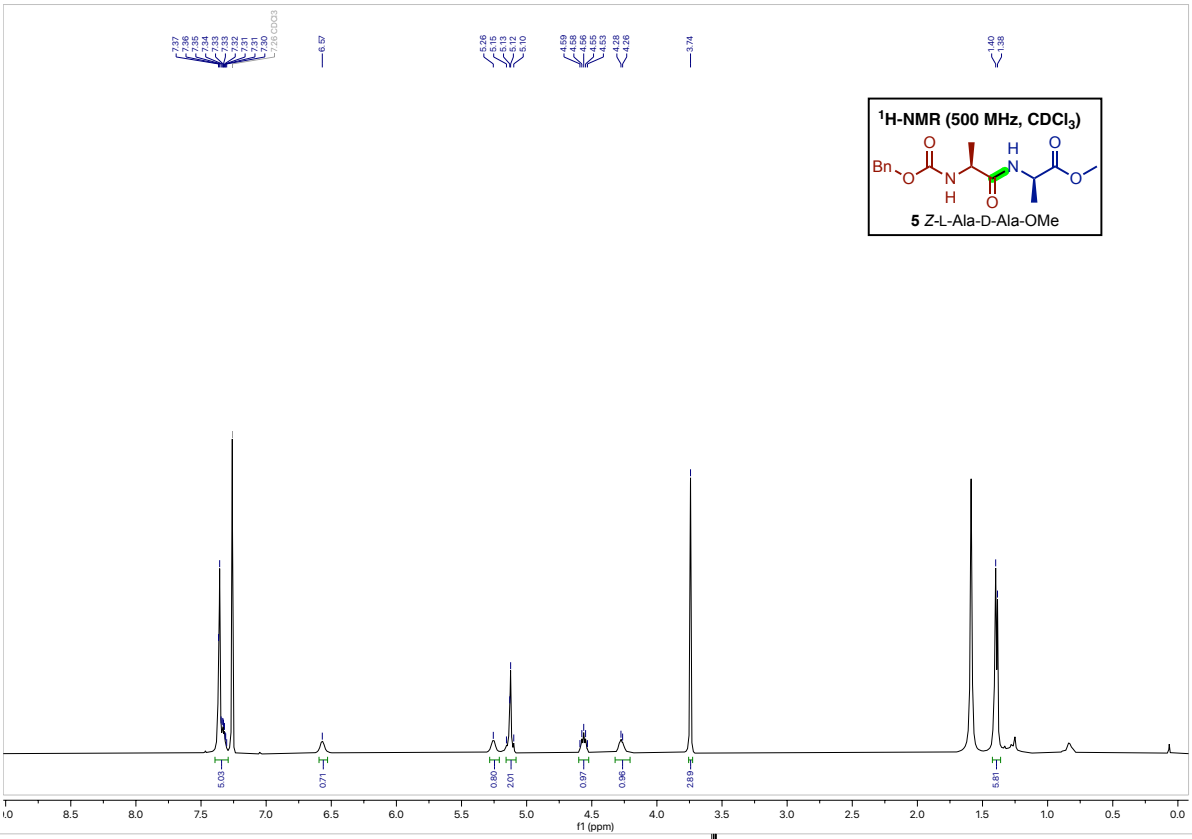
^{1}H-NMR (500 MHz, CDCl$_3$)
5 Z-L-Ala-D-Ala-OMe
f1 (ppm)

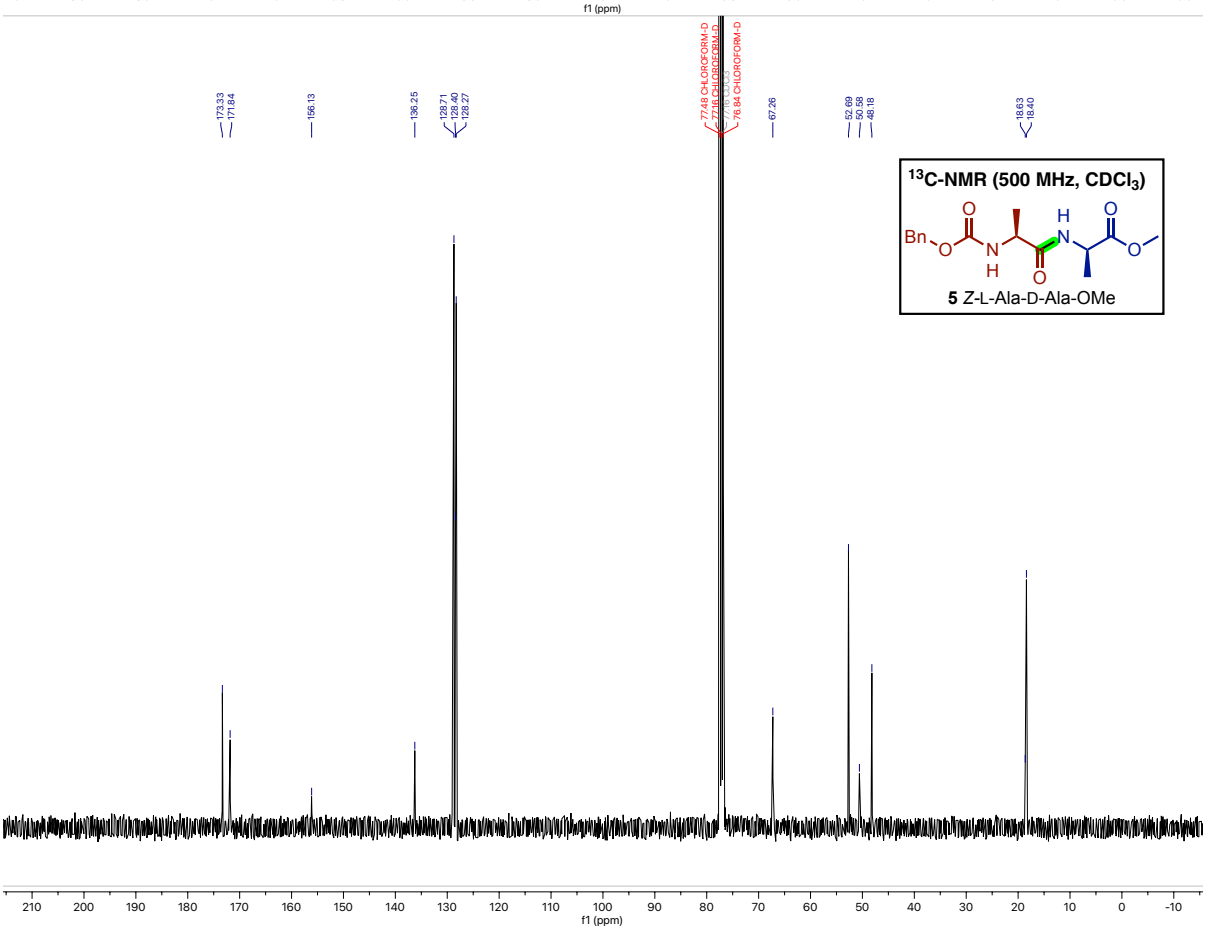
^{13}C-NMR (500 MHz, CDCl$_3$)
5 Z-L-Ala-D-Ala-OMe
f1 (ppm)

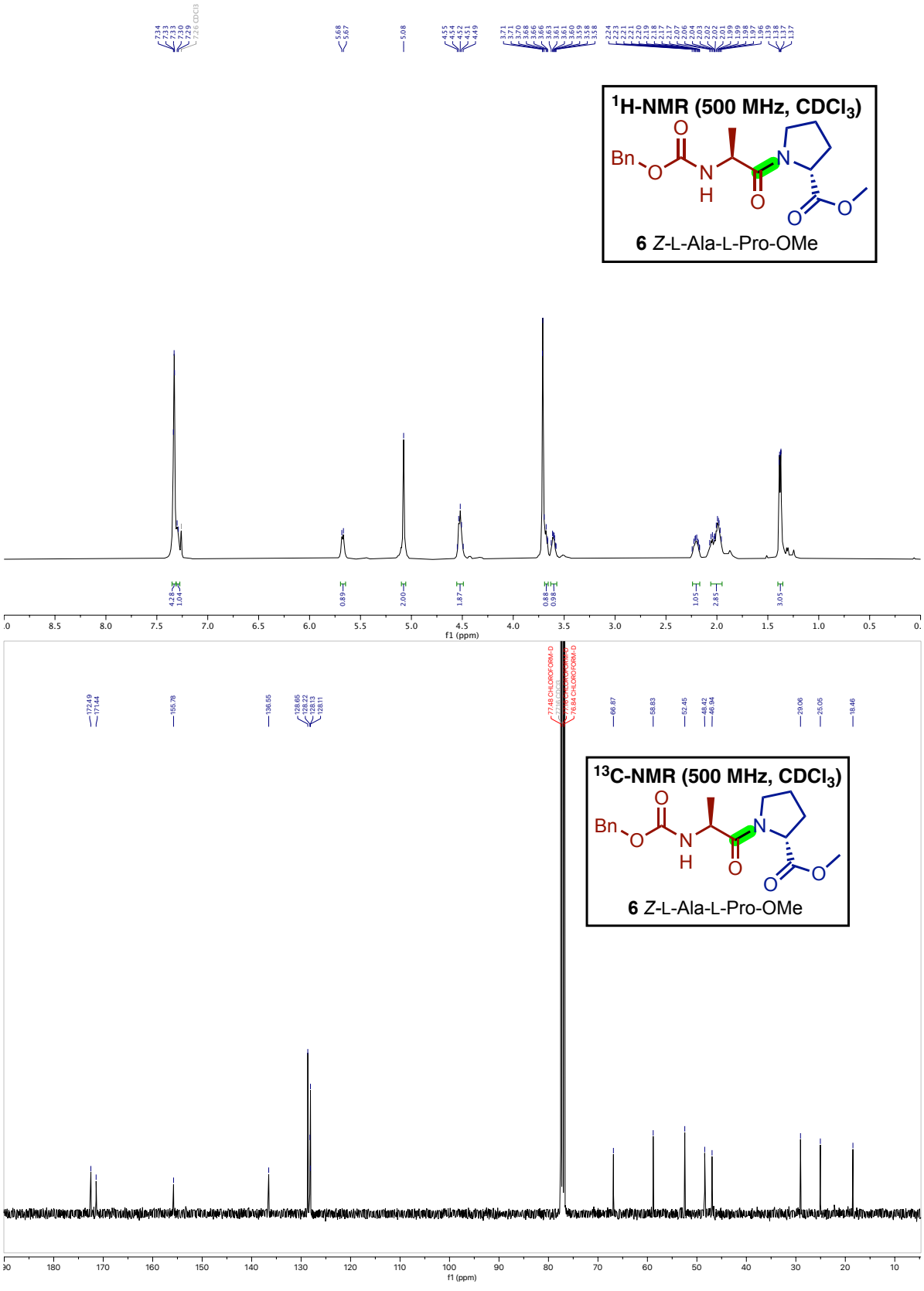
^{1}H-NMR (500 MHz, CDCl$_3$)
6 Z-L-Ala-L-Pro-OMe
f1 (ppm)
^{13}C-NMR (500 MHz, CDCl$_3$)
6 Z-L-Ala-L-Pro-OMe
f1 (ppm)

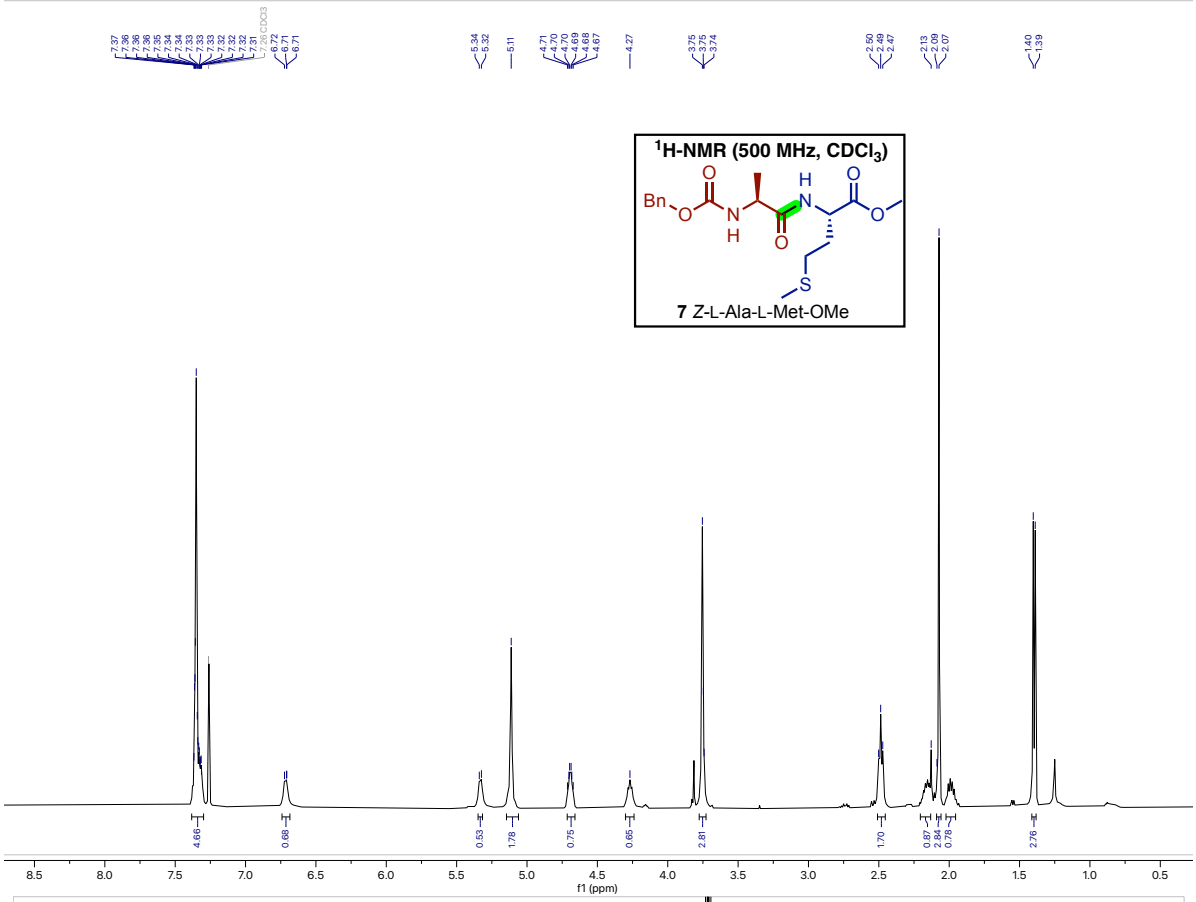
^{1}H-NMR (500 MHz, $CDCl_3$)
7 Z-L-Ala-L-Met-OMe
f1 (ppm)

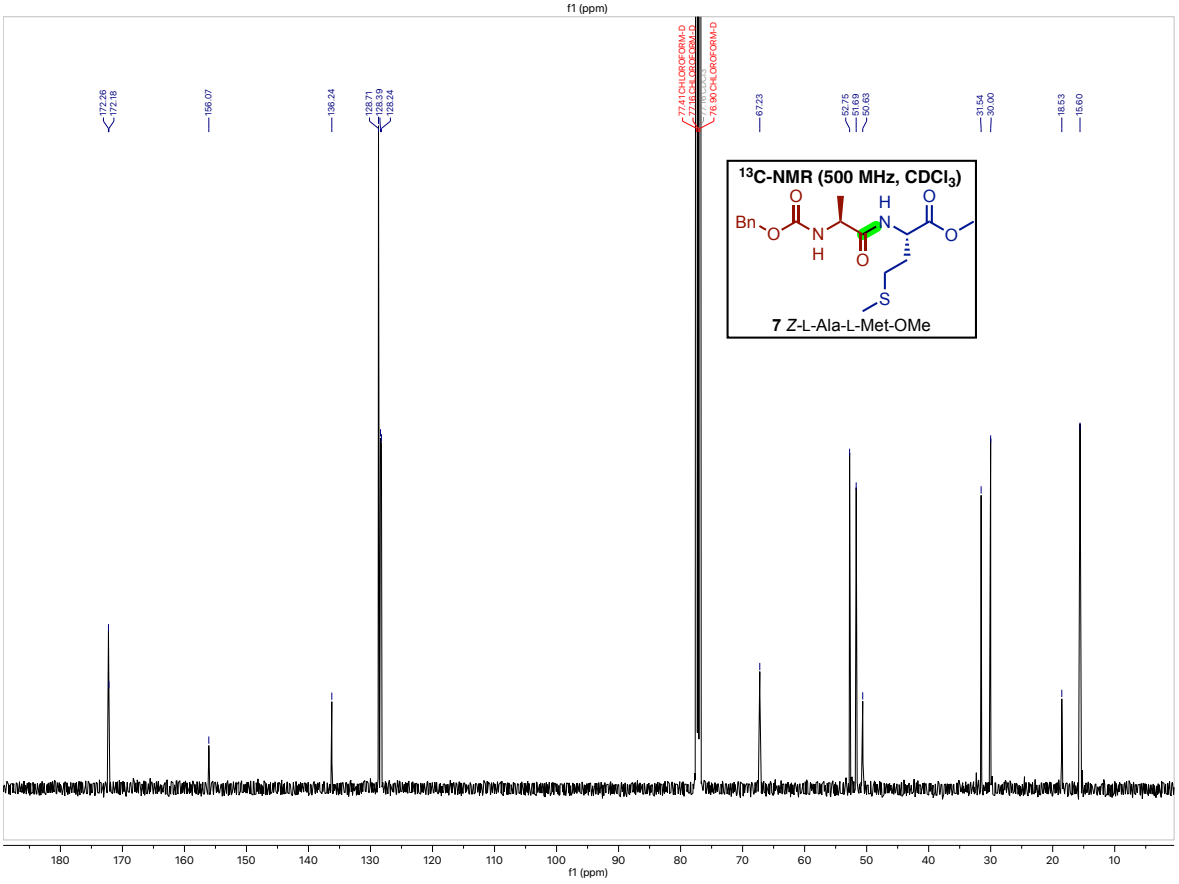
^{13}C-NMR (500 MHz, $CDCl_3$)
7 Z-L-Ala-L-Met-OMe
f1 (ppm)

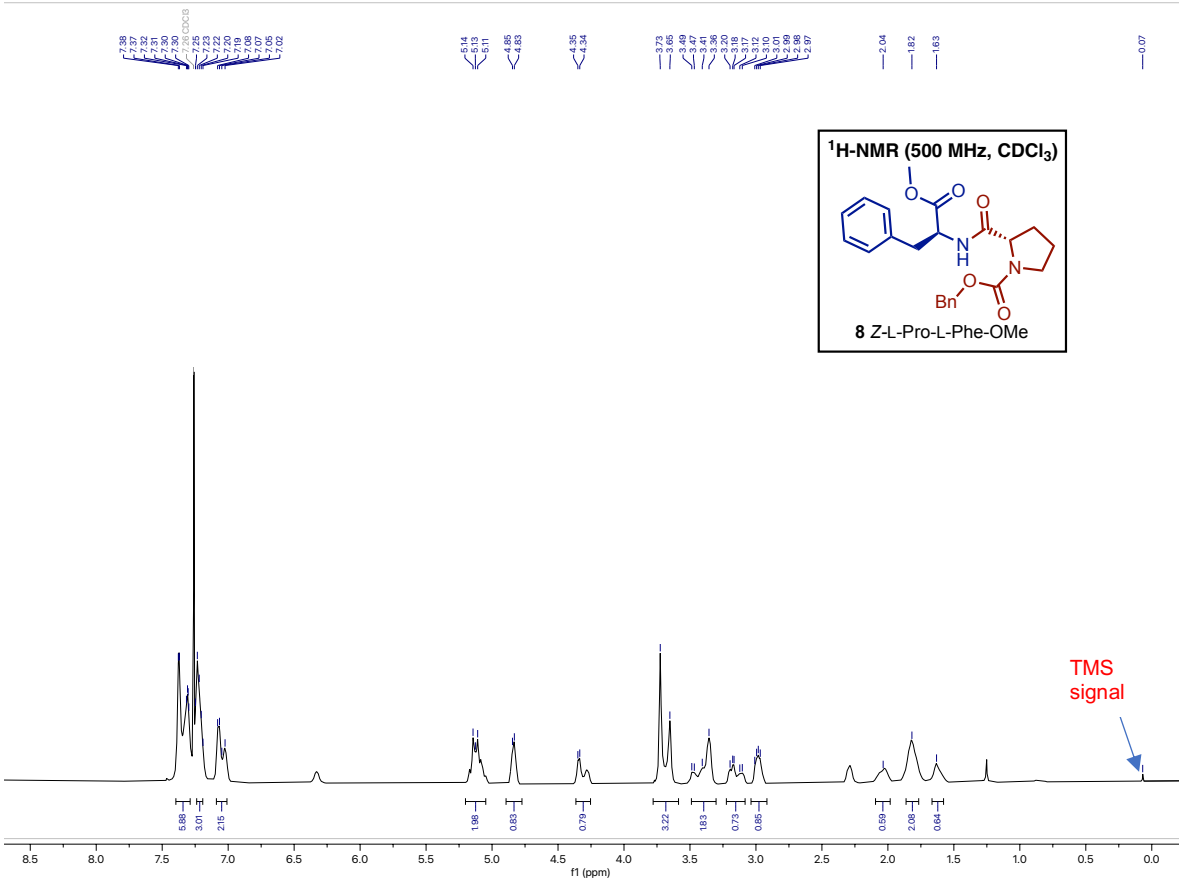
^{1}H-NMR (500 MHz, CDCl$_3$)
8 Z-L-Pro-L-Phe-OMe
TMS signal
f1 (ppm)

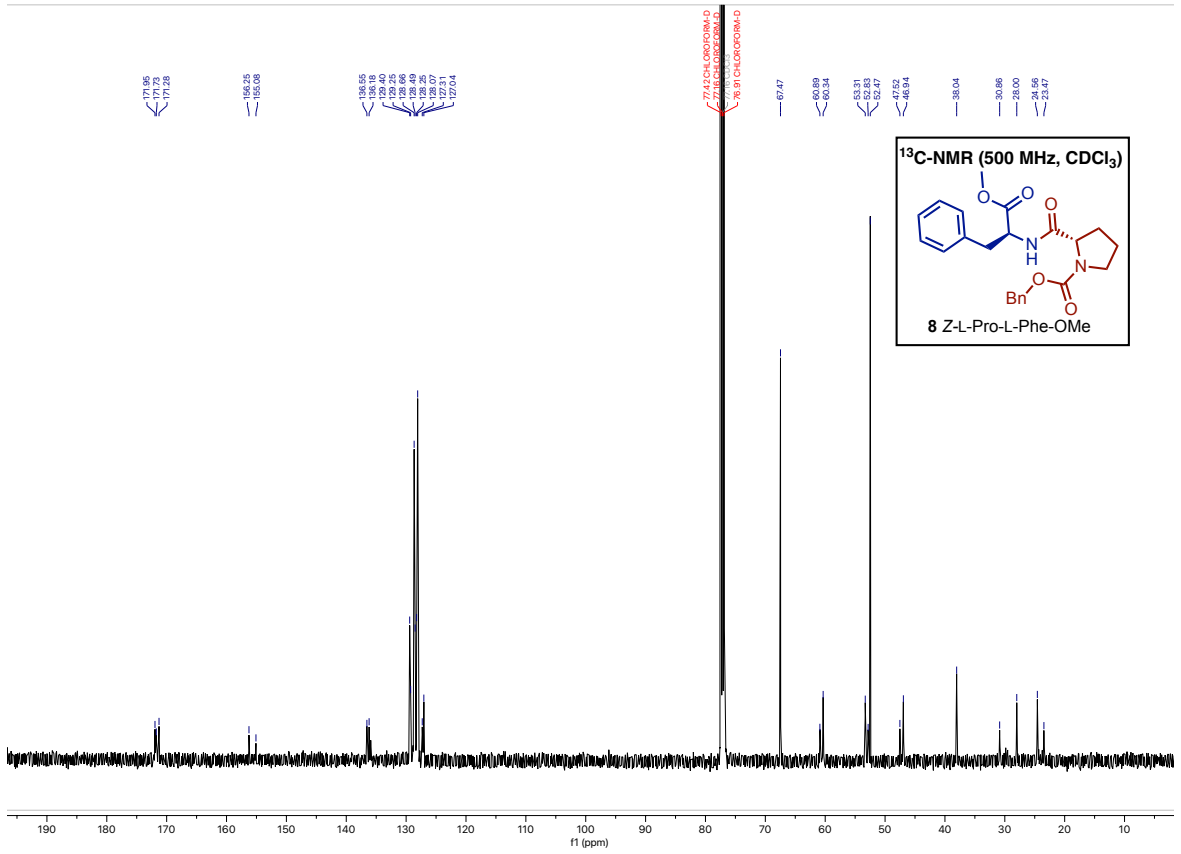
^{13}C-NMR (500 MHz, CDCl$_3$)
8 Z-L-Pro-L-Phe-OMe
f1 (ppm)

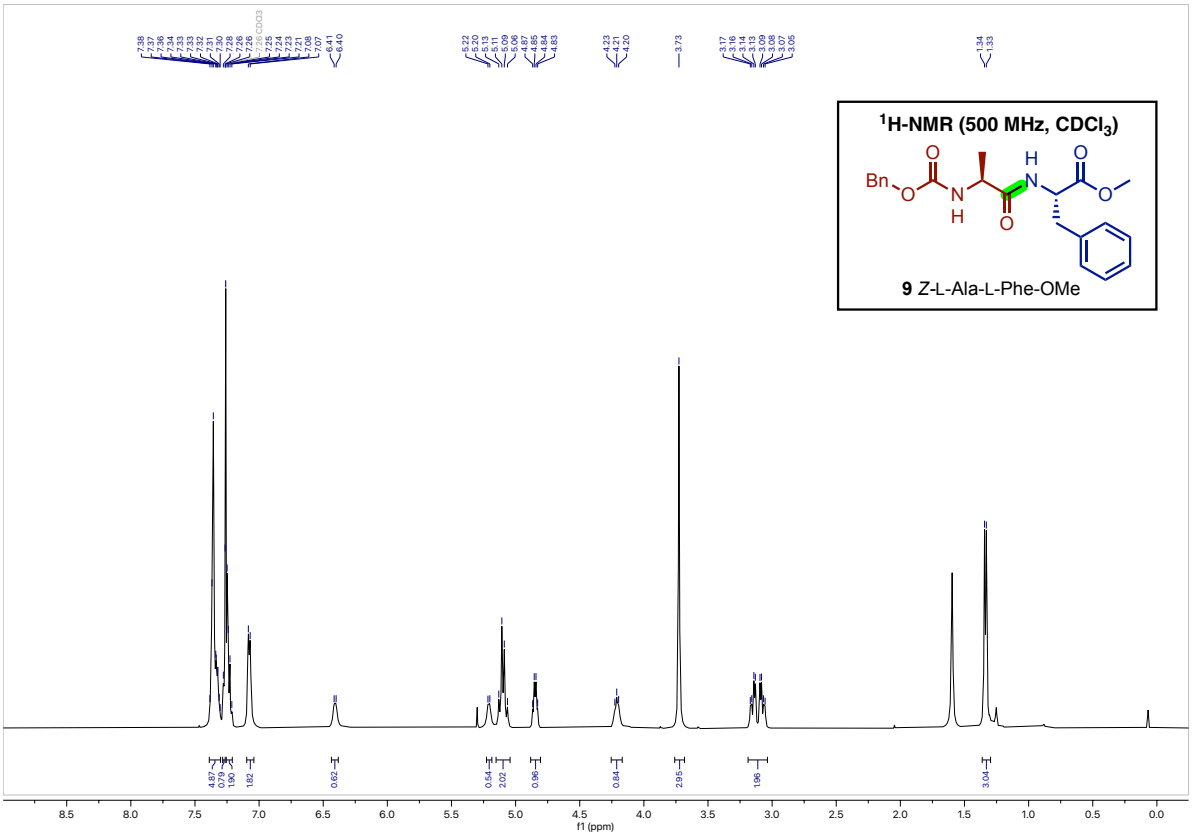
^{1}H-NMR (500 MHz, $CDCl_3$)
9 Z-L-Ala-L-Phe-OMe
f1 (ppm)

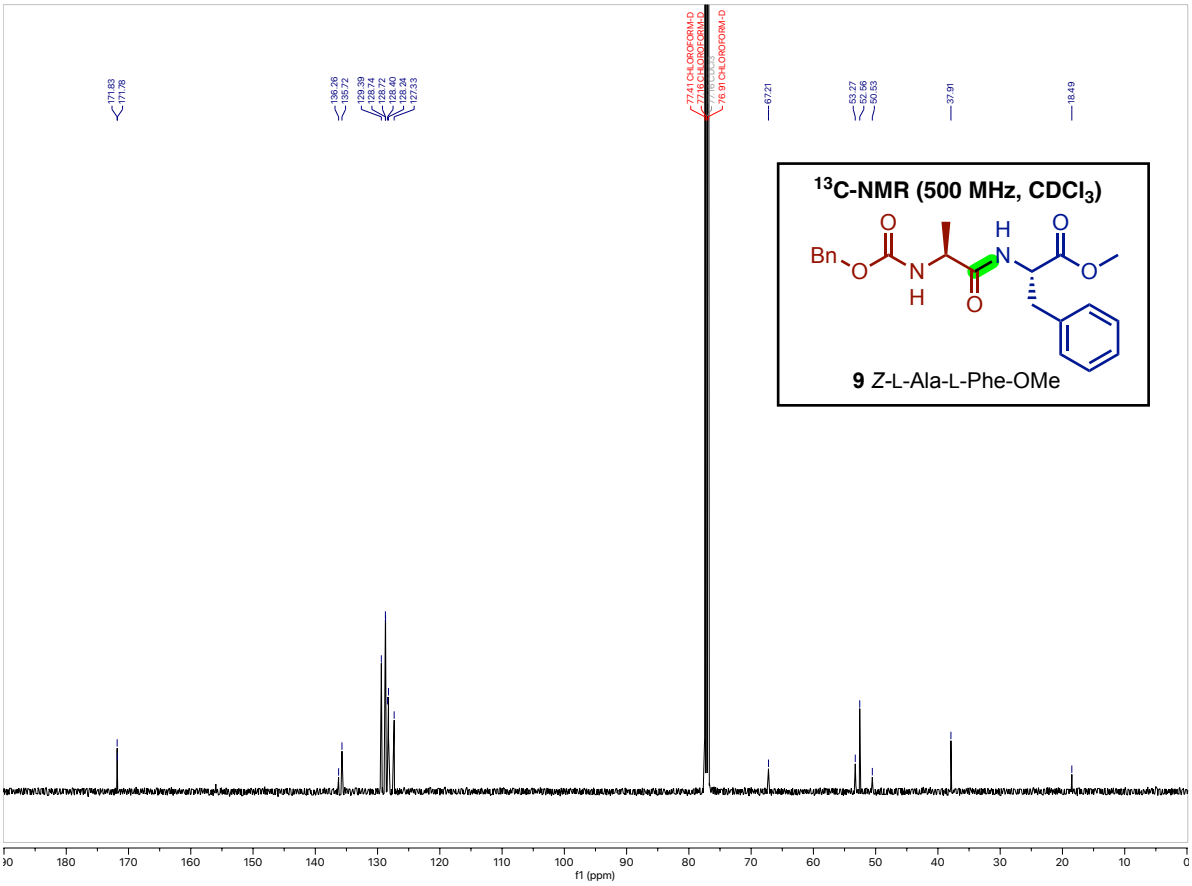
^{13}C-NMR (500 MHz, $CDCl_3$)
9 Z-L-Ala-L-Phe-OMe
f1 (ppm)

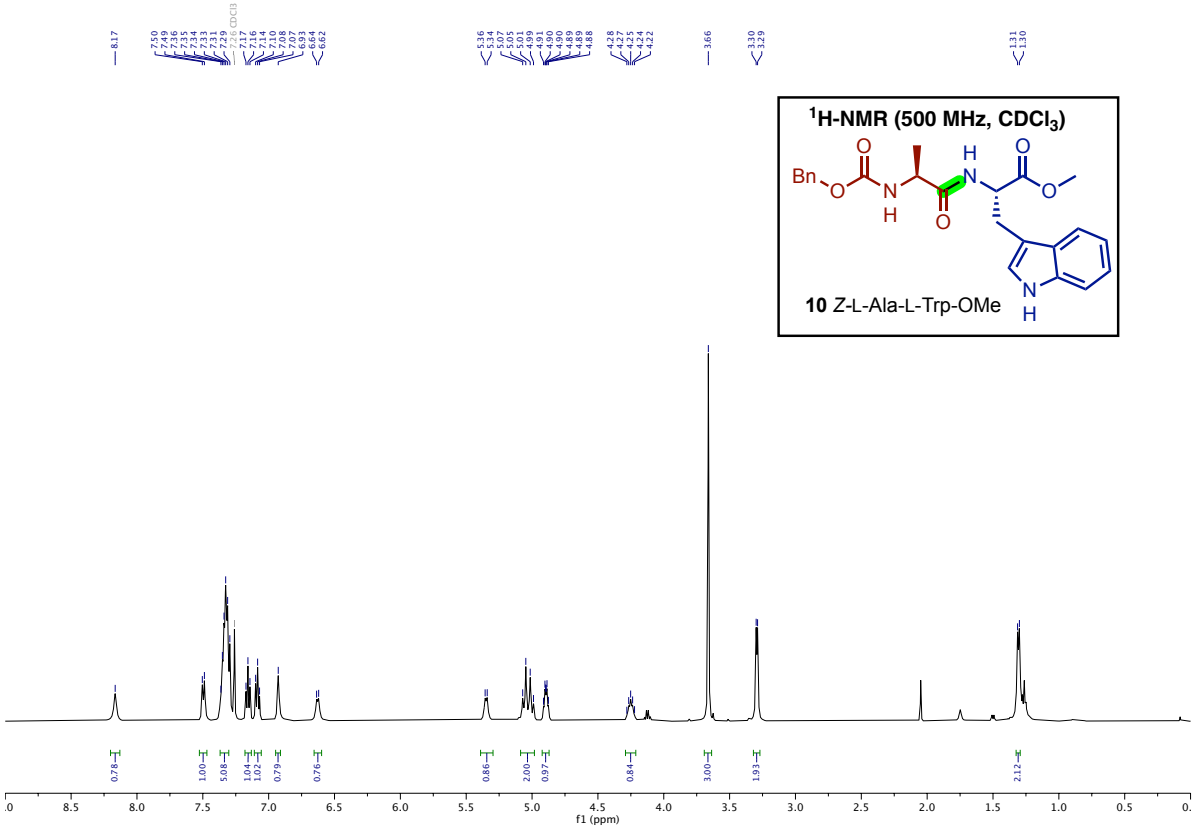
8.17
7.50
7.49
7.36
7.35
7.34
7.33
7.31
7.30
7.26 CDCl3
7.17
7.16
7.14
7.10
7.08
7.07
6.93
6.64
6.62
5.36
5.34
5.07
5.05
4.91
4.91
4.90
4.90
4.89
4.89
4.88
4.28
4.27
4.25
4.24
4.22
3.66
3.30
3.29
1.31
1.30
0.78
1.00
5.08
1.04
1.02
0.79
0.76
0.86
2.00
0.97
0.84
3.00
1.93
2.12
f1 (ppm)
1H-NMR (500 MHz, CDCl3)
Bn
O
N
H
O
H
N
O
O
N
H
10 Z-L-Ala-L-Trp-OMe

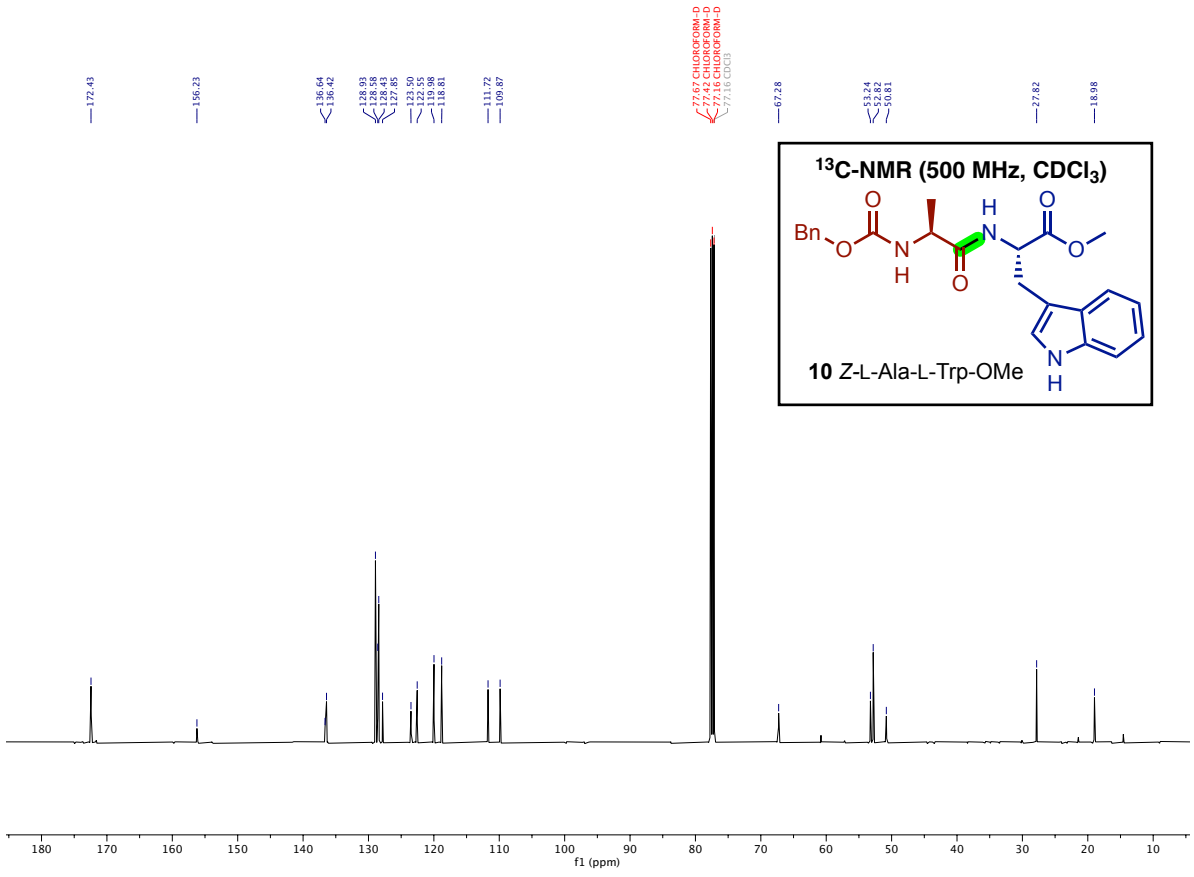
172.43
156.23
136.64
136.42
128.93
128.58
128.43
127.85
123.50
122.55
119.98
118.81
111.72
109.87
77.67 CHLOROFORM-D
77.42 CHLOROFORM-D
77.16 CHLOROFORM-D
77.16 CDCl3
67.28
53.24
52.82
50.81
27.82
18.98
f1 (ppm)
13C-NMR (500 MHz, CDCl3)
Bn
O
N
H
O
H
N
O
O
N
H
10 Z-L-Ala-L-Trp-OMe

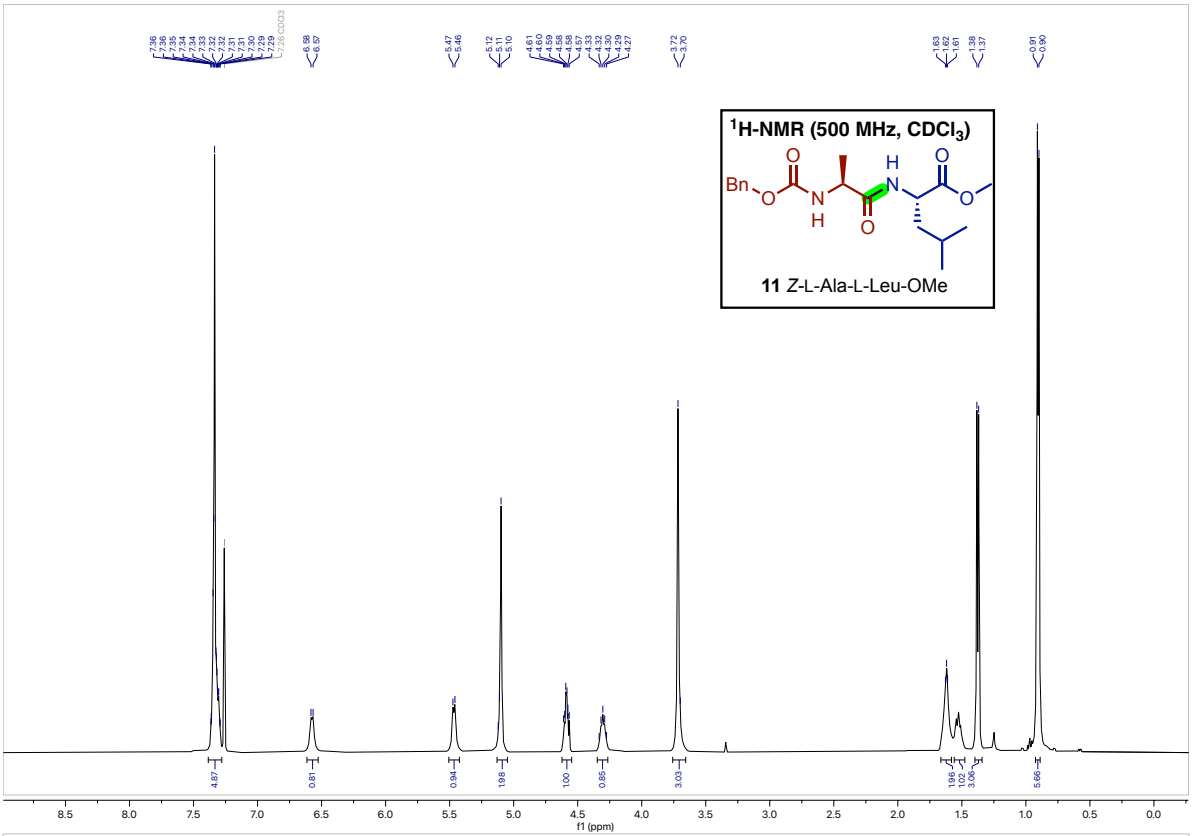
^{1}H-NMR (500 MHz, CDCl$_3$)
11 Z-L-Ala-L-Leu-OMe
f1 (ppm)

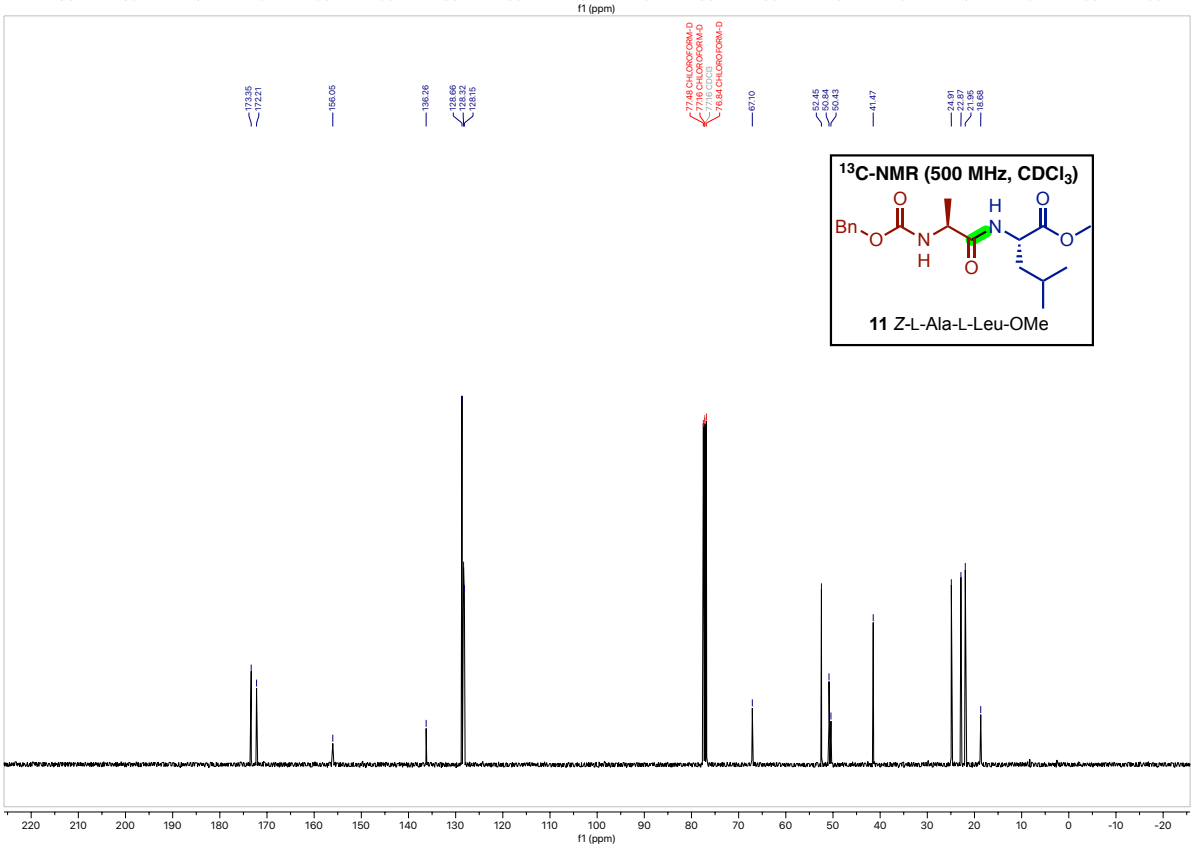
^{13}C-NMR (500 MHz, CDCl$_3$)
11 Z-L-Ala-L-Leu-OMe
f1 (ppm)

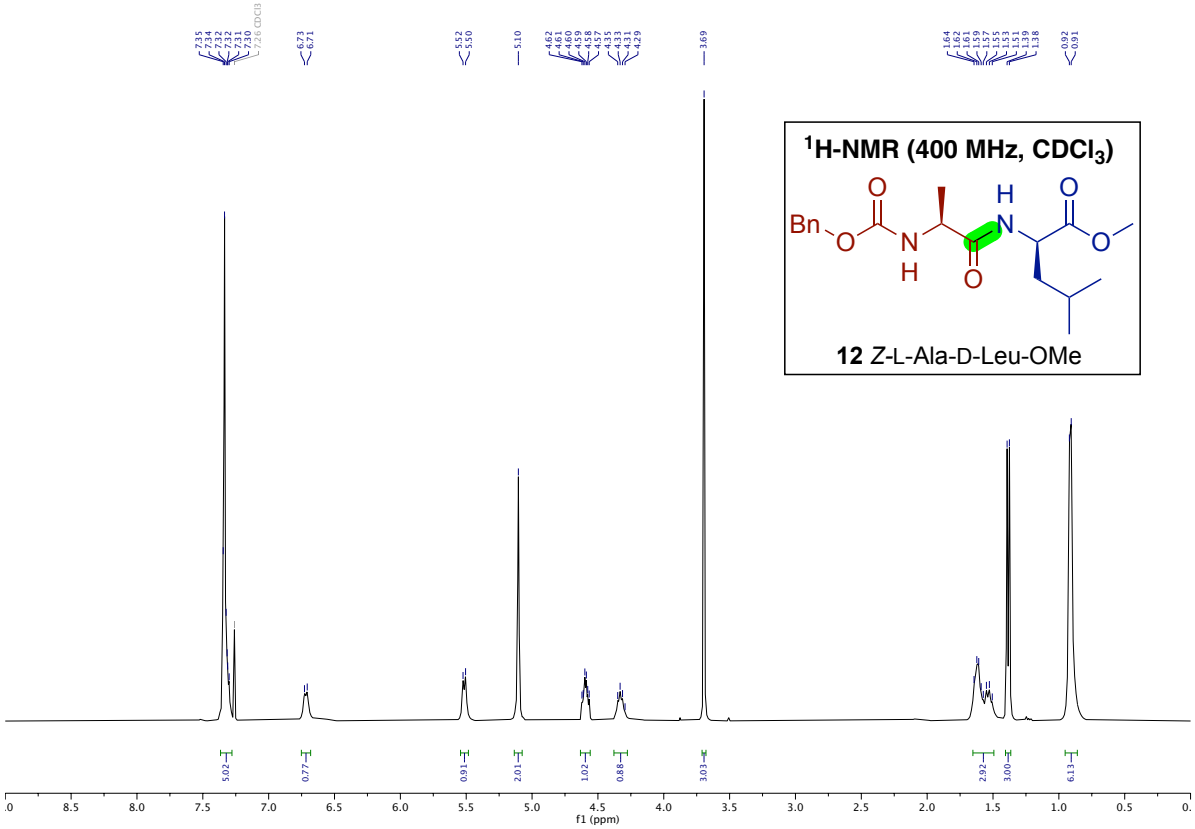
^{1}H-NMR (400 MHz, CDCl$_3$)
12 Z-L-Ala-D-Leu-OMe
f1 (ppm)

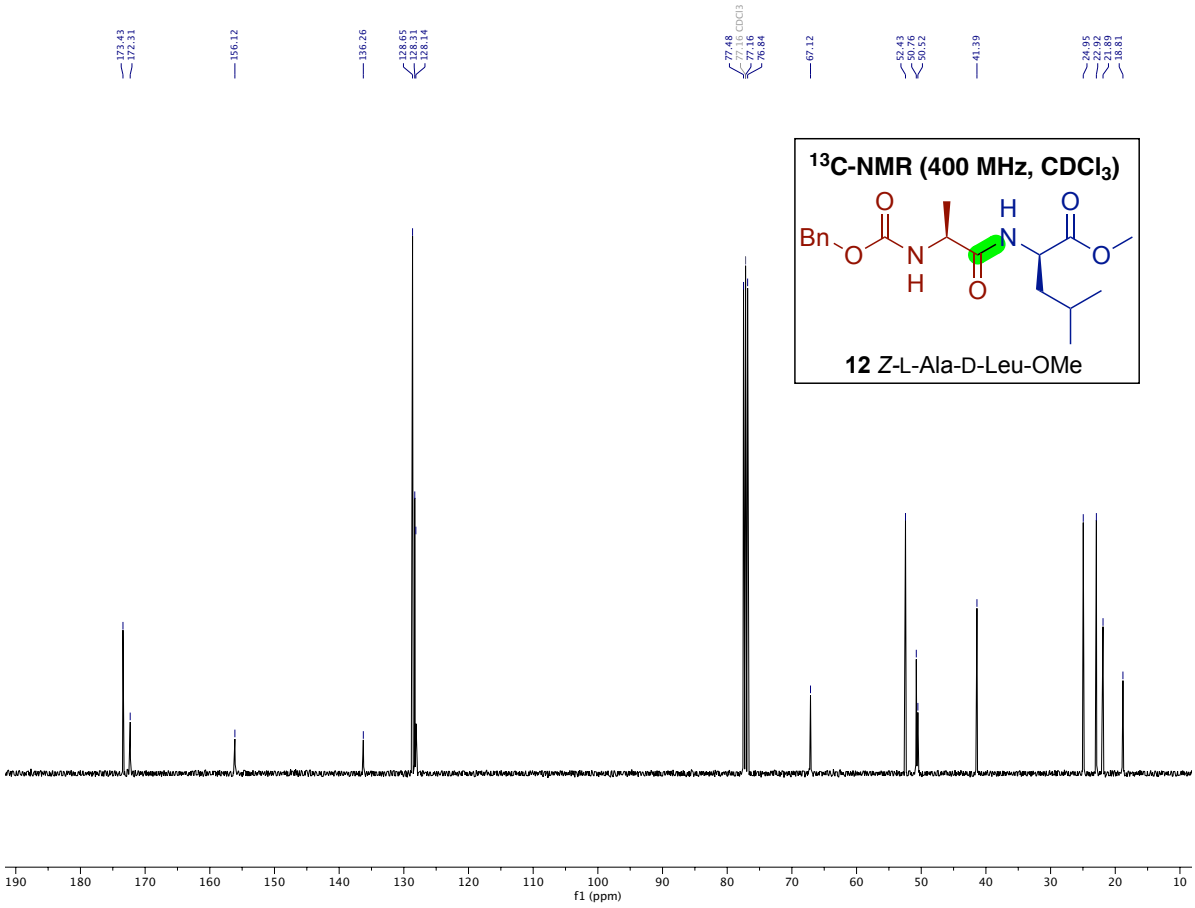
^{13}C-NMR (400 MHz, CDCl$_3$)
12 Z-L-Ala-D-Leu-OMe
f1 (ppm)

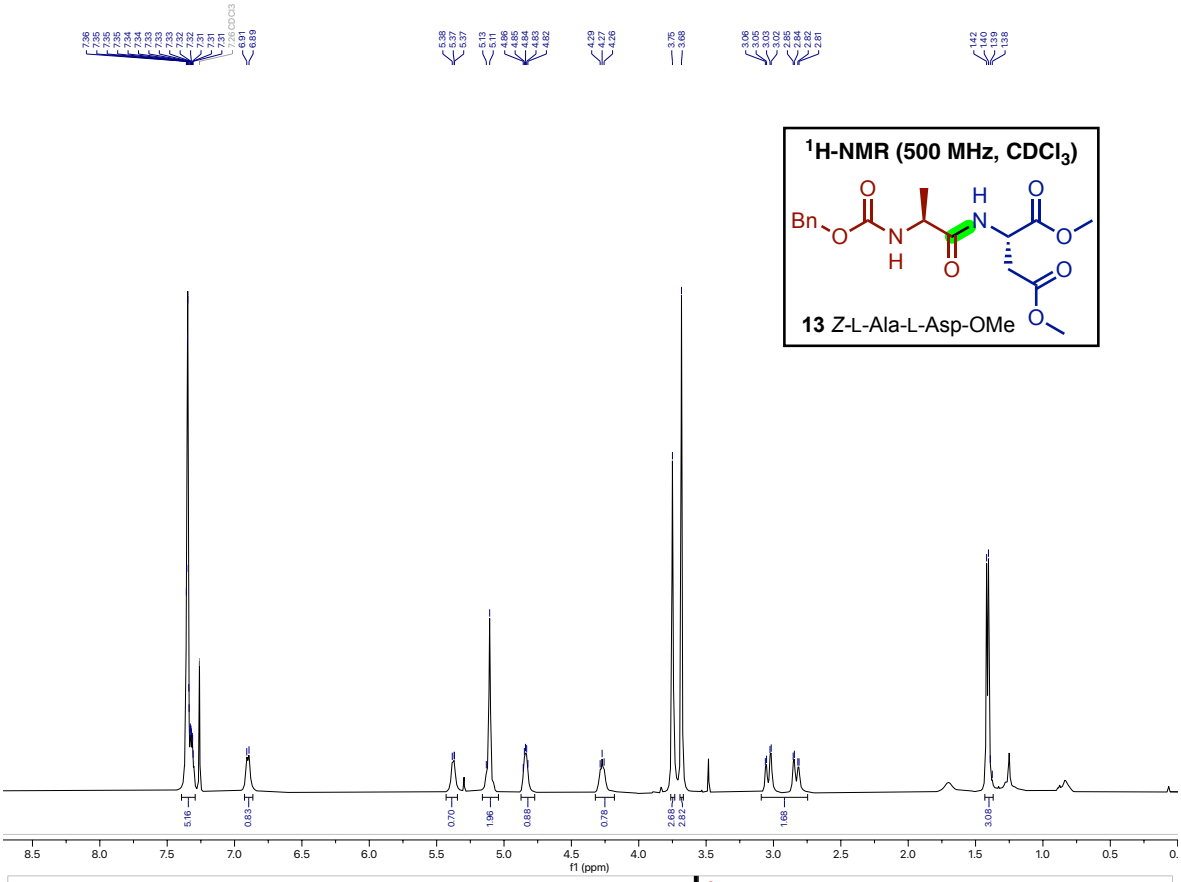
^{1}H-NMR (500 MHz, $CDCl_3$)
13 Z-L-Ala-L-Asp-OMe
f1 (ppm)

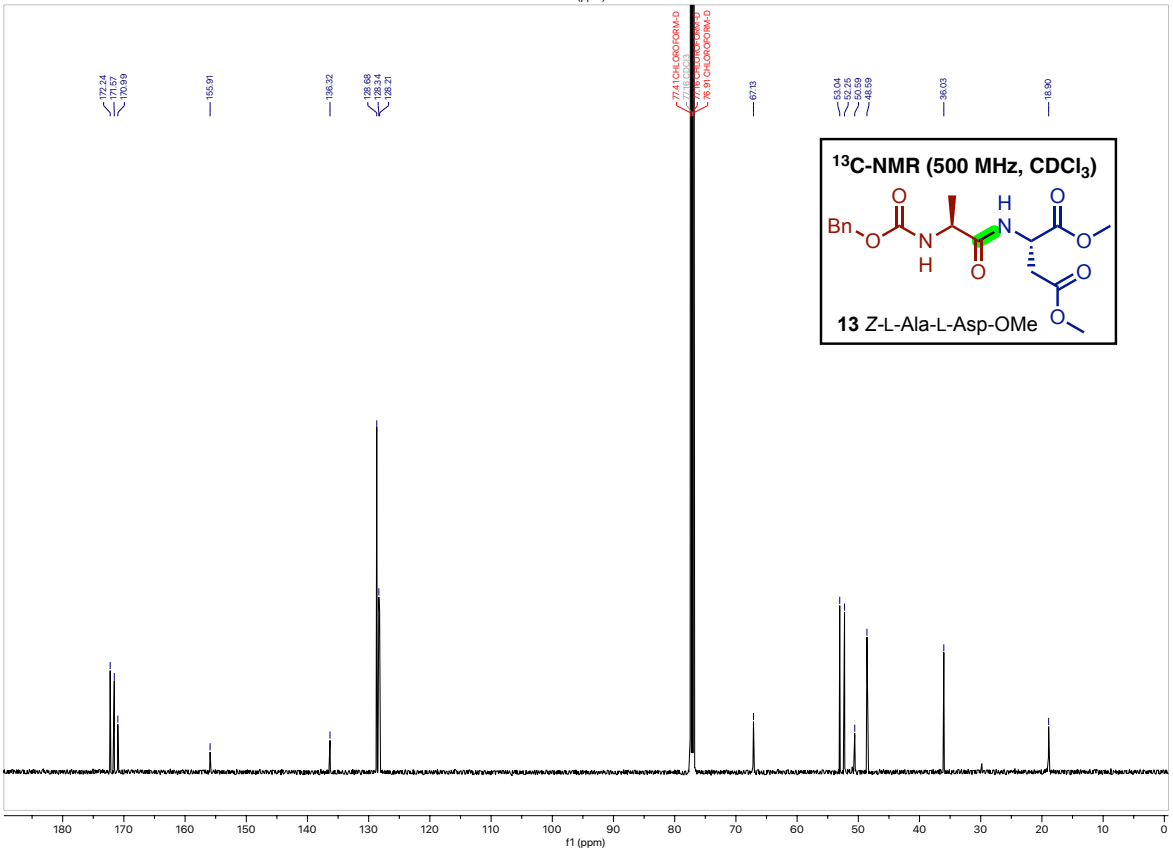
^{13}C-NMR (500 MHz, $CDCl_3$)
13 Z-L-Ala-L-Asp-OMe
f1 (ppm)

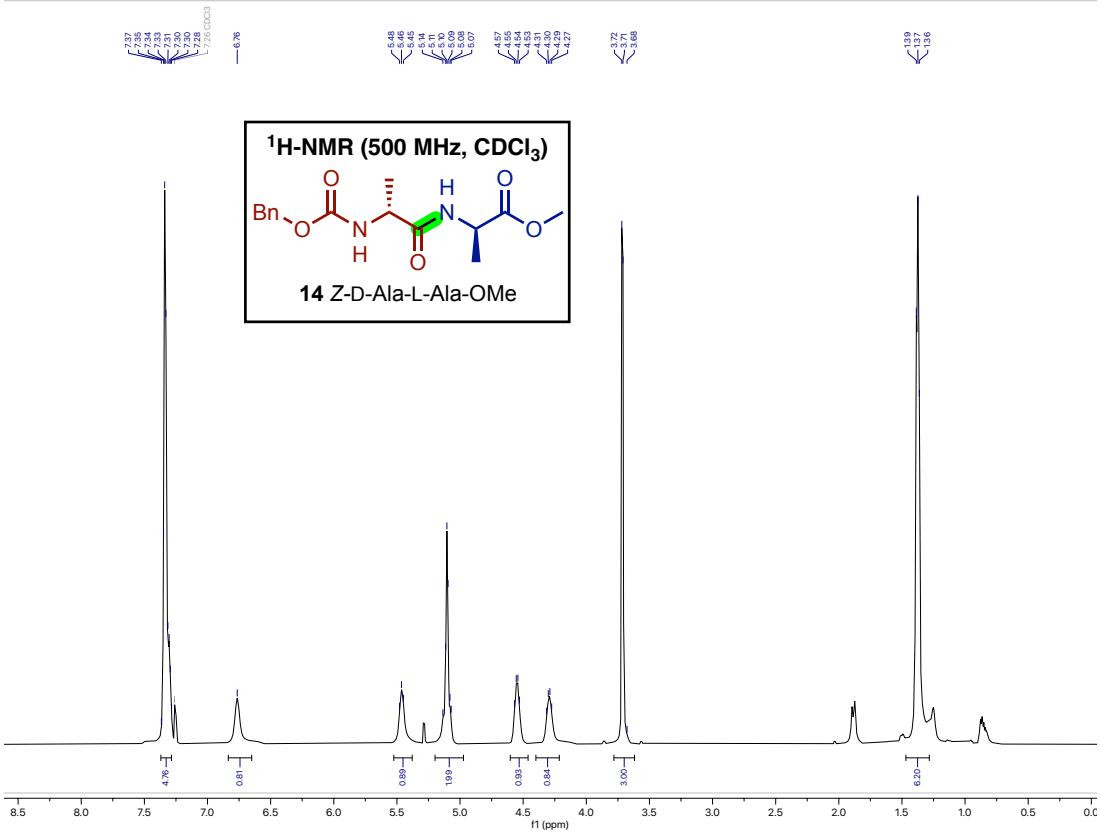
^{1}H-NMR (500 MHz, $CDCl_3$)
14 Z-D-Ala-L-Ala-OMe
f1 (ppm)

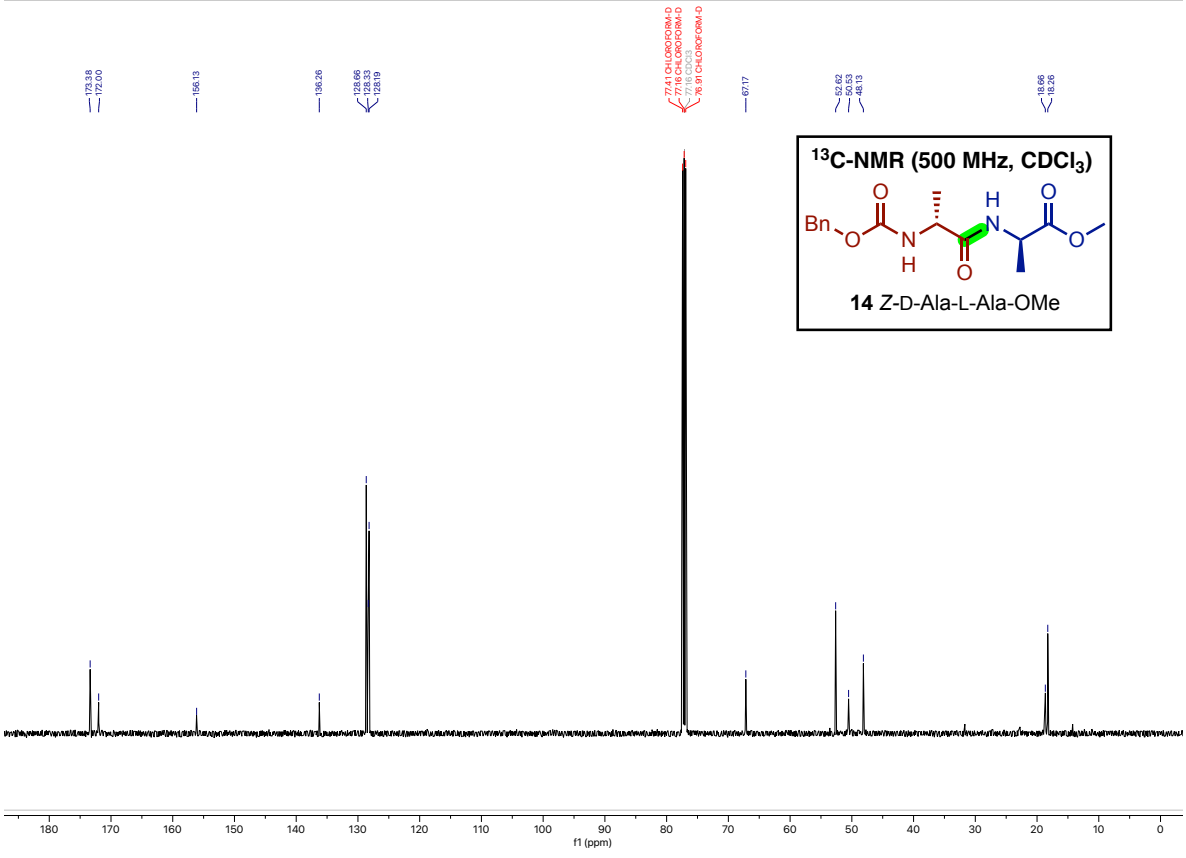
^{13}C-NMR (500 MHz, $CDCl_3$)
14 Z-D-Ala-L-Ala-OMe
f1 (ppm)

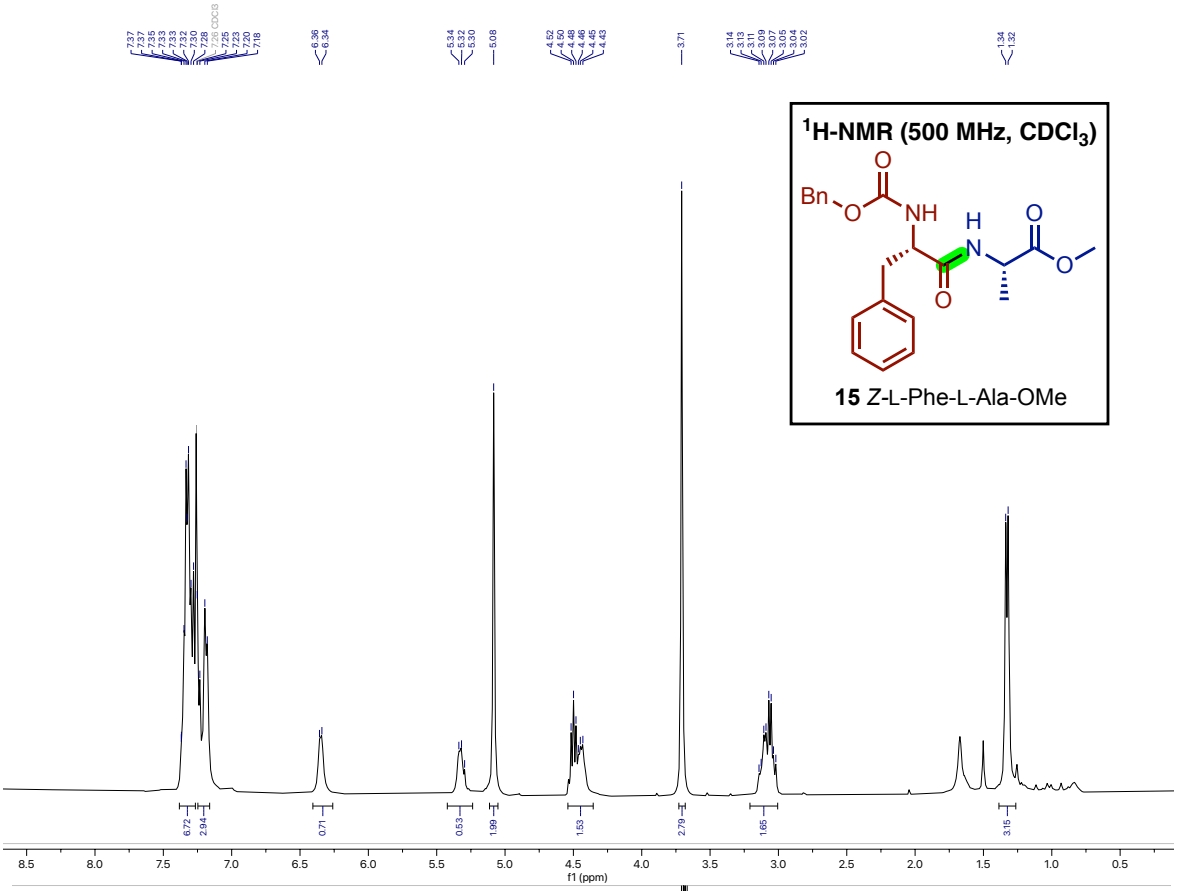
^{1}H-NMR (500 MHz, $CDCl_3$)
Bn
O
NH
H
N
O
O
O
O
15 *Z*-L-Phe-L-Ala-OMe
f1 (ppm)

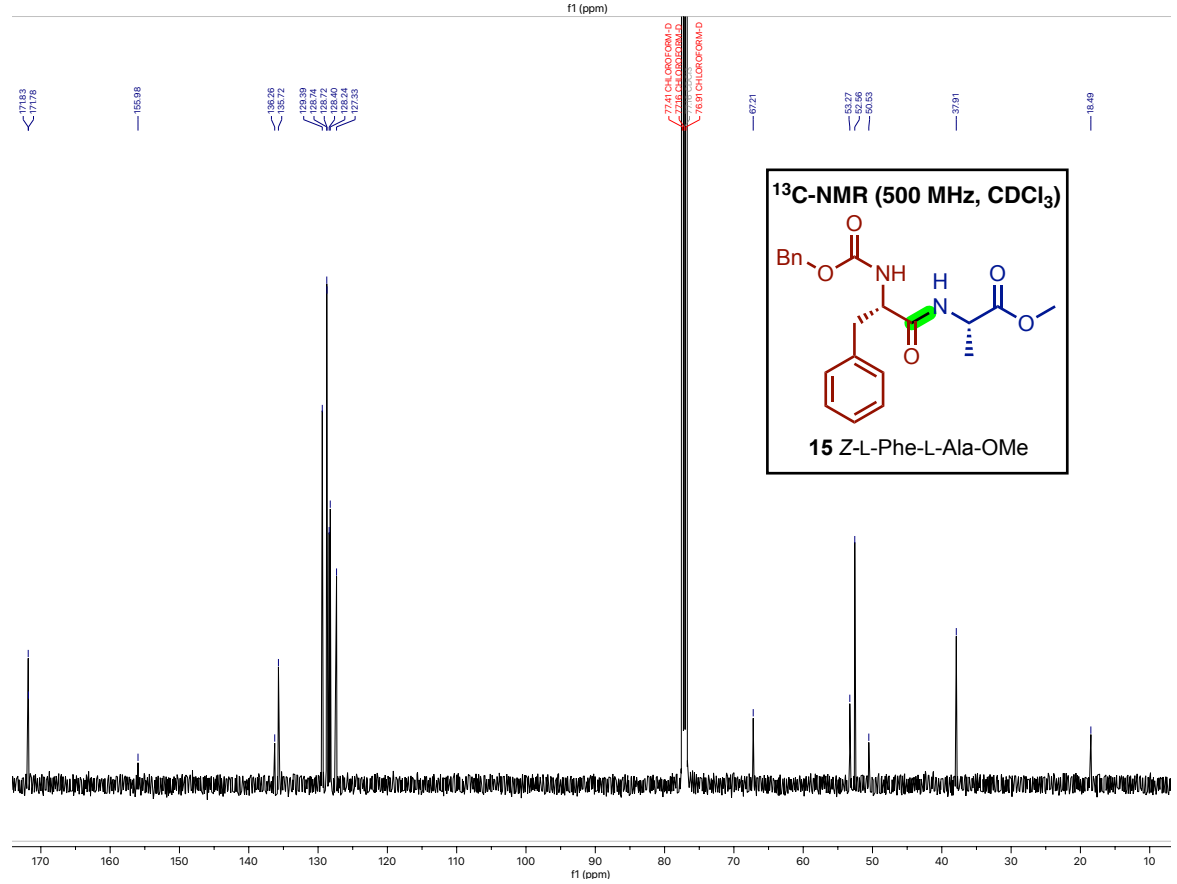
^{13}C-NMR (500 MHz, $CDCl_3$)
Bn
O
NH
H
N
O
O
O
O
15 *Z*-L-Phe-L-Ala-OMe
f1 (ppm)

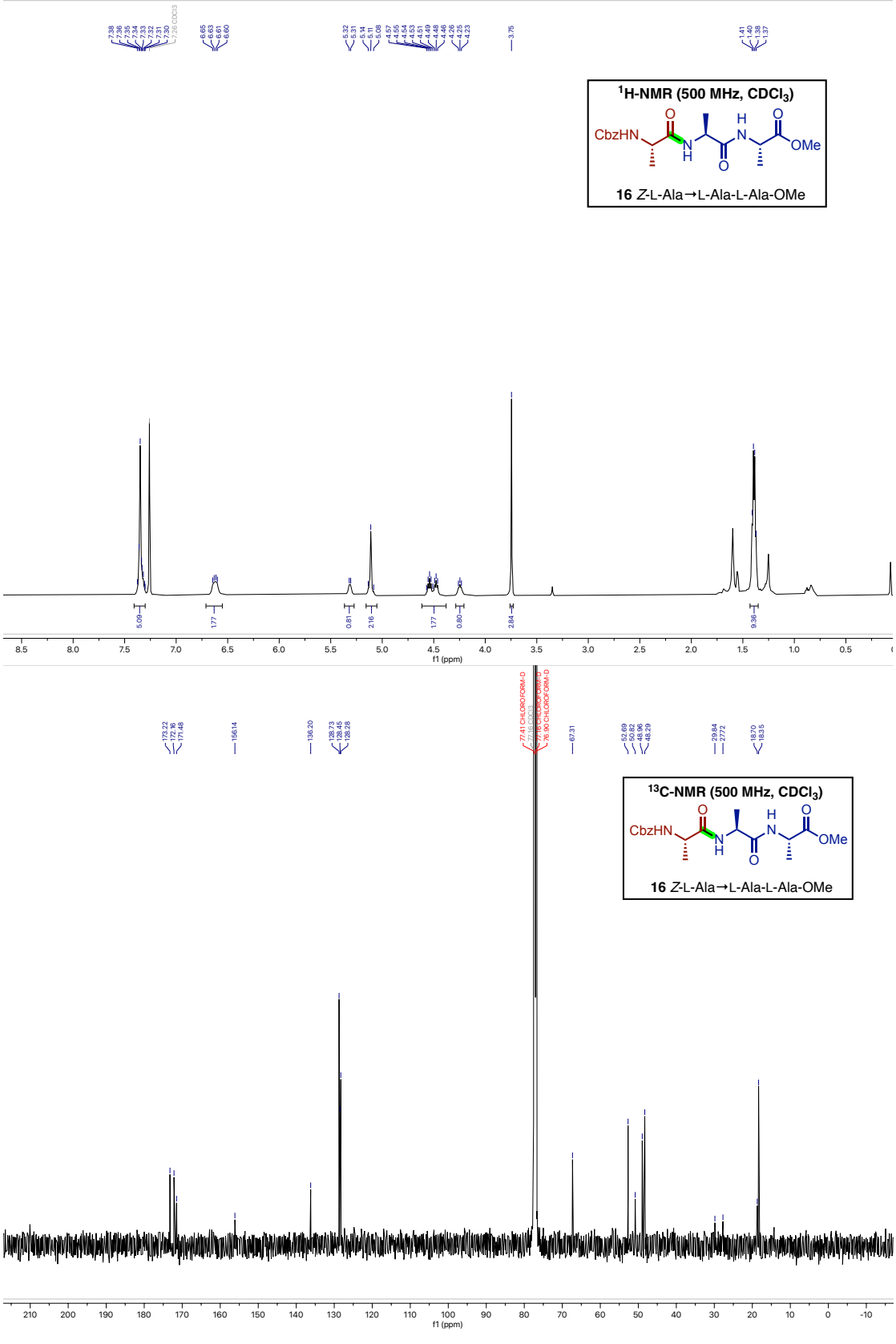
^{1}H-NMR (500 MHz, $CDCl_3$)
CbzHN
OMe
16 Z-L-Ala→L-Ala-L-Ala-OMe
f1 (ppm)
^{13}C-NMR (500 MHz, $CDCl_3$)
CbzHN
OMe
16 Z-L-Ala→L-Ala-L-Ala-OMe
f1 (ppm)

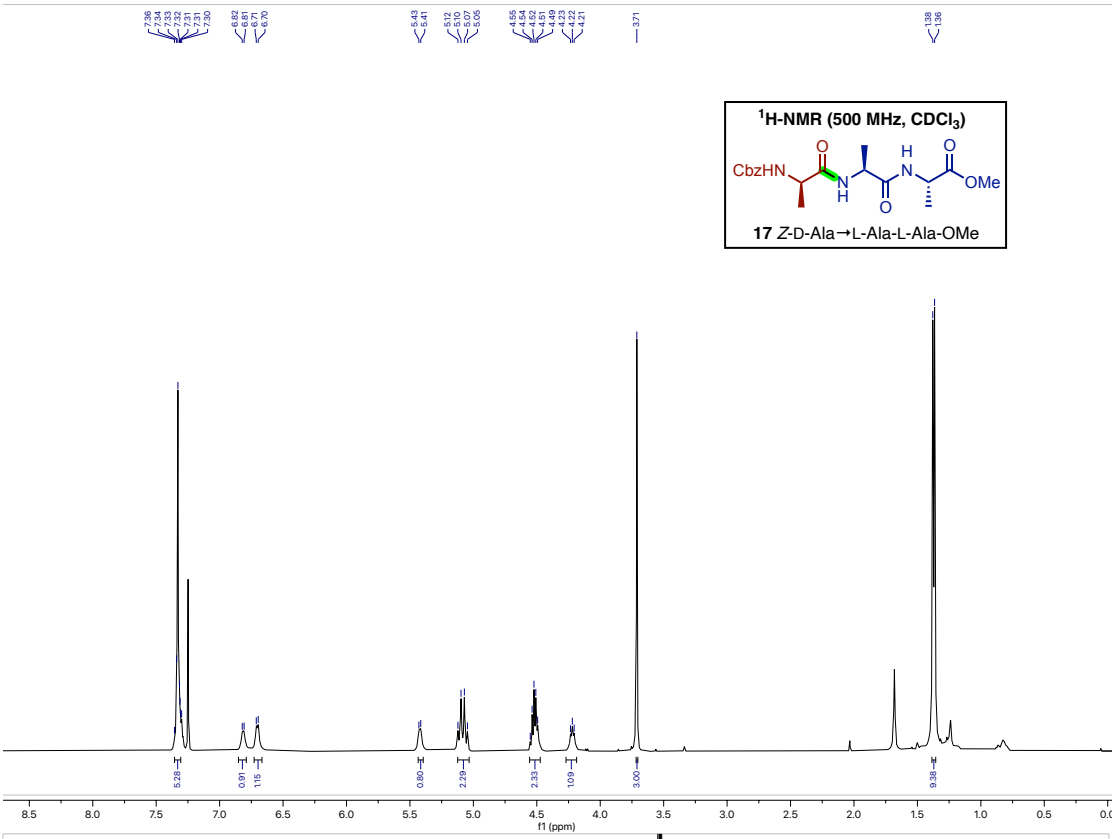
7.36
7.34
7.33
7.32
7.31
7.31
7.30
6.82
6.81
6.71
6.70
5.43
5.41
5.12
5.10
5.07
5.05
4.55
4.54
4.52
4.51
4.49
4.23
4.22
4.21
3.71
1.38
1.36
5.28
0.91
1.15
0.80
2.29
2.33
1.09
3.00
9.38
f1 (ppm)
^{1}H-NMR (500 MHz, CDCl$_3$)
CbzHN
OMe
17 Z-D-Ala→L-Ala-L-Ala-OMe

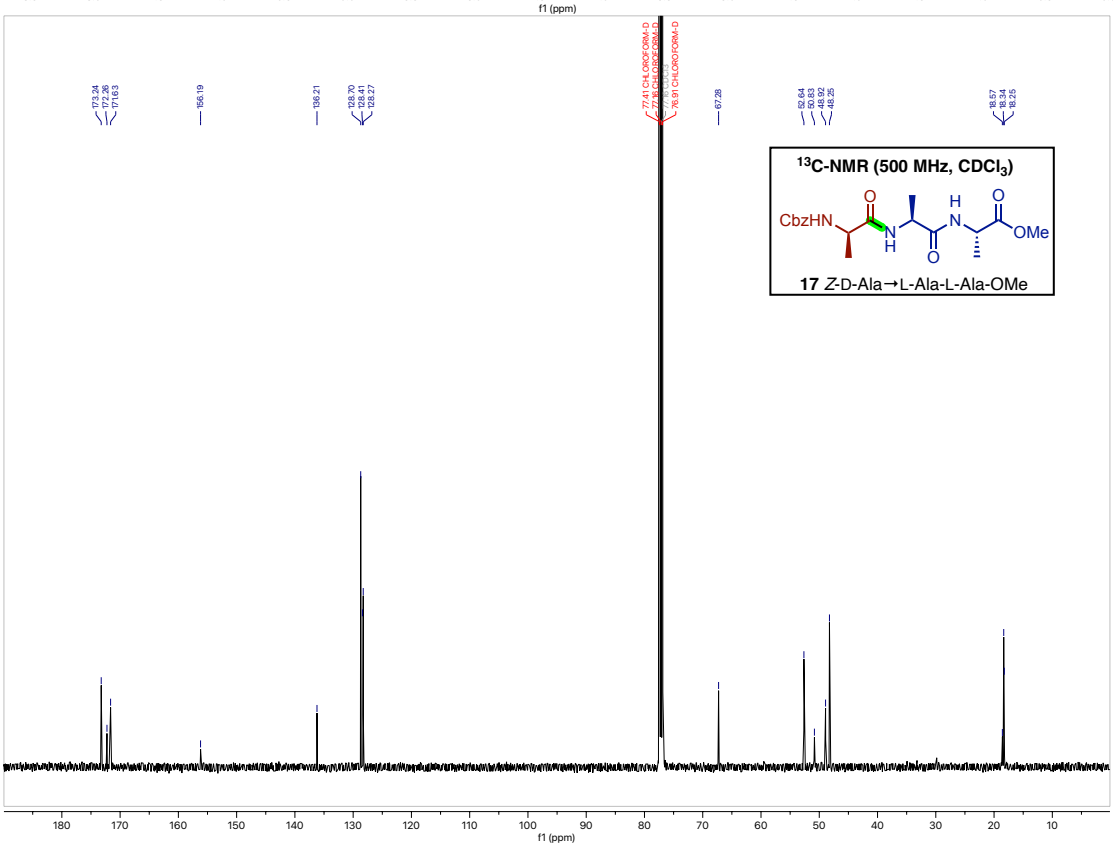
173.24
172.26
171.63
156.19
136.21
128.70
128.41
128.27
77.41 CHLOROFORM-D
76.91 CHLOROFORM-D
67.28
52.64
50.83
48.92
48.25
18.57
18.34
18.25
f1 (ppm)
^{13}C-NMR (500 MHz, CDCl$_3$)
CbzHN
OMe
17 Z-D-Ala→L-Ala-L-Ala-OMe

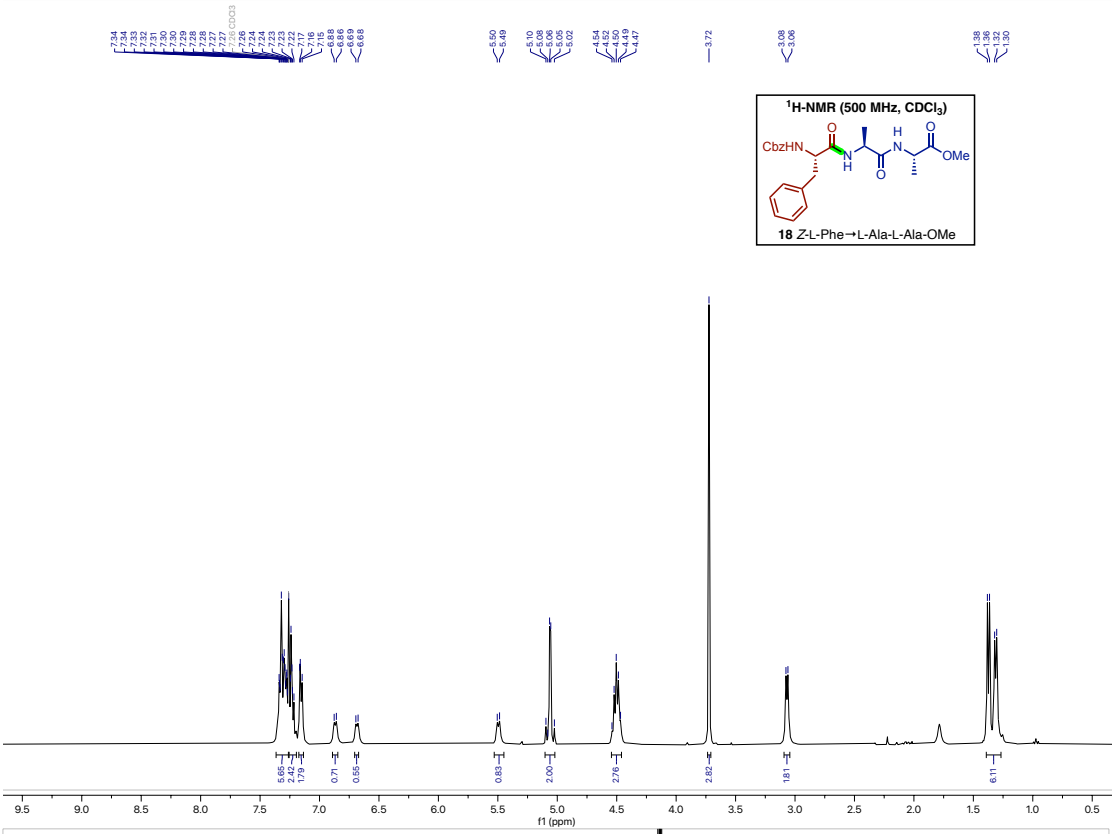
7.34
7.34
7.33
7.32
7.31
7.30
7.30
7.29
7.28
7.28
7.27
7.27
7.26 CDCl3
7.26
7.24
7.24
7.23
7.23
7.22
7.17
7.16
7.15
6.88
6.86
6.69
6.68
5.50
5.49
5.10
5.08
5.06
5.05
5.02
4.54
4.52
4.50
4.49
4.47
3.72
3.08
3.06
1.38
1.36
1.33
1.30
^{1}H-NMR (500 MHz, CDCl$_3$)
CbzHN
OMe
18 Z-L-Phe→L-Ala-L-Ala-OMe
5.65
2.42
1.79
0.71
0.55
0.83
2.00
2.76
2.82
1.81
6.11
f1 (ppm)

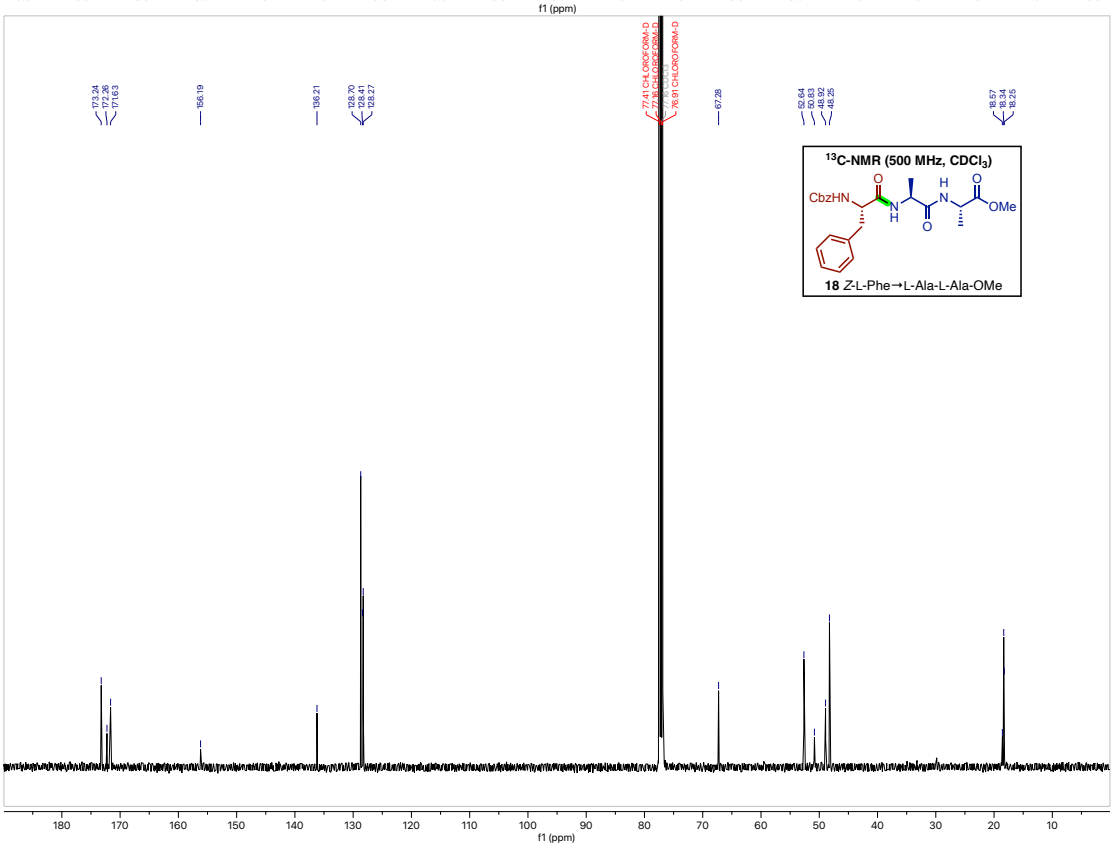
173.24
172.26
171.63
156.19
136.21
128.70
128.41
128.27
77.41 CHLOROFORM-D
77.16 CHLOROFORM-D
76.91 CHLOROFORM-D
67.28
52.64
50.83
48.92
48.25
18.57
18.34
18.25
^{13}C-NMR (500 MHz, CDCl$_3$)
CbzHN
OMe
18 Z-L-Phe→L-Ala-L-Ala-OMe
f1 (ppm)

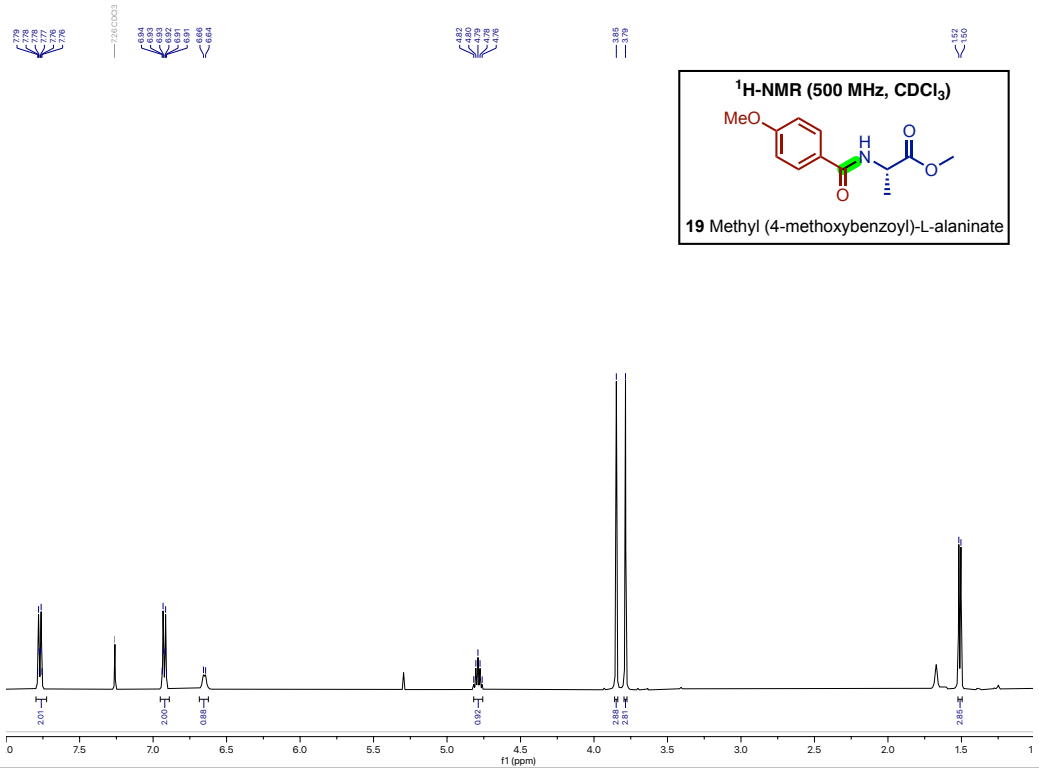
^{1}H-NMR (500 MHz, $CDCl_3$)
MeO
H
N
O
O
O
O
19 Methyl (4-methoxybenzoyl)-L-alaninate
f1 (ppm)

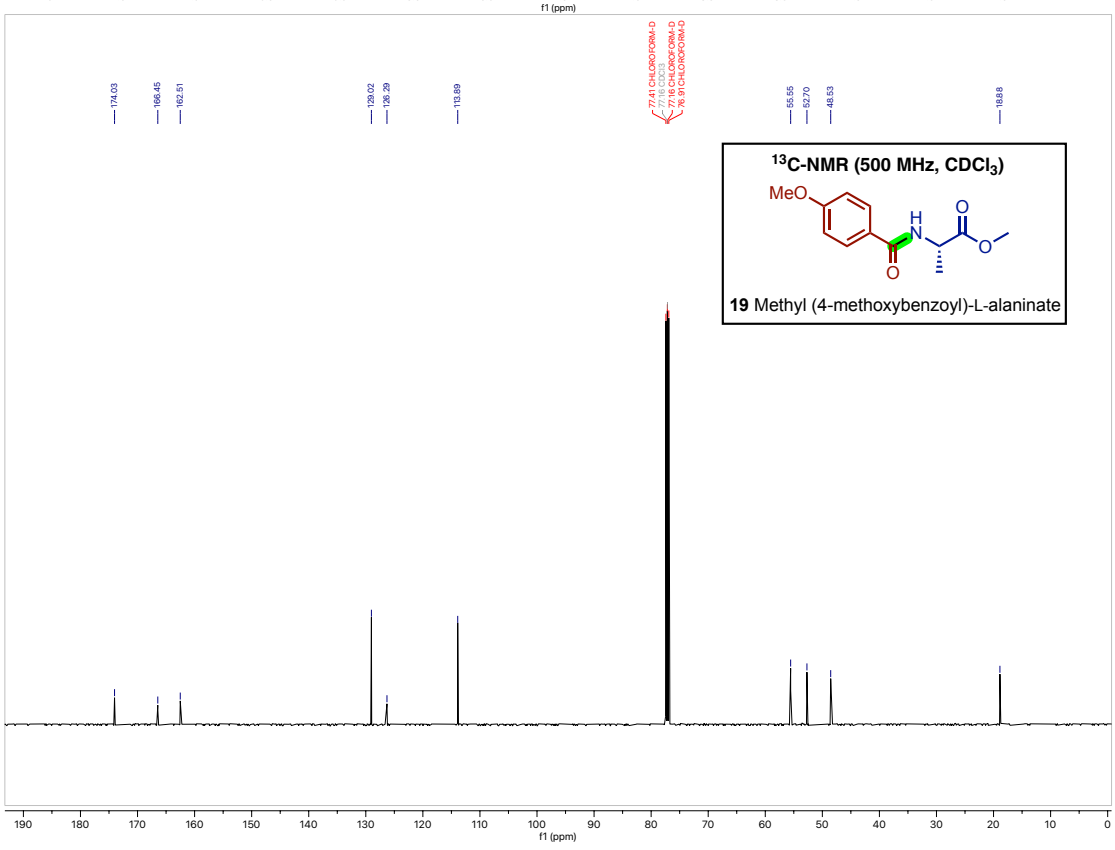
^{13}C-NMR (500 MHz, $CDCl_3$)
MeO
H
N
O
O
O
O
19 Methyl (4-methoxybenzoyl)-L-alaninate
f1 (ppm)

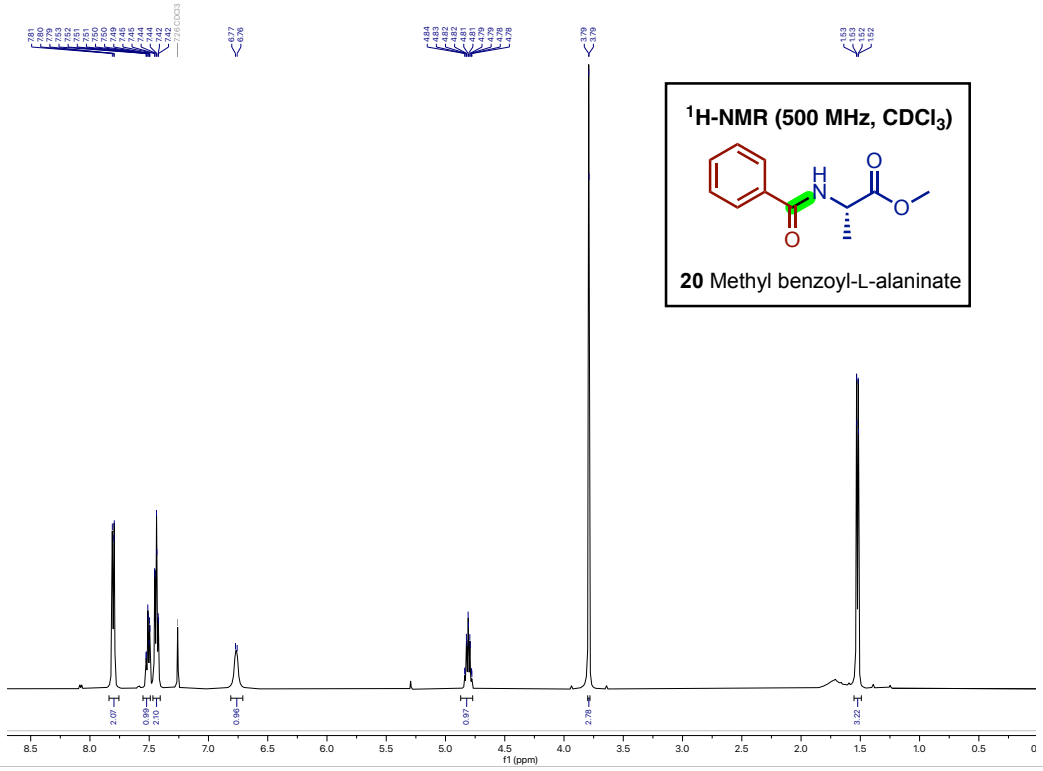
^{1}H-NMR (500 MHz, $CDCl_3$)
20 Methyl benzoyl-L-alaninate
f1 (ppm)

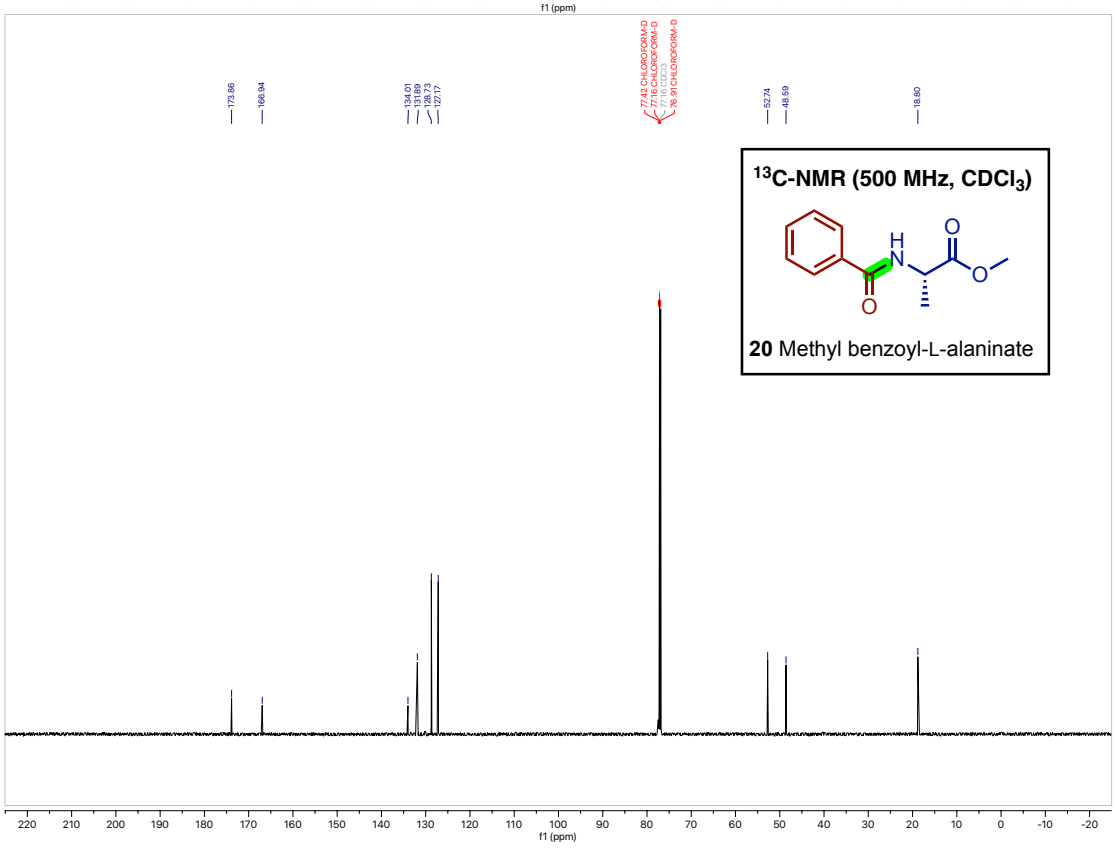
^{13}C-NMR (500 MHz, $CDCl_3$)
20 Methyl benzoyl-L-alaninate
f1 (ppm)

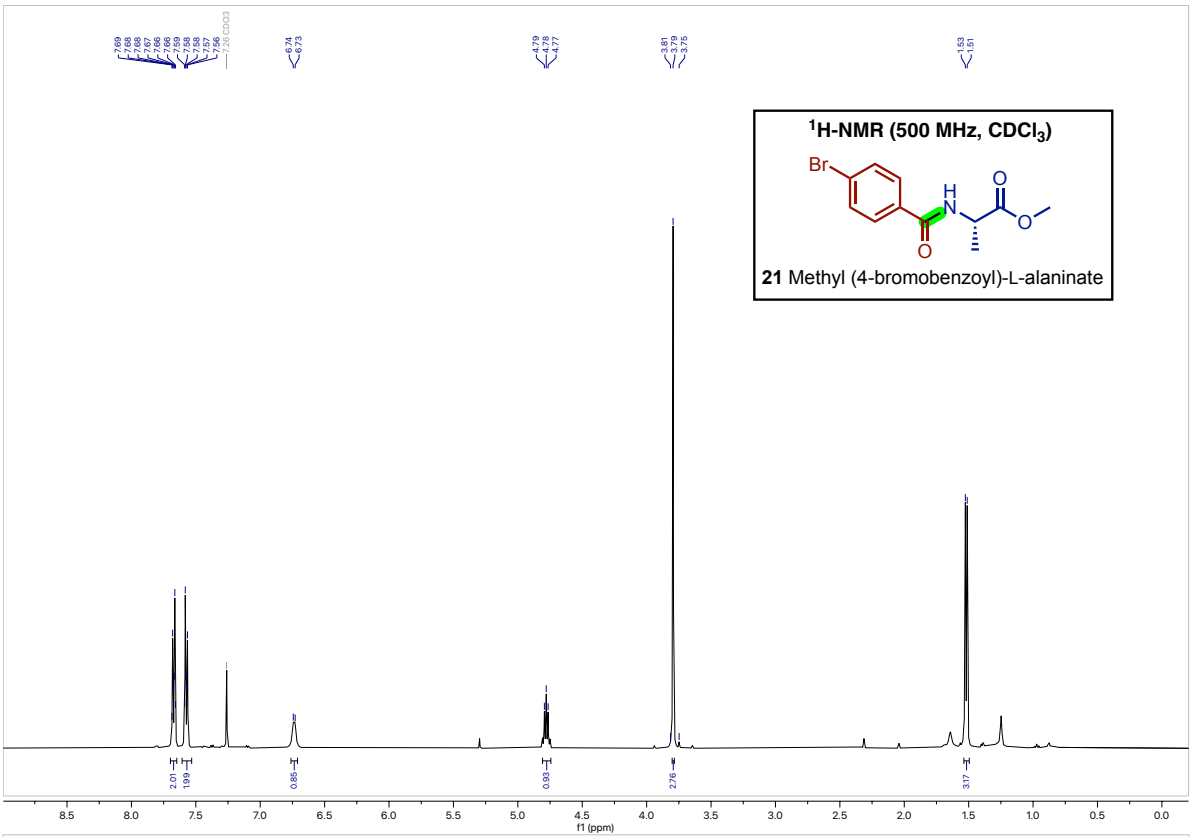
^{1}H-NMR (500 MHz, $CDCl_3$)
Br
H
N
O
O
O
21 Methyl (4-bromobenzoyl)-L-alaninate
f1 (ppm)

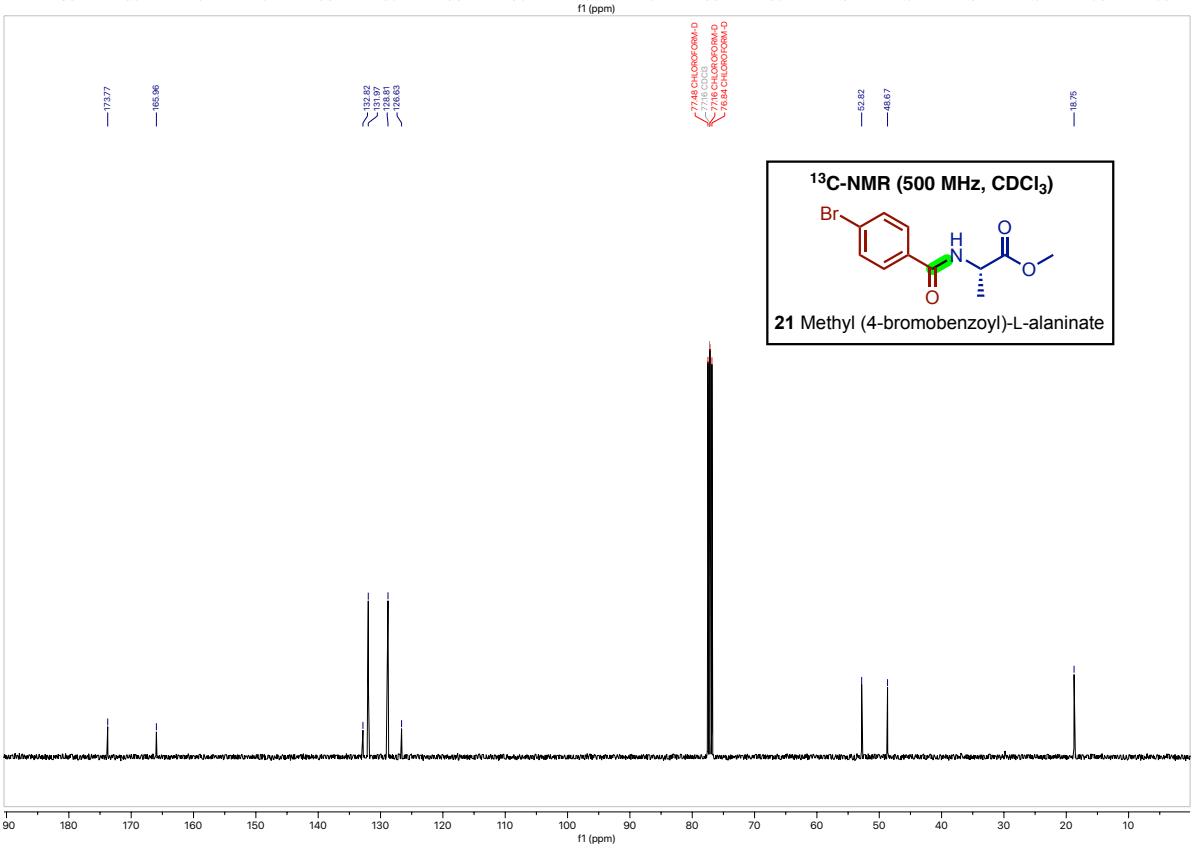
^{13}C-NMR (500 MHz, $CDCl_3$)
Br
H
N
O
O
O
21 Methyl (4-bromobenzoyl)-L-alaninate
f1 (ppm)

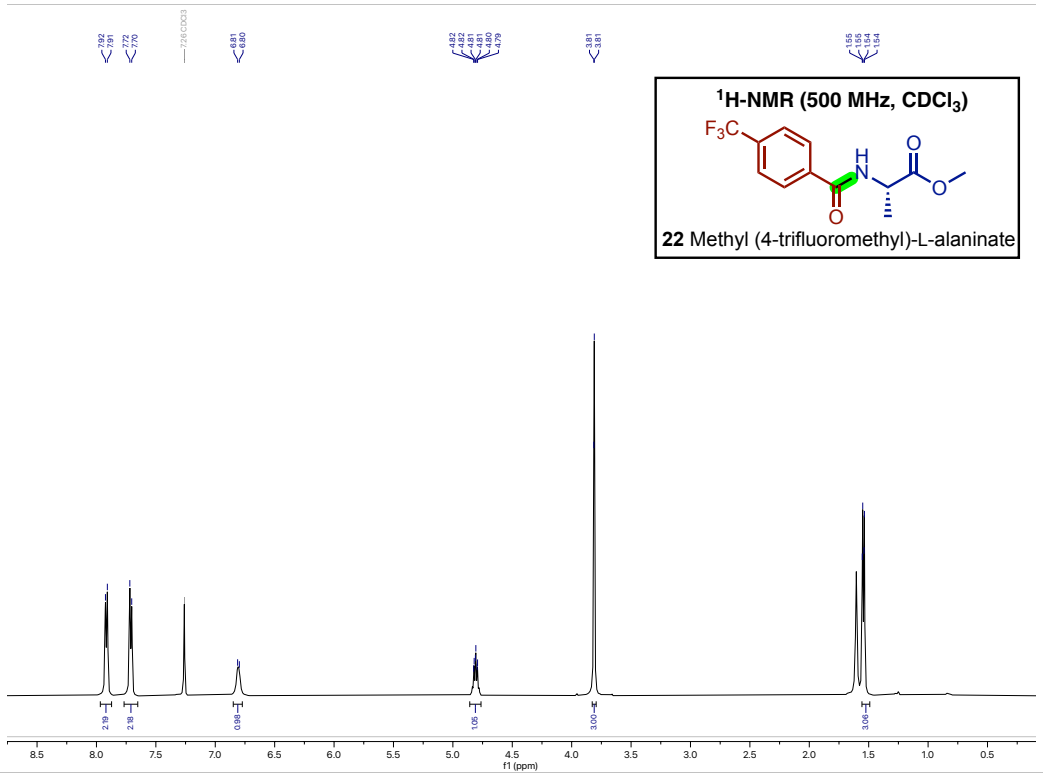

^{1}H-NMR (500 MHz, $CDCl_3$)

22 Methyl (4-trifluoromethyl)-L-alaninate

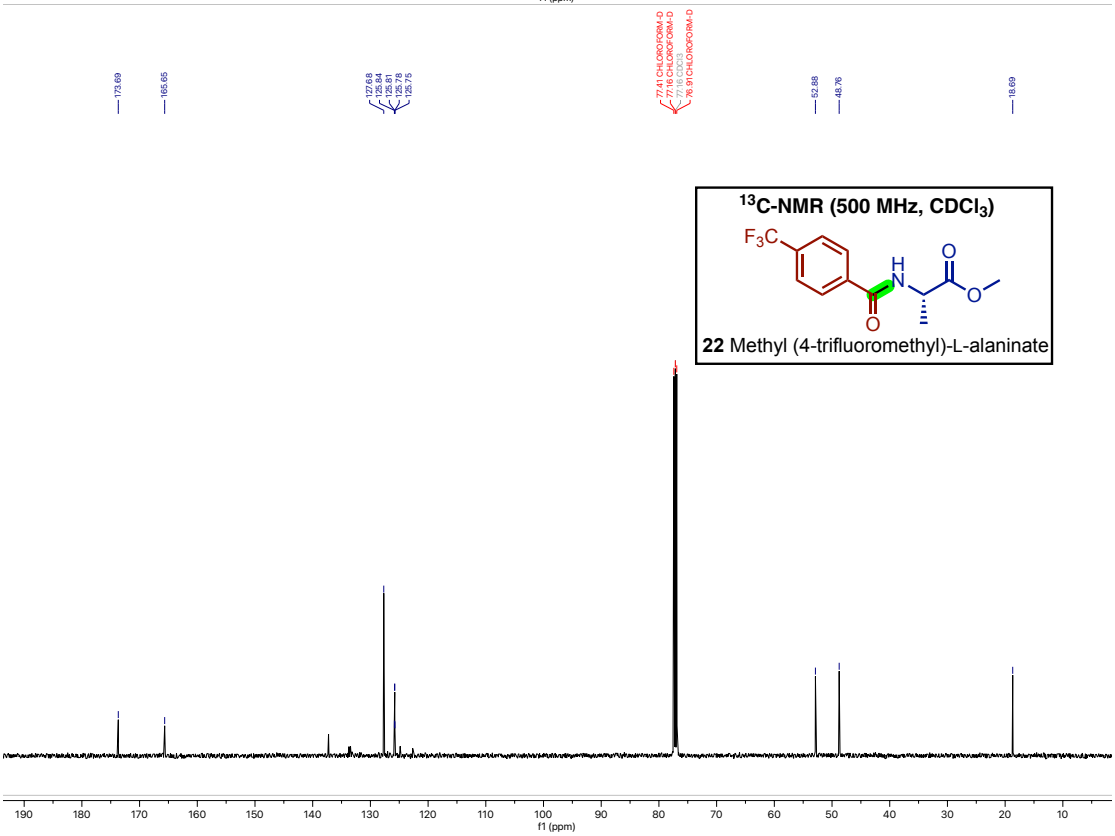

^{13}C-NMR (500 MHz, $CDCl_3$)

22 Methyl (4-trifluoromethyl)-L-alaninate

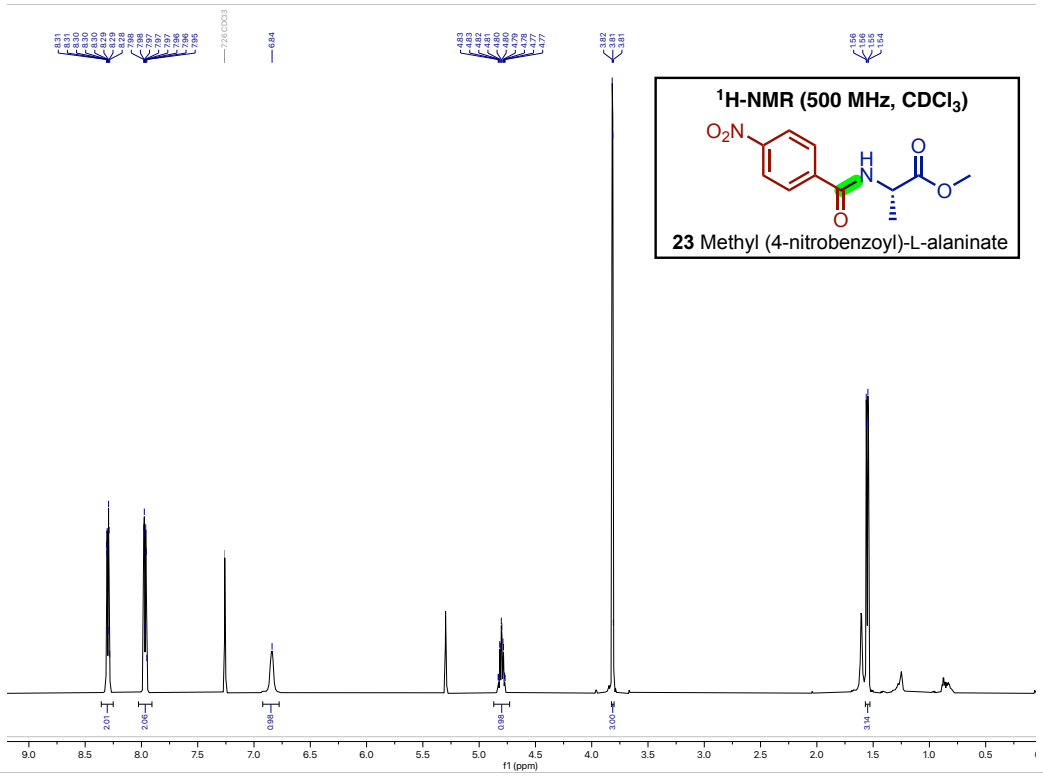
^{1}H-NMR (500 MHz, $CDCl_3$)
O_2N
H
N
O
O
O
23 Methyl (4-nitrobenzoyl)-L-alaninate
f1 (ppm)

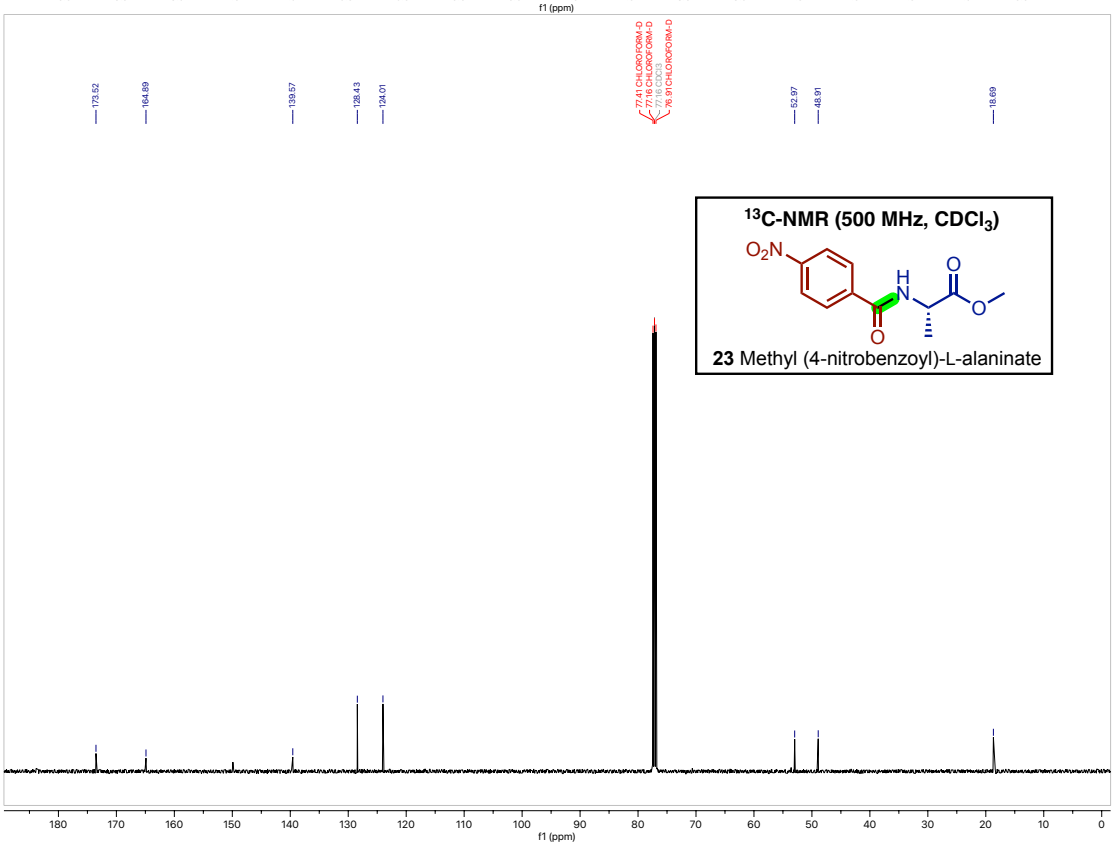
^{13}C-NMR (500 MHz, $CDCl_3$)
O_2N
H
N
O
O
O
23 Methyl (4-nitrobenzoyl)-L-alaninate
f1 (ppm)

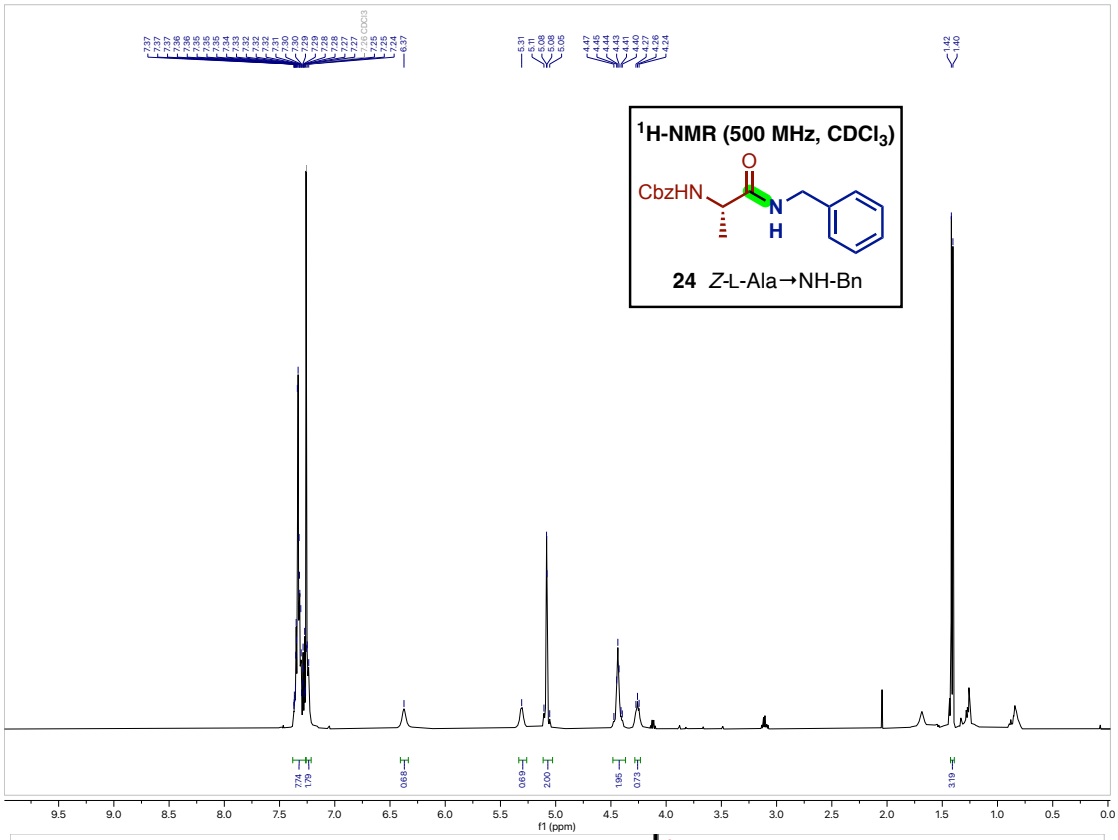
^{1}H-NMR (500 MHz, $CDCl_3$)
CbzHN
O
N
H
24 Z-L-Ala→NH-Bn
f1 (ppm)

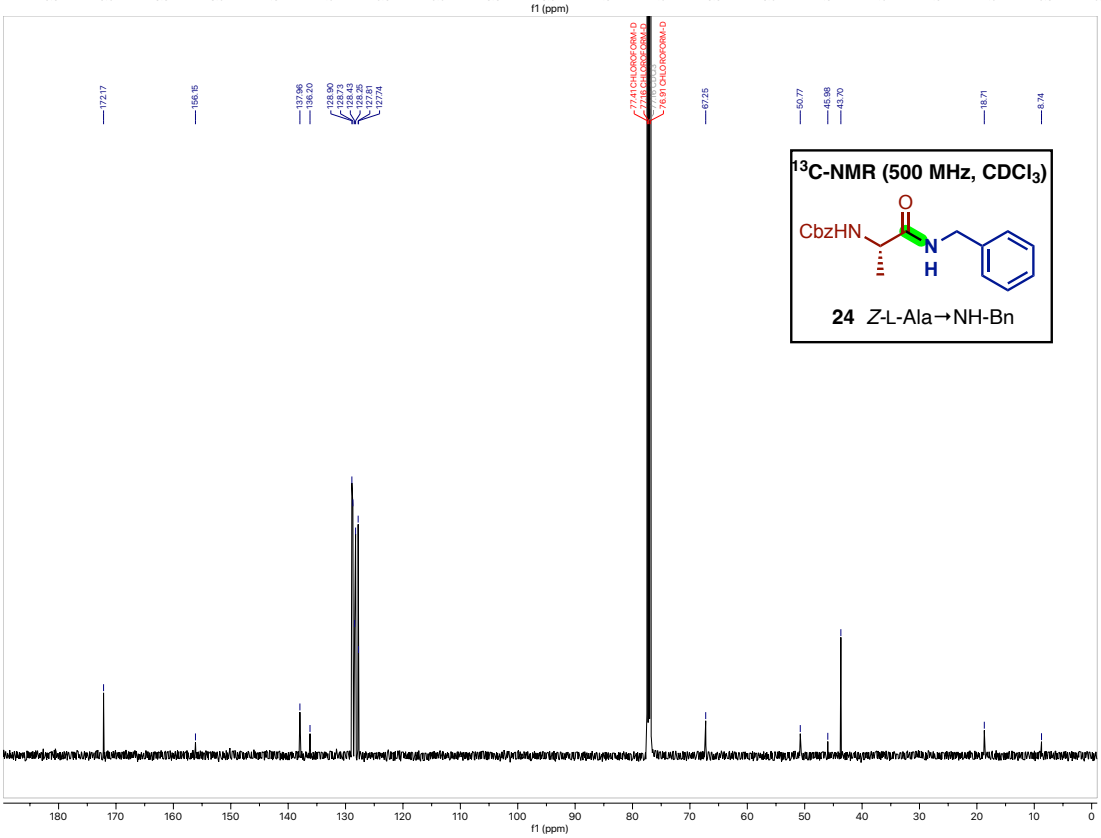
^{13}C-NMR (500 MHz, $CDCl_3$)
CbzHN
O
N
H
24 Z-L-Ala→NH-Bn
f1 (ppm)

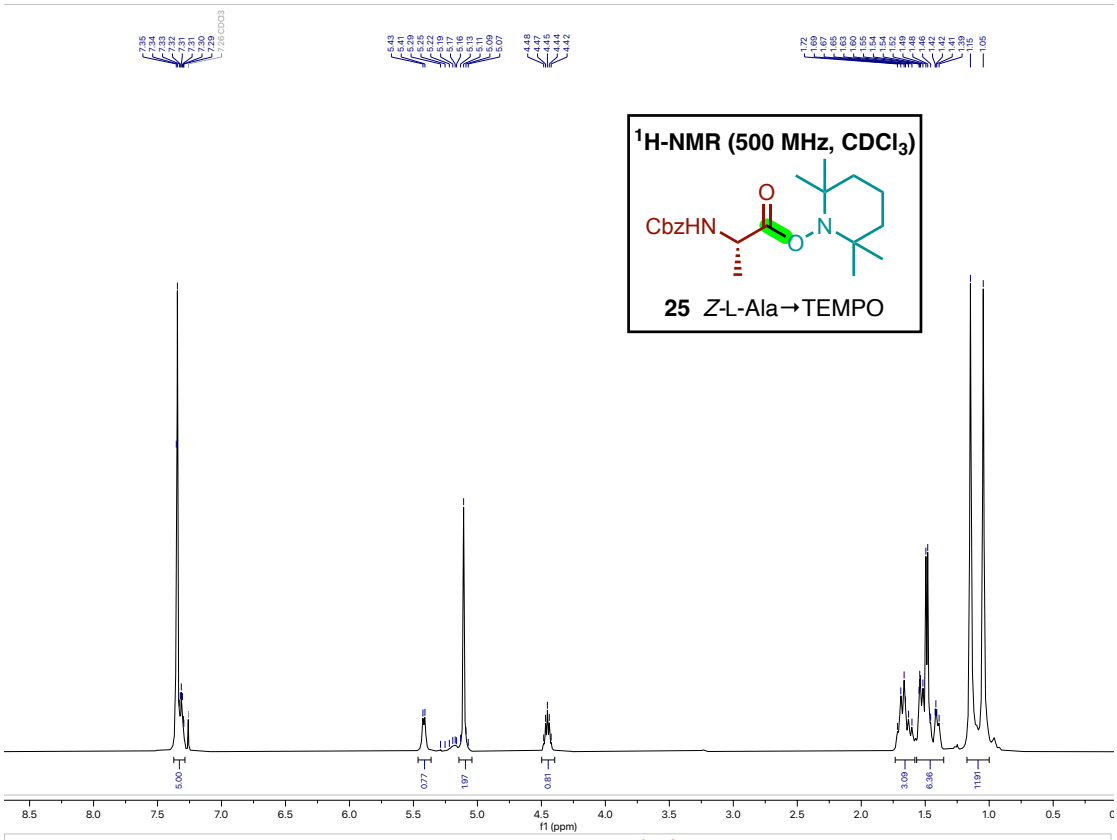
^{1}H-NMR (500 MHz, CDCl$_3$)
CbzHN
O
N
O
25 Z-L-Ala→TEMPO
f1 (ppm)

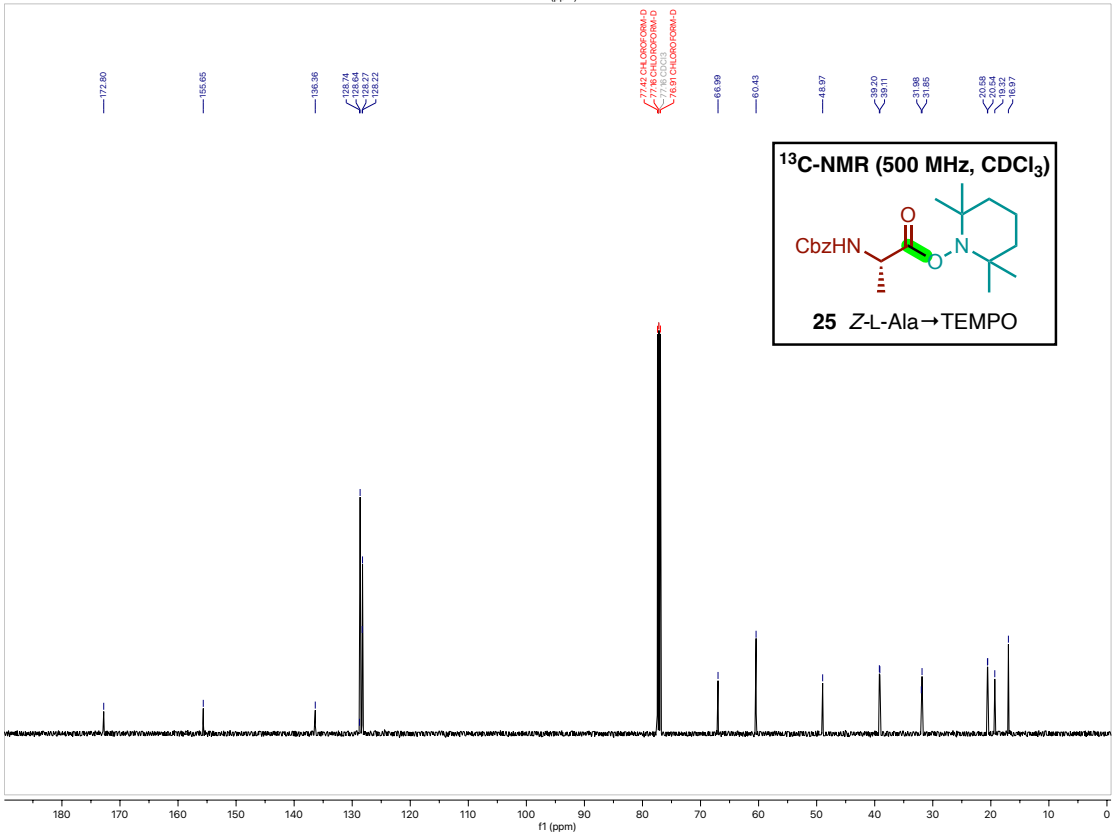
^{13}C-NMR (500 MHz, CDCl$_3$)
CbzHN
O
N
O
25 Z-L-Ala→TEMPO
f1 (ppm)